DECLARATION

No part of the work described in this thesis has been submitted in support of an application for another degree or other qualification of this or any other Institution.

A STUDY OF SOME FACTORS WHICH INFLUENCE SURFACE FINISH IN THE GRINDING PROCESS.

TREVOR JAMES VICKERSTAFF

BSc, MSc, CEng, MIMechE, MIProdE.

Thesis submitted for the degree of Doctor of Philosophy of the University of Aston in Birmingham

Department of Production Engineering

April, 1974

SUMMARY

This report deals with a research programme in which some of the factors which influence the surface finish produced in the grinding process have been studied.

In Part 1 a theory is proposed for the way in which the grinding wheel generates the workpiece surface. This theory explains why certain of the parameters in the wheel dressing process can be detected on the workpiece surface, whereas they do not appear on the surface of the grinding wheel. A special test rig is described which was developed to obtain data on wheel profiles. The data is analysed using a computer programme and confirms the theory.

In Part 2 the effects of wheel dressing and wheel wear on the surface finish produced are investigated.

The results of grinding tests show that the shape of the dressing diamond and its traverse rate across the wheel have a significant influence on the surface finish produced. Theoretical profiles are developed and compared with actual test results.

The influence of wheel wear is initially studied for plunge cut surface grinding in which the wheel passes only once over each part of the workpiece surface. It is concluded that, depending on the nature of the wear process, wheel wear may either improve the surface finish or cause it to deteriorate.

Wheel wear in crossfeed surface grinding is investigated. It is noted that some authors have reported a wear mechanism for this process which is different to that observed for other grinding

processes. In this work an alternative wear theory is proposed and grinding tests show that it is consistent with the generally accepted theories of wheel wear.

The proposed wear mechanism has certain theoretical effects on the workpiece surface finish. Grinding test results are presented to confirm these effects.

ACKNOWLEDGEMENTS

An undertaking of this magnitude cannot be completed without the support, encouragement and understanding of many people.

I would first thank Professor R H Thornley, both for allowing the use of equipment, material and services in the Department of Production Engineering at the University of Aston in Birmingham and also for his constant advice and encouragement.

The research was made possible by the supply of equipment and materials by the De Beers Industrial Diamond Division and the British Iron and Steel Research Association. Their support is gratefully acknowledged.

The active and willing support of technical staff is essential for this type of research and I am grateful for the assistance I have received from staff in the Machine Tools and Metrology Laboratories. My special thanks go to Mr Eric Langton and his staff for their invaluable assistance with electronic equipment.

Mr John Driscoll provided considerable assistance in the development of the computer programme.

I would like to thank Mrs Carol Robinson for typing the manuscript.

Finally my special thanks to my wife. Her willingness to provide encouragement without complaint over very many months has made this project possible.

LIST OF CONTENTS

LIST OF FIGURES

28. Wheel profile sampling intervals.
29. Hardened steel blade and fixture on the grinding machine.
30. Hardened steel blade and stylus on Talysurf 4.
31. Technique to ensure wheel and workpiece profiles start from the same point.
32. Test conditions for comparison of wheel and workpiece profiles.
33. Typical wheel profiles.
34. RAXEVCO matrix - coarsely dressed wheel.
35. RAXEVCO matrix - finely dressed wheel.
36. Wheel and workpiece profile comparison - coarse dressing.
37. Wheel and workpiece profile comparison - fine dressing.
38. Mean errors for each comparison of wheel and workpiece profiles - coarsely dressed wheel.
39. Mean errors for each comparison of wheel and workpiece profiles - finely dressed wheel.
40. Mean errors between wheel and workpiece profiles - coarse dress.
41. Mean errors between wheel and workpiece profiles - fine dress.
42. Mean error for different workpiece start positions - coarse dress.
43. Mean error for different workpiece start positions - fine dress.
44. Wheel profile envelope and workpiece profile - coarse dress.
45. Wheel profile envelope and workpiece profile - fine dress.
46. Comparison parameters calculated for wheel and workpiece profiles.
47. Profiling stylus failing to record a high point on a grit.
48. Effective diamond angle.
49. Calculation of theoretical workpiece profiles.
50. Comparison of theoretical and actual workpiece profiles - coarse dress.

1. INTRODUCTION

For a number of reasons it is becoming increasingly important to select the conditions to be used in a machining process at the planning stage, rather than to leave these decisions to the skill of the machine operator. First of all there is a serious shortage of skilled labour. Secondly, the rapid rate of development in new workpiece and tool materials makes specialised experience redundant in a relatively short period. A third problem is caused by the increasing cost and complexity of machine tools. With expensive equipment it is not adequate to merely use conditions which give satisfactory workpiece characteristics. The conditions must be optimised to give satisfactory workpieces at minimum possible cost. Finally, the increase in the application of automatic control systems and particularly adaptive control, demands that machining parameters are preselected.

The level of skill normally considered necessary for a grinding machine operator is probably higher than that for any other metal removal process. Indeed, grinding is still considered to be something of an 'art', rather than the application of scientific principles. One reason for this is that the grinding wheel is an extremely complex cutting tool, both in its structure and also in its performance during the cutting operation. Another factor is the degree of precision traditionally associated with the grinding process.

However, a study of any grinding operation will show that the machine operator adopts a standard procedure when asked to produce

a new type of component. First of all he uses his experience to decide if the job is similar to anything he has done before. If so, he will know that similar machining conditions must be used. The next step is to carry out a series of trials from which an appropriate method is developed. The method is then recorded, usually in a personal notebook and is used again for subsequent similar components.

The important implication of this procedure is that within acceptable limits the grinding process is repeatable. To predict the output of any repeatable process it is only necessary to establish those parameters which are significant in relation to the output and to quantify their significance. Hence it should be possible to obtain data which can be used as a basis for selecting grinding conditions. This will avoid the necessity for expensive 'trial and error' techniques.

The potential variables in a precision grinding operation have been listed by Wetton[1] and can be considered under three main headings.

1. The wheel selected.
2. The wheel preparation prior to grinding; the dressing process.
3. The grinding conditions being used.

For economic reasons an individual user will wish to place strict limits on the number of different wheels available for selection. Consequently the second two groups of variables will normally be the most important.

Figures in brackets refer to the list of references.

These variables must be manipulated to achieve certain criteria, usually defined by dimensional accuracy and workpiece surface condition. The former criterion is not a serious problem, providing that the machine tool being used is capable of the required degree of accuracy. In-process or post-process gauging can be used to control the inevitable drift which occurs in all processes. However, the latter is more difficult to control, because it is directly related to the wheel surface condition at any time. The surface of a grinding wheel sustains considerable wear during the grinding operation and the wear process can have very different effects on the wheel performance. Depending on the conditions being used the wheel can develop improved cutting properties or, alternatively, become so blunt that it may damage the workpiece surface, causing cracking, changes in microstructure or serious residual stresses. The wheel may gradually produce a smoother workpiece, or generate rougher surfaces as grinding is continued.

The nature and influence of the wear process occurring on a grinding wheel surface is a function of the way in which the wheel surface is prepared and the grinding conditions used. If the grinding process is to be controlled the influence of these factors must be fully understood. This work is a contribution to current knowledge in these areas.

2. DEFINITION OF THE PROBLEM

2.1 The Grinding Wheel

A grinding wheel is a bonded abrasive body consisting of a large number of abrasive particles held together by a bonding agent.

The main types of abrasive material are aluminium oxide, silicon carbide, diamond (natural and synthetic) and cubic boron nitride. The former two can be considered as conventional, being the most widely used. Aluminium oxide is generally used for grinding ferrous alloys, while silicon carbide is used for grinding glass, ceramic, or non-ferrous alloys. Natural diamond has been in use for many years to grind very hard materials. However, synthetic diamond and cubic boron nitride are now being applied to the grinding of relatively ductile materials. They are many times more expensive than conventional abrasives, but their wear characteristics are such that overall grinding costs may be reduced in certain cases. For the purposes of this investigation aluminium oxide abrasive was used throughout.

The type of bonding agent used depends on the grinding operation, for example rubber or shellac bonds are used for abrasive cut-off wheels which are subject to axial as well as radial loading. For the large majority of precision grinding operations the bond material is based on silica, containing soda, potash, lime, etc. Such wheels are termed 'vitrified' and are the type used in this work.

Grinding wheels are manufactured by mixing together controlled amounts

of abrasive grits, bonding materials and filler. The mixture is pressed into moulds of the required size and shape and then heated under controlled conditions. The application of heat vapourises the filler material to give the wheel controlled porosity and causes the bond to form a bridge structure in which the grits are supported The theoretical wheel structure is illustrated in Figure 1.

For given abrasive and bond materials the manufacturing process can be arranged to give various wheel parameters.

2.1.1 Grit type and size:

The majority of grit materials are synthetic and their physical and mechanical properties can be controlled to give the combination of hardness and toughness best suited to their application. Grit sizes are determined by grading according to a sieve or mesh system so that, for example, a 60 grit wheel would contain grits which have been graded in a sieve with 60 spaces per lineal inch. In practice grits are produced by crushing the synthetic abrasive and rigid control of both grit shape and size is too expensive for most applications. Consequently wheels contain grits which are nominally of a certain size, but which in fact are distributed around this nominal size.

2.1.2 Wheel grade:

The grade of a wheel is a measure of the tenacity with which the bond material holds the abrasive grits in the wheel. Using practical terms, a 'soft' grade of wheel is one from which the grits can easily be dislodged, whereas the removal of grits from a 'hard' wheel requires a

greater force. In general a harder grade of wheel contains more bonding material.

In practice the hardness or grade of a wheel has two meanings. Firstly, hardness is the nominal grading which is given to a wheel by the manufacturer. Hardness is designated according to a certain manufacturing formula composition and this implies that the same manufacturing process will produce identical wheels. Secondly hardness is assessed from the manner in which the wheel behaves in operation. A soft wheel wears quickly whereas, for the same operating conditions, a hard wheel has a much lower wear rate.

The wheel user is concerned to know the hardness of grinding wheels so that he can select the appropriate wheel for a given application. Various tests have been devised to determine wheel hardness. Peklenik[2] determined relative hardness by measuring the force required to cut or gouge a groove across the periphery of the wheel. These tests showed that the hardness obtained is influenced by the shape of the tool used to cut the groove and also that hardness values quoted by different manufacturers did not correlate with one another.

There are two major disadvantages of this type of test. Firstly it is destructive and consequently can only be applied to a sample of a batch of wheels. This type of testing will be carried out by the wheel manufacturer and unless different manufacturers can agree on a standardised test procedure, there is no guarantee that meaningful results are obtained. The second problem is the localised nature of the test. To a certain extent this problem can be overcome by taking several tests, at different positions around the wheel periphery, but

it is still only a surface test.

In recent years non-destructive tests of the whole wheel structure have been developed. A pneumatic method[3] determines wheel porosity, which is a first approximation to wheel hardness, by measuring an airflow through the wheel. The technique is able to show variations of structure within the wheel and this is particularly important when wheels are to be used at high cutting speeds. An alternative method of testing[4,5] measures the modulus of elasticity of a wheel from a sonic test. The modulus is computed from a knowledge of the shape, density, dimensions and natural frequency of the wheel. Hardness is assumed to be a function of the modulus of elasticity and the friability of the grits in the wheel. Good agreement was noted[4] between the results for the sonic test and those obtained from the destructive methods[2].

There is reasonable correlation between the wheel hardness determined by these tests and the wheel performance in practice. However, it has been shown[6,7] that the effective grade of a wheel is influenced by factors such as relative wheel and work dimensions, wheel and work speeds, grinding fluids, machine stiffness and wheel dressing. The nominal wheel grade designated by the manufacturer or determined by one of the above tests is not affected by these conditions.

2.1.3 Wheel structure:

The structure of a grinding wheel is a measure of the degree and size of the porosity in the wheel. It is effectively the relative spacing of the abrasive grits and is determined by the amount of filler material

and the pressure used during the manufacturing operation.

During the grinding operation each abrasive grit which contacts the workpiece surface is a potential cutting edge. Many authors, of which Krabacher[8] is only one example, have shown that the debris produced in the grinding operation contains chips which are similar in shape to those associated with other metal cutting processes. These chips are caused by the workpiece material sliding up the front, or rake face of the grits and because the wheel surface is porous many of these chips will penetrate the surface, rather than be thrown off.

An 'open' structure wheel has adequate space, or chip clearance for this material to enter the wheel surface. The surface of a wheel with a 'close' structure can easily become clogged with workpiece material. In this condition the wheel is termed 'loaded'. A loaded wheel will give a smooth, possibly burnished workpiece surface, but may well cause undesirable changes in microstructure and surface cracking.

It can be seen that the grinding wheel is an extremely complex cutting tool. Relatively small changes in wheel characteristics can cause significant changes in wheel performance. The performance of nominally identical wheels can be significantly altered by the selection of the operating variables.

2.2 Grinding Wheel Wear

The wear processes occurring on the surface of a grinding wheel can

be broadly classified as either attricious wear or fracture wear. Attricious wear is caused either by the rubbing process between the grit and the workpiece, or by a chemical reaction between these materials. In either case the result is a worn, flat grit face of the type shown at (A) in Figure 1. Fracture wear is the removal of abrasive particles from the wheel, either by dislodgement from the bond, (B) in Figure 1, or by actual fracture within the grit itself, (C) in Figure 1.

2.2.1 Attricious wear:

The smooth surfaces of grits which have sustained attricious wear reflect incident light. Malkin and Cook[9] used this property to quantify the wear by expressing the reflective areas as a percentage of the wheel surface area. They found that when grinding various types of steel the workpiece surface exhibited grinding 'burn' if a certain percentage of wear flat area was obtained. The presence of grinding burn indicates high cutting temperatures, which is normally associated with blunt cutting tools. Their findings agree with those of other workers such as Yoshikawa[11].

In practice attricious wear is termed 'glazing' due to the glazed, or glossy appearance of the wheel surface. Glazed wheels are known to produce smooth workpieces, but can cause damage to the workpiece surface. High levels of residual tensile stress, surface cracks and, when grinding hardened steel, the retention of austenite in the surface layers have all been associated with glazed wheels. Consequently attricious wear is normally regarded as being undesirable.

2.2.2 Fracture wear:

Malkin and Cook[9,10] also found that grinding forces increased with the incidence of attricious wear. With the correct selection of grit and bond strengths and grinding conditions this force increase may be sufficient to fracture or dislodge the worn grit. Fracture or dislodgement will produce new, sharp cutting edges and, in theory, this self-sharpening process could be continued indefinitely. However, the wear process is unlikely to be consistent across the whole wheel face and will be particularly rapid at the edges of plain wheels, or at sharp corners on formed wheels, where the grit support is relatively weak. Consequently for precision grinding operations fracture wear is only acceptable as long as the necessary geometrical accuracy is maintained.

2.2.3 The significance of wheel wear:

The attricious and fracture wear mechanisms discussed above apply to individual grits on the wheel surface. These processes affect the performance of the wheel, but in addition the cumulative effects of wear over the whole wheel surface are significant for a number of reasons. Firstly, a workpiece dimension is often determined by the relative position of the wheel axis and some other fixed point, such as the top of the worktable or the axis of the workpiece support centre. In this case the wheel radius is a critical dimension and it is important to know the rate of radial wheel wear so that appropriate compensation can be provided. The wear rate is also important in form grinding operations where the profile imparted to the workpiece is determined by that present on the wheel. Finally

there is an economic factor. Wheel cost is one aspect of the total cost and wheel life is directly related to radial wear rate.

Figure 2a shows the progression of wheel wear which has been measured by a number of authors[8,12-14]. Wear occurs in three phases.

Phase I - a short period of non-linear rapid wear during which any insecure grits are removed. The amount of wear occurring in this period is related to the dressing technique[14,15].

Phase II - a much longer period during which, under good grinding conditions, wear occurs at a constant and relatively slow rate.

Phase III - this phase has not always been identified, but is characterized by a rapid increase in wear rate and severe vibration. This is probably due to the formation of lobes on the wheel surface caused by inconsistent wear rates at various parts of the wheel.

The wear pattern is similar to that occurring on other types of cutting tool and in practice grinding would be terminated before the wheel enters Phase III. At this stage the total volume of metal removed and the volume of wheel lost can be calculated. The ratio of these quantities is termed the Grinding Ratio and is frequently used to assess the performance of different wheels.

In Figure 2b three possible wheel wear patterns are presented. Curve A is the ideal type discussed above. Curve B applies when the wheel is too soft for the grinding conditions being used. Grits are easily removed from the bond, the wear rate is rapid and Phase III wear occurs relatively quickly. If the wheel is too hard curve C is obtained. Wear is relatively slow, being mainly attricious, but if blunt grits are not fractured or dislodged the wheel becomes glazed and probably damages the workpiece surface.

It can be seen therefore that if the desired rate and type of wheel wear is to be obtained the wheel and the grinding conditions must be selected in conjunction with one another. The relationship is probably more critical for grinding than for any other cutting process.

2.3 Wheel Dressing

All cutting tools are subject to wear and must be periodically resharpened. In the grinding operation this process is termed wheel dressing. There are three objectives in the wheel dressing process.

1. To ensure that the wheel periphery is concentric to the wheel axis and is of the correct geometric form.

2. To remove the debris from the previous grinding operation.

3. To prepare the wheel surface for the grinding operation.

In many publications the first two of these objectives are termed wheel truing and only the latter objective is regarded as wheel dressing. In practice they are carried out in much the same way and no distinction is made in this work.

2.3.1 Methods used for dressing wheels:

The two principal techniques in common use are diamond dressing and crush dressing and both are normally used to true and dress the wheel simultaneously.

Various types of diamond dressing tool are available. In precision grinding operations a single point diamond tool is the most widely used. The tool can be used to dress all types of grinding wheel, both plain and profiled and is generally considered to be the most precise dressing tool available. Multi-point diamond tools, using a larger number of small diamonds set in a suitable matrix, are cheaper and are satisfactory for many applications. In recent years diamond coated rollers have been introduced as another alternative. They are very expensive and can only be justified for large production grinding operations, particularly when profiled wheels are being used.

Crush dressing is a technique whereby wheel grits are removed from the grinding wheel surface by pressing a metal disc or roller into the wheel periphery under a high load. The technique requires special machine design features to withstand the high dressing loads and is normally only used for production grinding applications where surface finish is not critical.

In this work single point diamond tools of precise geometry were used for all dressing operations.

2.3.2 The dressing mechanism using a single point diamond:

Kornberger[16] and Malkin[10] have examined the debris produced in the dressing process. In the latter paper size distributions were obtained for the grit particles removed from the wheel. In general larger particles and less grit fragmentation occurred with soft wheels, but more significantly the dressing particles were not much smaller than the grits used to manufacture the wheels. Kornberger[16] did not measure the particles, but photographs he presented show dressing particles approximately half the original grit size.

The results presented in these papers indicate that the dressing diamond either removes whole grits by causing bond fracture or shatters the grit into a small number of parts. However, in an earlier publication the author[17] has shown that the diamond shape and traverse rate across the wheel surface can be detected on the workpiece surface after grinding. Lindsay[18] suggests that these effects can be explained by the diamond actually reproducing its profile on individual grits. This explanation contradicts the results obtained by Kornberger and Malkin and an alternative solution is considered later in this report.

3. A REVIEW OF PREVIOUS WORK ON THE INFLUENCE OF WHEEL DRESSING AND WHEEL WEAR ON SURFACE FINISH

3.1 Introduction

A number of attempts[19-23] have been made to predict surface finish by simulating a workpiece profile from an analysis of the relative motion between the abrasive grits and the workpiece. The author has reviewed these papers in a previous publication[17].

For purposes of simulation the grits are assumed to have a precise shape, either spherical or fixed triangular, the number of grits is determined by direct measurement of the wheel surface and they are assumed to be distributed in some way which can be mathematically described. Good qualitative agreement is obtained with actual workpiece profiles and it is possible to successfully predict the influence of certain process variables on the workpiece surface roughness.

However, theoretical roughness values are significantly different from the results obtained in grinding tests and Yoshikawa[23] has discussed the reasons for these discrepancies. He suggests that an over simplified grit shape, machine vibration, wheel dressing and wheel wear will lead to errors in the simulation. A more realistic grit shape can be obtained by assuming a certain shape distribution about a mean value. A variable expressing this shape distribution can then be included in the simulation. Machine vibration will alter the position of the grits with respect to the workpiece and can probably be studied by the introduction of a systematic variable

into the mathematical expression for grit distribution. The effects of wheel dressing and wheel wear are more complex and they are also interdependent. Certain of the variables in the dressing process affect the workpiece surface finish. In addition these same variables influence the nature of the wear process occurring on the wheel surface and, consequently, the wheel profile. The workpiece surface is closely related to the wheel profile.

3.2 The Influence of Wheel Dressing on Surface Finish

When a grinding wheel is dressed with a single point diamond the following variables can be controlled[17]

1. The traverse rate of the diamond across the wheel surface.
2. The depth of cut or infeed of the diamond.
3. The total amount of wheel removed, i.e. the number of passes of the diamond across the wheel.
4. The wheel speed.
5. The setting angle of the diamond.
6. The diamond shape; this variable is time dependent due to diamond wear.

In a large series of statistically designed experiments[17,28] the author has shown that when the diamond is traversed across the wheel it tends to form a helical or screw thread pattern in the wheel rim. The thread pitch is equal to the movement of the diamond per revolution of the wheel and the thread shape is dependent on the diamond shape and infeed for a given traverse rate. When the wheel is used for a grinding operation these features appear on the work-

piece surface and consequently any factor which influences the shape dressed onto the wheel will influence the workpiece. Similar effects have been reported by other authors[18,26,30].

Diamond traverse rate has been thoroughly studied[14,17,18,24-30]. All the authors conclude that surface roughness increases as the traverse rate is increased. The effect can be explained by reference to Figure 3 which shows the influence of traverse rate on theoretical wheel profiles for given infeeds and diamond shapes.

Figure 3 also indicates the interdependence of traverse rate, infeed and diamond shape. If the relationship is such that the groove being produced in the wheel overlaps the groove produced during the previous revolution, infeed is theoretically not significant. For many practical conditions this relationship holds true and the author[17] found that in his experiments infeed was not significant over the range of values used. However, Pahlitzsch[29,30] found that at high values of traverse rate, when overlapping does not occur, the infeed is significant. In certain cases workpieces were found to have a roughness in excess of the diamond infeed. From Figure 3 it can be seen that this is theoretically impossible, but Pahlitzsch concludes that at very high traverse rates increased splitting and breaking of the brittle wheel material will cause a deviation from the theoretical wheel profile.

Wheel dressing must be continued until any dull grits have been fractured or dislodged and all the workpiece material in the wheel rim has been removed. Because of excessive wear on the diamond it is uneconomic to remove the necessary wheel material in one pass of

the diamond. Increasing the number of passes distorts the wheel profile and consequently increases the workpiece surface roughness[17,30]. Pahlitzsch[30] suggests that the dressing operation should be separated into three phases; remove the debris from the previous grinding operation, fine dress to produce a stable wheel rim and finally dress to give the required wheel performance.

References to the influence of wheel speed during dressing are confused. Pahlitzsch[30] observed an increase in workpiece roughness if the wheel speed was increased, but the author[17] found that the wheel speed was insignificant. The manufacturers of dressing diamonds recommend low dressing speeds to reduce diamond wear[25] and on high speed grinding machines the wheel speed is normally reduced during the dressing operation. However, a report published by the Machine Tool Industry Research Association[31] suggests that diamond wear rate is not affected by wheel speed.

A dressing diamond should not be set radially to the centre of the wheel[25,27,30], but should be inclined as shown in Figure 4. Inclination reduces the possibility of damage due to shock loading and helps to maintain a sharp point. The inclination also influences the diamond profile presented to the wheel and the author[17] has shown that this profile can be detected on the workpiece surface. A number of other authors[13,25,27-30] also confirm that diamond shape is important.

3.3 The Influence of Wheel Dressing on Wheel Wear

Pattinson and Chisholm[14] have made a comprehensive study of the

influence of dressing traverse rate on wheel wear. Initially radial wheel wear occurs rapidly and during this primary phase the wear rate is influenced by the dressing conditions. An increase in the traverse rate increases the wear rate. Eventually a secondary phase is reached during which the rate of wheel wear is significantly reduced and is virtually independent of the dressing process used. The density of active cutting edges was also observed using a microscope and suitable illumination. In all cases the number of cutting edges increases during the primary wear phase, but the rate of increase is less at higher traverse rates. In the secondary phase the number remains substantially constant and attricious wear occurs on the grits. For the coarsely dressed wheels the number of active cutting edges is always less than that for wheels which are finely dressed.

The authors[14] conclude that the passage of a diamond through a brittle, complex material such as a grinding wheel, will disturb the wheel material to a substantial depth below the points of contact with the dressing tool. The disturbance will be greater for coarsely dressed wheels. Consequently many of the active cutting edges on a coarsely dressed wheel will be unstable and will be lost, due to fracture or pull out, as soon as they contact the workpiece. The more stable grits produced by a finer dressing process will not be removed. The increased instability explains both the increased wear rate and the lower number of active cutting edges on a coarsely dressed wheel.

Lindsay[18] obtained similar wear curves, but he argues that the dressing diamond actually machines a profile onto the abrasive grits.

His model of attricious grit wear is reproduced in Figure 5. In the initial wear phase, region 1, wear occurs on the sharp edges of the freshly dressed grit until the wear, 'h' has reached the depth of the initial diamond penetration, '$Co/_2$'. Rapid wear occurs in this first region because the 'sharp threads' wear quickly. In region 2, the secondary wear phase, the diamond-dressed grooves have been removed and the main body of the grit wears at a slower rate.

Pahlitzsch and Appun[29] obtained workpiece profiles produced by a wheel dressed with a single pass of the dressing diamond. The profiles show the regular features attributable to diamond shape and traverse rate and as grinding continues the profiles become flatter. These results tend to confirm the arguments put forward by Lindsay[18].

The influence of the dressing diamond infeed on wheel wear has been investigated by Pacitti and Rubenstein[15]. In this paper four stages of wheel wear are identified.

Stage A : Which is characterized by high wheel wear rate and a reduction of grinding force with time. This is the primary wear phase identified by Pattinson[14]

Stage B : Which is characterized by a low rate of wheel wear and a slow increase in grinding force. This is the secondary, attricious wear phase.

Stage C : Which is characterized by an increase in wheel wear rate and a rapid increase in grinding force with time. This phase can be attributed to the generation of high

grit temperatures due to excessive worn areas on the grits.

Stage D : Which is characterized by a decrease in grinding force with time, while the wheel wear rate may be higher or lower than that of Stage C. This is caused either by grit fracture or by pull out, or a combination of both.

The authors[15] suggest that a grinding wheel reaches the end of its useful life at the onset of Stage C.

The infeed of the dressing diamond was found to have a marked effect on the amount of grinding which could be carried out before Stage C occurred. At low infeed values the grits are virtually flat before grinding commences and consequently Stage B is very short. As the severity of dressing increases the plateau area per grit prior to grinding is reduced and the length of Stage B increases. Conversely if the dressing process is too severe Stage D may occur immediately due to excessive instability in the wheel rim.

The above conclusions are in direct opposition to recommendations made by Fisher[27]. He suggests that infeeds should be very low for maximum wheel life because a low infeed gives a stable wheel rim. Pacitti and Rubenstein[15] used infeeds ranging from 0 - 0.0010 in. and recommended the higher values. Fisher suggests that infeeds of 0.0002 in. or less are beneficial. The probable reason for these differences is the diamond shape used by Pacitti and Rubenstein. In their tests the diamond had a 0.025 in. x 0.025 in. wear flat and was traversed across the wheel at 0.015 in. per wheel revolution. Such

conditions would always tend to produce a glazed wheel, but at high infeed values the wheel rim would be unstable. Consequently the grinding forces would dislodge or fracture some grits and produce at least some sharp cutting edges. Fisher recommends a sharp diamond and indeed makes the point that as the diamond wears traverse rate must be increased to achieve a similar wheel performance.

The discrepancy between the conclusions reached by different workers serves to emphasise the importance of considering the implications of Figure 3. Diamond traverse rate, infeed and shape are interelated and should not be considered in isolation from one another.

3.4 The Influence of Wheel Wear on Surface Finish

In some grinding operations the wheel is dressed at least once for each component produced and wheel wear due to grinding is virtually negligible. This is done either because the finish requires a rough dress and finish dress procedure, or as a means of controlling component size. However, for many operations the wheel is allowed to cut until the component proves to be unsatisfactory, for some reason such as surface finish. In these cases the influence of wheel wear is important.

Very few authors have studied the effects of wheel wear on surface finish and those that have published data reach different conclusions. Grisbrook[13] and McKee[32] found that surface finish deteriorates with grinding time, whereas Pahlitzsch and Appun[29] observed improvements as grinding continued. Kaczmarek and Kornberger[33]

found that grinding time had little effect on surface finish.

The different results obtained by these authors can probably be explained by the different wear processes occurring on the wheel surfaces during grinding. A grinding wheel can either wear due to attrition or to fracture. If attrition is predominant the surface finish will probably improve. Attrition is the type of wear occurring in the secondary wear phase discussed in section 2.2.3 and wear results given by Pahlitzsch[29] indicate that in his tests wheel wear was restricted to this phase. Consequently the improvements in surface finish are to be expected. The author[34] has studied wheel wear and surface finish for prolonged grinding times. During the primary and secondary wear phases surface finish improves, but in the tertiary wear phase, when rapid wear is occurring the surface finish deteriorates. In this tertiary phase fracture or dislodgement of grits is the dominant wear mechanism, creating new, sharp cutting edges. In addition vibration could be a problem in this stage of wheel wear due to excessive wheel lobing[35] and both of these effects would tend to cause a deterioration in surface finish. McKee[32] did not publish wear data, but if the grinding conditions were severe, vibration and grit pull out could cause the finish to deteriorate. Lindberg[35] obtained similar results for certain grinding conditions.

4. THE GENERATION OF THE WORKPIECE SURFACE

4.1 Introduction

In previous publications[17,28] the author has shown that a grinding wheel produces features on the workpiece surface which can be directly attributed to the wheel dressing process. The traverse rate and shape of the single-point dressing diamond are particularly important. Similar effects have been reported by other authors[18,26, 29,30, 36-38]

Lindsay[18] and Pahlitzsch[29] suggest that the diamond actually cuts through the abrasive grit to form what is effectively a form tool. The dimensions of this form are determined by the diamond traverse rate, shape and infeed. When the wheel is used for grinding the abrasive grits transfer their profile to the workpiece. A model suggested by Lindsay[18] is reproduced in Figure 5.

Bhateja[39] has recorded both wheel and workpiece profiles by stylus measurement. He concludes that although dressing features clearly appear on the workpiece, they cannot be detected on the wheel surface. He suggests that this is probably because any grooves produced in the grit by the dressing process would be very small compared to the total roughness of the wheel.

In a series of recent papers[9,10,40] Malkin et al have examined the debris produced when a grinding wheel is dressed. Wheels were dressed by passing the flat side of a pyramidal diamond across the wheel face at an infeed of 0.001 in. and a traverse rate of 0.0035 in.

per wheel revolution. A minimum of ten dressing passes was taken beyond what was required for truing the wheel.

The dressing particles produced in the last dressing pass were collected by placing a glass slide coated with petrolatum grease vertically opposite the forward face of the grinding wheel. The particles adhered to the grease and were later separated out by dissolving the grease in boiling trichlorethylene. The size distribution was determined with a series of sieves and an electric balance.

Figure 6 shows the size distributions of dressing particles obtained by Malkin[40] for wheels of various grit sizes and hardnesses. For comparison purposes the size distribution of the grits used to manufacture the wheels are included. It can be seen that the dressing particles are not very much smaller than the original abrasive grits.

These results throw considerable doubt on the 'grit machining' theory proposed by Lindsay[18] and implied by Pahlitzsch[29]. From the dressing conditions used by Malkin for an 80 grit wheel, the 'grit machining' theory would yield a maximum possible particle volume of 1.03×10^{-8} in.^{3}; the volume is calculated in Figure 7. On a weight basis such a particle is equivalent to a spherical grit of diameter 2.7×10^{-3} in., which is somewhat smaller than 200 grit size.

The size distribution for an 80 grit wheel in Figure 6 shows that the large majority of the dressing particles were larger than 200 grit

size. Consequently it would appear that the dressing diamond actually fractures grits to produce relatively large fragments or, possibly, dislodges them from the bond. The appearance of dressing features on the workpiece surface cannot be explained by the 'grit machining' theory and an alternative proposition is discussed below.

4.2 A Theory to Explain the Generation of the Workpiece Surface

In this theory it is assumed that when the dressing diamond passes through the brittle wheel material it causes fracture of the abrasive grits or dislodges them from the bond material. Consequently any one wheel profile in the dressing direction will not indicate regular features and will probably have a roughness considerably in excess of that appearing on the workpiece surface.

A wheel profile cannot penetrate inside the locus swept out by the diamond at any point, because material in this area will be removed by the diamond. However, a typical profile such as A-A in Figure 8 will probably contain some points which are coincident with the diamond locus. If the infeed during grinding is greater than the peak to valley height of the locus these coincident points will appear on the workpiece surface.

In all grinding operations the surface speed of the wheel is many times larger than the workpiece speed, a 100 : 1 ratio being commonly used. Consequently a number of wheel profiles A-A, B-B, C-C, etc., in Figure 8, will pass any one section of the workpiece. All of these profiles will potentially contribute to the ultimate

workpiece profile. If each wheel profile contains points which are coincident with the diamond locus the regular dressing features are gradually generated on the workpiece surface.

If this theory is correct only those points on the wheel profile which fall within the peak to valley height of the diamond locus will contribute to the final workpiece surface. The position of any one point on the surface will be determined by the highest point on the wheel which actually passes this point. If each wheel profile passing the workpiece is obtained these high points can be determined by combining the profiles and choosing the highest value at each point along the profiles. This profile envelope should, when inverted, be the same shape as the workpiece produced by the wheel.

A dressing and profiling test rig was developed for use on a standard surface grinding machine. The rig enabled precise dressing conditions to be obtained and was capable of recording wheel profiles with the required degree of accuracy. The data obtained was used to evaluate the theory. A general view of the equipment is given in Figure 9.

Wheel profiles were digitally recorded on punched paper tape. The wheel was indexed by a small amount between profiles. The recording of each profile was commenced at the same distance from the edge of the wheel. Hence a three dimensional network of the wheel face was built up as shown in Figure 10. The indexing interval between profiles determined the spacing along the wheel periphery; the interval between wheel height samples determined the spacing along the wheel axis and the actual reading recorded was a measure of the height of the sampled point relative to the other points on the wheel

surface.

A computer programme was written to develop the envelope of the wheel profiles. The procedure was to sample all points in column 1, Figure 10, to find the highest reading. Sampling was repeated for all columns, 2, 3, 4, etc., and the consequent series of highest points represented the profile envelope. This envelope was inverted and compared with a digitised version of the workpiece surface produced by the wheel.

4.3 Grinding Facilities

4.3.1 The grinding machine:

A standard Jones and Shipman 540 surface grinding machine was used as the basis of the test rig. The machine specification is given in Figure 11.

4.3.2 The grinding wheel:

An aluminium oxide grit wheel with a vitrified bond was used throughout. The wheel specification was 6A60 L8 V75, 7 in. diameter by $\frac{1}{2}$ in. wide, supplied by the Carborundum Company Ltd.

The wheel was carefully balanced before being used for grinding, using the static balancing system normally considered adequate for this wheel size. The wheel flanges were locked onto the wheel and then the wheel was mounted on the machine spindle and trued. The assembly was removed from the wheelhead and located on a balancing mandrel. A balancing unit, consisting of two suitably levelled

parallel knife edges was used to check the balance. A pair of balance weights, mounted in the flange, were adjusted until the assembled wheel and mandrel remained static in any position on the knife edges. Finally the mandrel was removed, the wheel assembly replaced on the machine spindle and the wheel dressed before use.

4.3.3 The grinding fluid:

The workpieces were ground dry, but for the dressing operations Solvac 68 grinding fluid was used at a dilution of 100 parts water to 1 part fluid. This is a non-petroleum fluid developed to overcome wheel gumming which can be a problem when using conventional cutting fluids. Dressing diamond manufacturers[25] recommend dressing wet to minimize the wear on the diamond.

4.4 Wheel Dressing System

4.4.1 The dressing diamonds:

Two single-point diamonds were used and they are illustrated in Figure 12. A standard commercial diamond was used to true the wheel and to stabilize the wheel rim. Precise dressing conditions were obtained with a special diamond tool supplied by the De Beers Industrial Diamond Division. This diamond was lapped to a pyramidal shape with an included angle of 150° and a flat face of the pyramid was presented to the wheel as shown in Figure 13. The diamond fixture was designed to give a setting angle of $7\frac{1}{2}^{\circ}$ (Figure 3) and the dressing tool was periodically rotated in the fixture to avoid excessive wear.

4.4.2 Diamond traversing system:

Many authors[8-11,12,18-24] have stressed the importance of diamond traverse rate in the dressing process. However, for the type of grinding machine used the standard procedure was to mount the dressing tool on the machine table and then traverse the table across the wheel surface using leadscrew operated by a handwheel. The wheel was attached to the end of the leadscrew which meshed with a nut fixed to the machine base. Consequently when the handwheel was rotated the machine table, the leadscrew and the handwheel moved parallel to the wheel axis on the cross slide. The handwheel was graduated in increments of 0.001 in., but could be operated through a fine feeding system to give graduations of 0.0001 in. The fine feed arrangement was also manually operated.

Manual operation was not considered satisfactory for controlled, and repeatable dressing conditions and consequently special equipment was required.

A motorised sub-table, mounted on the machine table, was considered. This sytem was rejected on the grounds that it would be difficult to ensure that the path traversed by the dressing diamond was parallel to the wheel axis in both the vertical and horizontal planes. An error in the vertical plane produces a truncated conical wheel whereas any horizontal misalignment gives a hyperbolic wheel. These effects are shown in Figure 14.

The alternative was to make use of the accuracy already built into the machine by providing a suitable drive system for the machine table and

it was decided to use this method.

An 0.25 H.P. fractional horsepower d.c. shunt wound motor was mounted on a bracket, which was in turn attached to the cross slide on which the machine table moved. The bracket was constructed in such a way that it replaced the hydraulic valve box cover and held the motor shaft in the vertical position. The motor shaft was connected to the input shaft on the fine feeding system with a simple chain drive, giving a constant gear ratio of 3.8 : 1.

Consequently when the motor drove the feed shaft the machine table was traversed across the wheel and the motor also moved with it. Mounting the motor in this way avoided the necessity for an extending drive shaft from the motor to the cross slide leadscrew. The system is illustrated in Figure 15.

The dressing motor speed was controlled by a standard rectifier unit, providing a static conversion from a.c. single phase supply to d.c. by means of silicon diodes. Speed control was effected by varying the armature voltage, the field voltage remaining constant. A switching circuit was incorporated to reverse the motor and hence allow cross-feed in both directions. The wiring diagram for the motor is given in Figure 16 and the available traversing speeds for the machine table are given in Figure 17.

4.4.3 Standardised dressing procedure:

The number of passes of the dressing diamond across the wheel has been found to influence the surface roughness produced by the wheel[17,30].

This effect is thought to be due to an increase in the instability of grits on the wheel as the number of passes is increased[17].

However, several diamond passes are necessary to remove the debris of the previous grinding operation from the wheel and consequently a standardised dressing procedure was adopted throughout these tests. The author has used a similar procedure in previous work[17] and obtained repeatable results.

1. Using the commercial diamond, dress to remove debris with a diamond traverse rate of 0.005 in. per wheel revolution and an infeed of 0.001 in. per pass.

2. With the same diamond, dress to stabalise the wheel rim and produce a smooth wheel surface. A diamond traverse rate of 0.005 in. per wheel revolution was used with six passes at an infeed of 0.0005 in., six at 0.0002 in. and finally four passes at zero infeed.

3. Using the special diamond dress the wheel with one pass at the required traverse rate and infeed.

4.5 Wheel Profiling System

4.5.1 Design considerations:

The stylus used to check the wheel profile had to be capable of following geometric features on the wheel of a similar magnitude to features appearing on the workpiece surface. At the same time it was essential

that the stylus did not distort the profile in passing over the wheel material. Consequently a diamond stylus was used, applied with a very light load and having the same dimensions as the stylus used for workpiece surface measurement.

The next problem was to ensure that the profiles checked were in precisely the same planes as the path of the dressing diamond. Any misalignment would cause errors of the type previously discussed in section 4.4.2. It was decided that the best approach was to mount the stylus on the machine table and move it across the wheel face using similar arrangements to those adopted for the dressing process.

It was anticipated that a large number of wheel profiles would be required before the 'profile envelope' approached the workpiece profile. Each individual profile had to commence in precisely the same position along the wheel axis, so that the envelope would correctly represent the series of wheel profiles presented to the workpiece. The problem was solved by using a triggering system to activate the recording facility when the stylus reached a specific point on the wheel.

In order to obtain the envelope of a large number of profiles a digital recording system was considered essential. The large volume of data required could not readily be manipulated in analogue form. The profiling stylus used gave an analogue voltage output and, after amplification, this was digitised using an A-D Convertor and recorded on punched paper tape.

In addition to ensuring that each profile commenced at the same point

it was essential that the sampling intervals along each profile were exactly the same. The A-D Convertor sampled the analogue output on a time base and consequently it was decided that the stylus traversing system should be similarly operated. A stepping motor drive was used and by deriving the impulses to the motor and the sampling frequency from the same time standard the sampling intervals were precisely controlled.

4.5.2 Profiling stylus:

The stylus shape used is illustrated in Figure 18. The dimensions of the stylus point are the same as those for the stylus used on the surface measuring instruments described in section 4.6. Consequently the stylus was capable of following all the relevant features on the wheel surface. The stylus shape was periodically checked to ensure that it had not worn significantly.

The stylus was mounted in a Talymin, Series 3, Side Acting Gauge Head supplied by Rank Taylor Hobson. The force required to operate the gauge was approximately $3\frac{1}{2}$ grams. To ensure that this force was not sufficient to damage the wheel a number of traces were taken across a wheel with the stylus in the recording position. Sections were cut from the wheel rim and examined using a scanning electron microscope. It was impossible to detect any wheel damage, either to the abrasive grit or to the bond.

In early profiling tests it was noted that the peak to valley heights recorded from the wheel profiles were many times greater than those measured on a workpiece produced by the wheel. A typical wheel trace

is compared with a workpiece profile in Figure 19. This height difference was expected, partly because any voids in the wheel surface would be recorded as low spots and partly because, in the theory discussed in section 4.2, the dressing diamond breaks up the wheel surface causing considerable roughness values.

In order to record the whole of the wheel profile it was necessary to use a very much lower magnification than that used to record the workpiece profile. The low magnification was considered undesirable due to the consequent loss of accuracy when comparing the wheel profile envelope with the workpiece. In section 4.2 it is argued that only those points in the wheel profile which fall within the peak to valley height of the diamond locus will contribute to the final workpiece roughness. Hence it was only necessary to record the upper portion of the wheel profiles to obtain sufficient data to test the theory.

Consequently a 'cut-off' system was used to prevent the stylus from penetrating a greater distance than was necessary below the upper levels on the wheel surface. The system used physically restrained the stylus from moving towards the centre of the wheel. The limit of stylus movement in this direction was adjustable by means of a micrometer drum. The system used is shown in Figure 20 and a comparison of full and 'cut-off' wheel profiles is given in Figure 21.

The stylus system is shown in position on the machine table in Figure 22.

4.5.3 Stylus traversing arrangements:

It was not possible to obtain a stepping motor with a speed range wide enough to provide machine table traverse speeds suitable for both dressing and profiling. The dressing traverse rates were considerably higher than those required for profiling and so it was necessary to provide separate motors.

The dressing motor bracket described in section 4.4.2 incorporated an arrangement for locating the stepping motor directly above the fine feed input shaft on the grinding machine table. The stepping motor specification is given in Figure 23 and the system is illustrated in Figure 15.

Both motors were driving the fine feed input shaft and information received from the stepping motor suppliers indicated that it was essential to disconnect this motor when operating at the higher speeds provided by the dressing motor. Consequently, for safety reasons, it was decided to use a common drive system for both motors with a motor selection arrangement for dressing or profiling. An electromagnetic friction clutch was provided to connect the stepping motor to the feed shaft and this clutch was automatically disconnected when the dressing motor was selected. The machine table drive system is shown in diagrammatic form in Figure 24.

The stepping motor drive was derived from a 100 kHz crystal controlled time standard and a block of frequency dividers. The dividers were arranged to give a number of frequency outputs in the forward, or profiling direction and a single, high speed output in the reverse

direction to return the stylus to the start position. The consequent profiling speeds are given in Figure 25.

Adjustable limit switches were provided to limit the movement of the machine table in both the forward and reverse directions when the stepping motor was being used. The switches effectively controlled the limits of stylus travel and the forward limit served to cut off both the motor drive and the recording facility. Coarse and fine datum systems were used to trigger the recording facility and these are described in section 4.5.5. The stepping motor drive system and the functions of the stylus traversing system are described in Figures 26 and 27 respectively.

4.5.4 Wheel indexing system:

It was necessary to index the wheel by a small amount between each wheel profile. Indexing was carried out by fixing an indexing bar to the wheel flange and mounting a micrometer on the fixed part of the wheelhead above this bar. The vertical movements of the micrometer were calculated to give an indexing interval of 0.002 in. on the wheel surface.

The system can be seen illustrated in Figure 22.

4.5.5 Profile recording facilities:

It was anticipated that a large number of wheel profiles would be required before a satisfactory profile envelope was obtained. Consequently it was decided to use an analogue output system for setting

purposes, etc., but to digitise the profile for recording purposes. The analogue recording was obtained from a standard amplifier and rectilinear recorder of the type normally supplied by Rank Taylor Hobson for use with the profiling stylus. The amplifier output was also fed to a Solartron Type LP942 Analogue-Digital Convertor and the digitised profile was recorded by a Tally, Model 420 Tape Perforator.

The recording facility was required to have two essential features. Firstly, each profile had to commence at the same position relative to the edge of the wheel and secondly the sampling intervals along each profile had to be precisely the same.

The first requirement was met by the use of coarse and fine datum detectors for the machine table position. The coarse system was a photo-cell arranged on one side of the machine table and capable of locating a particular rotation of the stepping motor. This gave an accuracy of $\pm$ 0.0025 in. The fine detector was another photo-cell activated by a single hole in a disc mounted beneath the clutch on the fine feed input shaft. This cell was not actuated until a positive signal was received from the coarse detector and consequently located a single step on the motor. Hence an overall accuracy of approximately $\pm$ 1×10^{-5} in. was obtained. Tape perforation was commenced when both coarse and fine position detectors gave positive signals.

To ensure that precise sampling intervals were obtained on all wheel profiles the sampling instruction was derived from the crystal controlled time standard used to drive the stepping motor. In its normal form the A-D Convertor had an internal 100 Hz signal from which the

sampling rate was derived. The internal facility was replaced by an external 100 Hz signal obtained from the frequency dividers, section 4.5.3, at an appropriate stage. Consequently the steps of the motor and the sampling signals were synchronised so that if the same sampling frequency was used for each profile the interval between samples was precisely the same.

The available sampling intervals are tabulated in Figure 28.

4.6 Workpiece Surface Measurement

4.6.1 Production of the workpiece profile:

In a previous publication[17] the author has described a method which can be used to obtain the workpiece profile produced by a grinding wheel, without incurring significant wear on the wheel surface. This method was used in these tests.

A thin hardened steel blade, with a hardness of approximately 680 VPN, was mounted in a special fixture held on the machine table. The wheel-head was lowered to give a wheel infeed of approximately 0.003 in. into the blade and the table traversed once only past the blade at its maximum speed. The advantages of the system are that because the blade is only 0.005 in. thick wear on the wheel is negligible and only a short length of the wheel periphery is used to form the workpiece.

The fixture is shown in position on the machine table in Figure 29.

4.6.2 Recording the workpiece profile:

The workpiece surface was recorded using a Talysurf 4 Surface Measuring Machine supplied by Rank Taylor Hobson. The hardened steel blade, still in its fixture, was removed from the grinding machine table and mounted on a co-ordinate table. This table was in turn mounted on another fixture which fitted into the tee slots in the base of the Talysurf 4. Consequently the blade was accurately aligned parallel to the stylus movement on the surface measuring machine. The co-ordinate table was used to locate the narrow blade beneath the stylus. A view of the blade and the stylus is shown in Figure 30.

An analogue recording of the workpiece profile was obtained using the standard amplifier and rectilinear recorder. For comparison with the digitised wheel profiles a digital version was derived with the Solartron Convertor and Tape Perforator used for recording the wheel profiles.

The recorded wheel profiles were only a part of the wheel width and consequently it was necessary to ensure that the recorded portion of the workpiece profile was equivalent to that part of the wheel. The position of the wheel profiling stylus relative to the edge of the wheel when recording commenced was measured on the grinding machine with a travelling microscope. The edge of the wheel could easily be detected on the surface measuring machine and so it was only necessary to commence recording the workpiece profile at the appropriate distance from the wheel edge. The procedure is illustrated in Figure 31. Any inaccuracy in the measurement of the distance from the

wheel edge to the stylus was allowed for in the comparison section of the computer programme.

4.7 Comparison of Wheel and Workpiece Profiles

A computer programme was written to develop the envelope of the wheel profiles. The envelope was then compared with the digitised workpiece profile to determine the errors and various other parameters such as mean error and standard deviation. The flow chart and the computer programme are given in Appendix I and the procedure is discussed below. The terms EVCO, RAXEVCO and RCR are defined in Appendix I and are simply a computer code.

4.7.1 Development of the EVCO matrix:

The term EVCO was used to describe an individual value on a wheel profile. For the tests reported here 200 wheel profiles were recorded and each profile was at least 150 samples in length. Consequently the EVCO matrix contained 30,000 readings. Each EVCO value was a three digit number between 000 and 999, where these figures represented the lower and upper limits on the analogue output from the profiling stylus.

Each wheel profile constituted a column in the EVCO matrix and to identify the beginning of a profile on the punched tape a negative sign was punched before the first reading. The data reader was required to look for a negative value and then to ignore it. The next value was taken as the first sample in a wheel profile and the first column in the EVCO matrix was generated to a maximum length of 150 readings. The data reader then looked for the next negative value, ignoring all

intervening values, and commencing the next column with the subsequent value to the negative one.

The process was continued until the whole of the EVCO matrix had been generated.

4.7.2 Generation of the RAXEVCO matrix:

Each row in the EVCO matrix represented a series of points on a line, along the wheel periphery, parallel to the edge of the wheel. The highest value in the row would determine the height of the work-piece at that particular distance from the wheel edge. The number of values in a row was 200, the total number of wheel profiles recorded.

A new matrix was commenced by forming a column from the highest values appearing in each row of the first 20 columns in the EVCO matrix. The second column in the new matrix was derived from the first 40 columns and so on in steps of 20 until the last column was formed from the highest values in the whole 200 columns of the EVCO matrix. During the generation of this matrix the original integer numbers were changed to real numbers.

Each column in this new matrix represented the profile envelope of the number of wheel profiles used to generate the column. The mean value of each column was then substracted from each individual value in the column to give a matrix in a zero standardised form. This matrix was termed the RAXEVCO matrix.

4.7.3 Generation of the RCR trace:

The RCR trace was a digitised version of the workpiece profile, manipulated in such a way that it could be directly compared with each column in the RAXEVCO matrix.

Initially the workpiece profile was recorded at a much higher magnification than the wheel profile. This was due to the very much greater roughness on the wheel profile. Hence the first step was to vertically scale the workpiece to give the same magnification as the wheel.

The sampling interval on the workpiece trace was 0.0002 in. and was fixed by the surface measuring machine being used. Figure 28 shows that the sampling intervals available on the wheel profiling system were different from this value and it was necessary to derive a modified workpiece profile with sampling intervals equivalent to those on the wheel. The modification was done by interpolation between the actual values obtained for the workpiece profile.

The mean value of the vertically scaled and interval adjusted trace was subtracted from individual values to give zero adjusting. Finally each value was multiplied by -1 to invert the profile. Inversion was necessary because peaks on the wheel generate valleys on the workpiece and vice versa. Consequently for direct comparison the workpiece profile must be inverted.

4.7.4 Comparison section:

For a correct comparison it was essential that the first figure used in the RCR trace was precisely the same distance from the edge of the wheel as the first row in the RAXEVCO matrix. In section 4.6.2 it was explained that the distance from the edge of the wheel to the recording point of the first row in the RAXEVCO matrix was measured with a travelling microscope. However it was difficult to determine the edge of the wheel precisely and the accuracy obtainable was no better than $\pm$ 0.002 in. The sampling intervals used on the wheel profiles were either 0.0005 in. or 0.00025 in. Consequently the stylus position was not measured with sufficient accuracy.

To overcome this problem a number of tests were carried out for each column in the RAXEVCO matrix. In the first test both the wheel profile envelope and the workpiece profile were assumed to be correctly lined up with respect to one another when the first number in each was used to start the profiles. In the next test the wheel profile envelope was used in the same way, but the workpiece was assumed to start with the second reading, the first being ignored. In subsequent tests the workpiece start position was stepped along one reading for each test. A total of 20 tests were carried out giving a movement of 0.005 in. for sampling intervals of 0.00025 in. and 0.010 in. for intervals of 0.0005 in.

Hence by examination of each comparison to find the best one, the correct lining up of the wheel and workpiece profiles was achieved.

Each column in the RAXEVCO matrix was in turn compared with the RCR

trace, taking 20 tests for each column. The following data was calculated for each test.

1. The individual errors between points in the RAXEVCO column and the RCR trace.

2. The maximum error in the comparison.

3. The minimum error in the comparison.

4. The range of the errors in the comparison.

5. The total error in the comparison.

6. The mean error in the comparison.

7. The error variance in the comparison.

8. The error standard deviation in the comparison.

4.8 Results and Discussion

The purpose of these tests was to establish whether or not the surface generation theory proposed in section 4.2 is correct. The important factors in this theory can be summarised as follows:

1. When the dressing diamond passes through the brittle wheel material it does not machine a profile onto the grits. Grits and bond are fractured and some grits are dislodged from

the bond so that an individual wheel profile will be irregular and probably have a high roughness value.

2. However, each wheel profile will contain some points which are coincident with the locus swept out by the dressing diamond.

3. When the wheel is used for grinding these coincident points will appear on the workpiece profile and, because a large number of wheel profiles pass any one section of the workpiece the number of coincident points will increase with the number of profiles. Consequently the workpiece surface will have regular features which can be attributed to the dressing process.

The test conditions used for two complete tests are tabulated in Figure 32. One test is on a coarsely dressed wheel and the other on a finely dressed wheel. The results obtained indicate that the theory is correct.

4.8.1 Wheel profiles:

A series of wheel profiles is shown in Figure 33. These profiles were taken in random positions across the wheel surface and at different places around the wheel periphery. The wheel sampled produced the workpiece surface profile illustrated in Figure 19. A number of important conclusions can be drawn from these profiles.

The first point is that they do not show regular features of the

type appearing on the workpiece. The peaks are the abrasive grits whereas the deep valleys are probably caused by voids between the grits on the wheel surface. These results agree with the conclusion reached by Bhateja[39].

Secondly the profile roughness is very much greater than that appearing on the workpiece. If, as proposed by Lindsay[18], the dressing diamond machines a profile into the abrasive grit, the high points on the wheel profile would be relatively flat, with a consistent undulation due to the dressing parameters. There is no evidence that these flat areas are present on the grits and hence it can be concluded that grits are fractured or dislodged, confirming the results obtained by Malkin[40].

Finally the similar level of the highest points is important. The similarity applies not only to an individual profile, but also to profiles taken at different places on the wheel surface. Because the wheel material is splintering on impact with the dressing diamond these consistent heights can only be explained by assuming that at some points on the wheel surface fracture occurs in such a way that a point on the grit is coincident with the diamond locus. These coincident points must be at the highest levels on the wheel surface and if several coincident points appear on an individual profile they will be contained within the peak to valley height of the locus.

Consequently the wheel profiles shown in Figure 33 confirm the first two factors in the surface generation theory.

4.8.2 The effect of increasing the number of wheel profiles used to generate a profile envelope:

Figure 34 shows a part of the RAXEVCO matrix obtained for a coarsely dressed wheel before the values were zero standardised. The RAXEVCO matrix is discussed in section 4.7.2. A similar matrix for the finely dressed wheel is given in Figure 35. The number of columns in the EVCO matrix used to generate each column in the RAXEVCO matrix is equivalent to the number of wheel profiles considered.

It can be seen that for both wheels, as the number of profiles increases the values in the columns become more consistent. Effectively this means that the roughness of the wheel profile envelope is being reduced and is caused by the high points on wheel profiles gradually filling in the gaps left by preceding profiles.

In the surface generation theory it is argued that as the number of wheel profiles is increased there will be a tendency for the number of points on the workpiece which are coincident with the diamond locus to increase. The results confirm this tendency.

4.8.3 Comparison of wheel profile envelopes and workpiece profiles:

Figures 36 and 37 show typical wheel profiles and the workpiece profiles produced by the coarse and finely dressed wheels used in the tests.

The two wheels produce very different workpiece surfaces. The

coarsely dressed wheel gives a workpiece with a peak to valley height of 0.00020 in. whereas the workpiece produced after fine dressing has a peak to valley height of only 0.00012 in. In both cases a regular frequency wave appears on the workpiece. The frequency is equivalent to the traverse rate of the dressing diamond per revolution of the grinding wheel. These results are consistent with previous tests reported by the author[17].

However, the recorded wheel profiles do not indicate any significant differences between the two wheels. The roughness is similar in both cases and is very much greater than that of the workpieces. There are no regular features which can be attributed to the dressing process.

In Figures 38 and 39 the mean error obtained is presented for each comparison made between a profile envelope and the workpiece profile. Each row represents a comparison made by starting the workpiece profile from a different point. The reasons for doing this are discussed in section 4.7.4.

It can be seen that as the number of profiles used to generate the profile envelope is increased the mean error is reduced. The reduction occurs because more points coincident with the diamond locus are able to contribute to the profile envelope and consequently the envelope approaches the workpiece profile.

The reduction in mean error for the starting position giving the lowest mean error values is presented graphically in Figures 40 and 41. When relatively low numbers of profiles are being used the rate of

reduction in the mean error is rapid because there will still be many gaps left between high points on the profiles. Consequently there is a high probability that subsequent profiles will fill in at least some of these gaps, giving an improved fit. However, as the number of profiles is increased the number and size of the gaps become less and improvement will be more gradual.

A selection of the mean errors from Figures 38 and 39 are presented graphically in Figures 42 and 43. The purpose of these graphs is to show the way in which the mean error changes as the start position along the workpiece profile is varied.

For the coarse wheel in Figure 42 the lowest values of mean error are obtained at start positions 4 and 18. The gap between these positions is 14 sampling intervals on the profile and, at a sampling interval of 0.0005 in. the gap is 0.007 in. The gap corresponds to the traverse rate of the dressing diamond per revolution of the wheel. Similarly for the finely dressed wheel, the gap between the lowest mean error positions corresponds with the diamond traverse rate.

The above results clearly show that there is a strong periodic element in the wheel profile envelope and that the frequency is equivalent to that appearing on the workpiece. At position 4 in Figure 42 the profile envelope is in phase with the workpiece profile, giving a low mean error. The in-phase situation occurs again at position 18. At position 11, midway between these two positions, the profiles should be 180° out of phase giving maximum error. The graphs show that this is the case and emphasise the importance of precisely lining up the start positions of the wheel and

workpiece profiles before making comparisons. In addition, it is also clear that although individual wheel profiles do not have regular features the profile envelopes quickly develop a regular pattern determined by the dressing conditions.

In Figure 44 the profile envelope which gives the lowest mean error for the coarsely dressed wheel is compared with the corresponding workpiece profile. There is extremely good agreement between the two. The peak to valley height of the profile envelope is approximately 0.0004 in., compared with 0.0085 in. for the wheel profiles shown in Figure 36. This is a reduction of 95% and confirms the theory that the gaps left by individual wheel profiles are gradually filled in by subsequent profiles.

A similar profile comparison for the finely dressed wheel is shown in Figure 45. Apparently the agreement is not so good. but the scale used in this figure tends to emphasise the errors when compared with the coarsely dressed wheel in Figure 44. In this case the peak to valley height of the profile envelope is approximately 0.00016 in., a reduction of more than 98% compared with individual wheel profiles.

4.8.4 Reason for the differences between the profile envelopes and the workpiece profiles:

In Figure 46 all the parameters calculated in the comparison of the two sets of profiles in Figures 44 and 45 are tabulated. Where appropriate they are expressed as a percentage of the peak to valley height on the workpiece profile.

According to the generation theory the wheel profile envelope should be exactly the same as the workpiece profile. However, for the coarse wheel the mean error is 80×10^{-6} in. which is approximately 20% of the peak to valley height on the workpiece profile. The corresponding figures for the finely dressed wheels are 60×10^{-6} in. and 37% respectively.

These errors can be explained by considering the differences between the presentation of wheel profiles to the workpiece and the sampling technique used in these tests.

A given section of the workpiece is potentially influenced by each wheel profile which passes that section. However, in these tests only a sample of these profiles was recorded. A total of 200 profiles were obtained for each wheel, each profile being separated by a distance of 0.002 in. Hence a peripheral length of 0.4 in. was sampled. Figures 40 and 41 show that the mean error would not have been significantly reduced by taking further profiles at the same intervals around the periphery.

The errors probably result from all the profiles which were not recorded by indexing the wheel through a distance of 0.002 in. between profiles. The grits in the wheels were approximately 0.010 in. diameter and so several profiles were recorded over one grit. However, the grits are being fractured and will have sharp points, so it could still be possible to miss the highest point on a grit. This is shown in Figure 47. The highest point will determine the height of the workpiece profile whereas the profile envelope will give a different point for the workpiece. Inevitably some of the

highest points on grits will be recorded and consequently the sampling technique will give peak to valley heights on the wheel profile envelope which are greater than those appearing on the workpiece.

The only solution to this problem is to take wheel profiles at a much closer spacing, say 0.0005 in. In these tests some 30,000 height values were recorded for each wheel surface and the closer spacing would quadruple this figure. Such a large quantity of data would be extremely difficult to handle.

Even though there are these discrepancies between the profile envelopes and the workpieces, the comparability is extremely good, especially when the shape of individual wheel profiles is considered. The similarities are much more marked than are the errors and consequently it can be concluded that the theory proposed to explain the generation of the workpiece surface is confirmed.

In a paper concerned with the characterization of abrasive wheel profiles Baul, Graham and Scott[41] scanned wheel profiles with a fibre optic transducer. During the scan the wheel was rotated and the transducer was traversed slowly across the wheel surface. The output from the transducer was analysed into frequency mode and it was possible to record frequencies against density of occurrence for both new and worn wheels. The results indicated that peak frequencies occurred at a value corresponding to the traverse rate of the dressing diamond.

In the same paper, wheel profiles were recorded using a stylus trans-

ducer similar to the one used in this work. The authors attempted to correlate the profile obtained from the stylus with the results from the fibre optic transducer. It was not possible to obtain a successful correlation.

The results obtained from this work explain this lack of correlation. Individual wheel profiles cannot be related to the workpiece profile. It is only when a large number of profiles are arranged to give a profile envelope that similarities begin to appear.

5. THE INFLUENCE OF WHEEL DRESSING ON THE WORKPIECE SURFACE GENERATED

In the previous chapter it was shown that regular features appear on the workpiece surface which can be attributed to the parameters used in the dressing process. The purpose of the tests reported in this chapter is to study the relationship between theoretical and actual workpiece profiles and to determine the influence of the speed ratio between the grinding wheel surface and the workpiece.

5.1 Equipment and Test Procedure

The wheel dressing system and the standardised dressing procedure have already been described in section 4.4. These facilities enabled precise control of the dressing parameters to be maintained.

Sample workpieces were produced using the system described in section 4.6.1 and profiles were recorded using the Talysurf Surface Measuring Machine.

5.2 Comparison of Theoretical and Actual Workpiece Profiles

5.2.1 Effective dressing diamond shape:

A four sided pyramidal diamond with a sharp point and an included angle of 150° was used throughout. However, the diamond setting angle, shown in Figure 4, changes the effective angle presented to the wheel. The calculation presented in Figure 48 shows that this angle was $163^{\circ}34^{1}$.

5.2.2 Results and discussion:

Because the workpiece surface is generated by a series of points on the wheel surface which are coincident with the locus of the dressing diamond, the workpiece profile should theoretically be the same shape as this locus. The theoretical profiles for a diamond angle of $163^{o}34^{1}$ and diamond traverse rates of 0.007 in. and 0.002 in. per wheel revolution are presented in Figure 49. In Figures 50 and 51 these theoretical profiles are compared with the actual workpieces produced by wheels dressed using the above conditions.

The two sets of profiles compare very favourably. The influence of diamond traverse rate and shape can be very clearly seen on the workpieces.

It is noticeable that the workpiece peaks are more precisely and consistently formed than are the valleys. The workpiece peaks are produced by the valleys on the wheels, which are in turn formed by the point of the diamond. At these points the diamond only impacts the wheel material once. However, the valleys on the workpiece are produced by peaks on the wheel surface. These peaks are generated by the junction of adjacent grooves formed by the helical path of the diamond relative to the wheel. It is probable that the theoretically sharp points formed at these junctions are relatively unstable because the diamond has impacted the wheel on two occasions in forming the points. Consequently wheel material will break away in the grinding operation and produce flat valleys on the workpiece

The peak to valley height produced by the coarsely dressed wheel is approximately 0.000420 in. compared with a theoretical value of 0.000506 in. The corresponding values for the finely dressed wheel are 0.000120 in. and 0.000145 in. These discrepancies are due to the instability on the wheel peaks which is discussed above.

The results confirm that immediately after wheel dressing the workpiece profile is very closely related to the locus of the dressing diamond, emphasising the importance of the wheel dressing operation.

5.3 The Speed Ratio between the Wheel Surface and the Workpiece:

The path of the dressing diamond relative to the wheel surface is a helix. The pitch of the helix is equal to the diamond traverse rate per revolution of the grinding wheel. When this helically formed wheel grinds the workpiece the helix will influence the workpiece roughness. The roughness will be reduced as the proportion of the periphery passing any one section of the workpiece is increased. The effect is illustrated in Figure 52.

In theory, if the speed ratio between the wheel surface and the workpiece is such that one complete revolution of the wheel passes any section of the workpiece, the roughness at that section will be zero. However, in practice the helical profile dressed onto the wheel surface is not the only factor which influences the workpiece surface roughness. Each individual cutting edge on the grits potentially contributes to the roughness, depending on its shape and penetration into the wheel. Consequently the workpiece will never

have zero roughness.

Nevertheless the helix should have some effect and a series of tests were carried out using the coarse and finely dressed wheels described in the previous section. The speed ratio was varied by changing the table speed at which the workpiece profile was cut into the hardened steel blade.

Workpiece profiles produced at various speed ratios are shown in Figures 53 and 54 and the measured surface roughness values are tabulated in Figure 55.

Figure 52 shows that the theoretical influence of the helix is to reduce the peak to valley height on the workpiece and to produce a profile with sharp peaks and very much flatter valleys. The reduction in peak to valley height can be clearly seen in Figures 53 and 54 and is confirmed by the considerable reduction in surface roughnesses achieved at the high value of speed ratio. The sharp peaks and flattened valleys can be seen on the profiles produced by the coarsely dressed wheel. However, the effect is not clear for the finely dressed wheel, possibly because the peaks and valleys are too close together on the recording.

From a large series of statistically designed experiments Farmer et al[22] concluded that the table speed in surface grinding was the most significant parameter affecting surface finish. It should be low for a good finish. Farmer also concluded that wheel dressing was only one third as significant as table speed.

In the tests reported by Farmer et al[22] single point diamond wheel dressing was used. Consequently table speed would be important because of the helical nature of the wheel surface profile. However, the primary factor is the wheel dressing process rather than table speed itself. Therefore it would perhaps be more appropriate to conclude that the speed ratio between the wheel surface and the workpiece is the most significant parameter and that this is due to the nature of the wheel dressing process.

6. THE INFLUENCE OF WHEEL WEAR ON THE WORKPIECE SURFACE GENERATED

The conflicting data published by various authors[13,17,28,29,31] on the influence of wheel wear on surface finish has already been discussed in section 3.4. To this must be added the different conclusions reached by Pattinson[14] and Pacitti[15] on the influence of the dressing process on wheel wear rate. Pattinson reported that although the radial wheel wear in the primary wear phase shown in Figure 2a increases substantially as the wheel is dressed more coarsely, wear rate in the secondary phase is not greatly affected by the dressing process. The Lindsay model of wheel wear shown in Figure 5 supports this conclusion, but it has already been shown in Chapter 4 that Lindsay was incorrect in his assumptions. Pacitti found that wear rate in the secondary phase is strongly dependent on the dressing process.

In this research programme a series of grinding tests were carried out to try to clarify these conflicting reports. The first objective was to obtain data on the development of wheel wear with time. Secondly a study was made of the influence of wheel dressing on wheel wear and finally workpiece surface finish was examined at various stages in the wear process.

6.1 Experimental Equipment

6.1.1 Grinding facilities:

The Jones and Shipman surface grinding machine described in section

4.3.1 was used for these tests.

It can be seen from the machine specification in Figure 11 that the machine has a fixed spindle speed of 2800 revolutions per minute. At this rotational speed the wheel surface speed is approximately 5000 feet per minute, which is conventional for surface grinding. However, in recent years higher speeds, up to 12000 feet per minute, have been proposed and are in limited use in this country. It has been shown[42-45] that by using high grinding speeds it is possible to achieve a reduction in the grinding forces, an improvement in the surface finish and a significant reduction in wheel wear. Consequently these tests would be more complete if they included a variation in wheel speed.

However, the grinding machine available was not suitable for conversion to high speeds at an economical price. Conversion would require a complete modification to the drive arrangements, including a new motor and speed control system. In addition the wheel spindle and bearings would have to be changed and a more sophisticated wheel guarding system would be required.

It was decided to proceed with wheel wear testing at the conventional speed and a note on future work is included in section 9.4.

The grinding wheels were aluminium oxide in a vitrified bond. The wheel size was 7 in. diameter and ½ in. wide and the following specifications were used

1. 6A 60 G8 V75
2. 6A 60 I8 V75
3. 6A 60 L8 V75

Plunge cut surface grinding was used throughout, the workpiece traversing backwards and forwards beneath the wheel with no cross-feed. Infeed was applied at each end of the stroke, values of 0.0001 in. and 0.0005 in. being used.

6.1.2 Wheel dressing:

The dressing system has been discussed in section 4.4. The same equipment and procedure was used for these tests. Coarse dressing was achieved with a diamond traverse rate of 0.007 in. per wheel revolution and an infeed of 0.001 in. For fine dressing the traverse rate was reduced to 0.002 in.

6.1.3 Wheel wear measurement:

The determination of radial wheel wear by a direct measurement of the wheel radius is very difficult. The observed change in radius is very small relative to the radius itself. To overcome this problem wheel wear was measured using a method suggested by Grisbrook[13] and successfully used by the author in previous work[17].

The workpiece used was narrower than the width of the wheel and consequently, after grinding, a wear band was produced in the wheel rim. The wear band is illustrated in Figure 56. The wheel at either side of this wear band was not in use and consequently

retained the original wheel surface.

The profile of the worn wheel was produced in the hardened steel blade discussed in section 4.6.1. An amplified blade profile was obtained on the Talysurf and radial wheel wear was measured directly from this trace using the original wheel surface as datum. Using this technique wheel wear could be measured to $\pm$ .00001 in.

6.1.4 Workpieces:

The workpiece material was EN24, a 1½% Ni-Cr-Mo tool steel. Each workpiece was oil quenched and tempered to give a hardness of 550 VPN. The ground surface was 4 in. long and 0.25 in. wide. The material was supplied by the British Iron and Steel Research Association who also provided the chemical composition given in Figure 57.

The workpiece was mounted in a suitable fixture held on the magnetic table of the grinding machine. The set up is shown in Figure 58.

The table was allowed to traverse a distance of 10 in., giving an over run of 3 in. at each end of the stroke. The over run allowed the wheel to accelerate up to its unloaded speed before a new cut was commenced.

6.2 Results and Discussion

The results of the wear tests are presented graphically through

Figures 59-61. Consistent results were obtained for the influence of wheel dressing and grinding infeed, but the results obtained for different wheel hardnesses are very confused.

In section 2.1.2 it was explained that as the wheel hardness is increased it is more difficult to dislodge or fracture grits, because they are held more tenaciously by the wheel bond. Consequently wheel wear should be reduced if the wheel hardness is increased and other grinding conditions are retained constant. A comparison of Figures 59 and 61 shows that the soft, 'G' grade wheel wore more quickly than the hard, 'L' grade wheel. However, the intermediate 'I' grade shown in Figure 60 wore very quickly when used with the high grinding infeed of 0.0005 in. Repeated testing did not give significantly different results.

The above result is probably due to the problem of designated wheel grade discussed in section 2.1.2. Peklenik[2] found that in many cases a nominally hard wheel was in fact softer than other wheels with nominally softer gradings. Equipment to measure wheel hardness was not available for these tests, but it is possible that the 'I' grade wheel was in fact softer than the 'G' grade.

6.2.1 Wheel wear:

All the test results indicate primary and secondary phases in the wear process. In the first phase wear occurs rapidly and is probably due to the fracture or dislodgement of grits weakened by the dressing process. The amount of wear in this phase increases as the diamond traverse rate is increased because the wheel rim will be less stable

at the higher rates. The infeed during grinding is also significant in this primary region, because an increase in the infeed increases the force acting on each grit. Consequently for a given amount of instability in the wheel rim more grits will be dislodged or fractured with the increase in the force.

When the secondary wear phase is reached the wheel has become more stable and wears at a slower, more consistent rate. However, the rate of wear is still influenced by the dressing process and the grinding conditions. An increase in either the traverse rate of the dressing diamond or the grinding infeed gives a higher wear rate. This is most clearly seen in Figure 60.

These results for dressing are similar to data published by Pattinson[14] except that they show a somewhat greater influence of the dressing process in the secondary wear phase. In this respect they confirm a conclusion reached by Pacitti[15]. However, Figure 62a shows the wear curves obtained by Pacitti and it can be seen that the rate of wheel wear in the secondary phase decreases as the severity of dressing is increased.

The important difference between the results reported here and those obtained by Pacitti can be explained by considering the different dressing diamond shapes used in the two test programmes.

Pacitti used a pyramidal diamond with a flat wear band measuring 0.025 in. square. The diamond traverse rate was 0.015 in. per revolution of the wheel. These conditions would theoretically produce a flat workpiece when analysed in a similar way to Figure 49.

Due to the fact that the diamond tends to break up the wheel material the workpiece would never be entirely flat. However, the wheel rim would certainly be stable and may be equivalent to the glazed wheel discussed in section 2.2.1. A glazed wheel surface would give very high grinding forces, confirmed in Figure 62b, leading to severe bond failure and grit pull out. Consequently the wheel would wear very quickly.

An increase in the infeed of the dressing diamond would cause more breaking up of the material on the rim of the wheel and a consequent increase in the instability of the grits. Hence some of the grits would fracture giving a reduction in the grinding forces and less bond failure. The overall effect would be a reduction in the wheel wear rate.

However, this process cannot be continued indefinitely because ultimately the increased instability in the wheel rim will more than offset the grit pull out due to the glazed wheel. In Figure 62a it can be seen that the improvement in wear rate occurs at a decreasing rate. Consequently a diamond infeed greater than 0.001 in., the highest used in the tests, may well cause an increase in the wheel wear rate.

In the tests reported here the dressing diamond had a sharp point. This type of diamond could only produce a very stable wheel rim if it was repeatedly traversed across the wheel with a very low infeed. With only one pass of the diamond, at an infeed of 0.001 in., all the tests were conducted with a relatively unstable wheel rim and any increase in the instability would increase the wheel wear rate.

At high grinding infeeds the total wear obtained is also high. However, the results must be considered in relation to the material removed from the workpiece. A total of 100 passes at an infeed of 0.0005 in. is equivalent to 500 passes at the lower infeed of 0.0001 in. On this basis an analysis of Figures 59-61 shows that after the same amount of metal removal the radial wheel wear is less for a high infeed than it is for a low infeed.

The reduction in wear at this point is due to the fact that for the total radial wear measured in these tests a large proportion of the wear occurs in the primary phase, where wheel wear is occurring rapidly. After 100 passes the wheel has only just left the primary phase. At the high infeed 100 passes constitutes a total depth of cut of 0.050 in. which, for many precision grinding operations, will represent several components. Consequently all of these components will be ground during the primary stages of wheel wear. When grinding a similar number of components at a low infeed rate the wheel will operate in its secondary wear phase for most of the grinding time.

6.2.2 Surface finish:

For each stage in the wheel wear process the surface profile of the steel blade was recorded. A selection of the results is shown through Figures 63-66. Because only a part of the wheel width was used for grinding it is possible to compare the original surface produced by the wheel with the surface obtained after grinding.

Figures 63 and 64 represent two finely dressed wheels used at different

grinding infeeds. It can be seen that at the low infeed the peak to valley height produced on the workpiece after grinding is substantially the same as that originally produced. However, when the infeed is increased there is a marked increase in the peak to valley height, particularly during the latter stages of grinding. In addition, at the high infeed, the surface profile is much more irregular.

These results can be explained by reference to the pattern of wheel wear. In the primary stage the wheel wears quickly, indicating that grit fracture and grit pull out are the dominant wear mechanisms. However, in the secondary wear phase the rate of wheel wear is much slower, showing that a combination of attricious and fracture wear is occurring. For the low infeed values used in these tests this combination is such that surface finish remains substantially constant. Pahlitzsch[29] obtained similar results with finely dressed wheels.

When the infeed is increased there is an increase in the grinding forces. This tends to cause more wear due to fracture and pull out and consequently a deterioration in the surface finish. The surface profile will indicate more irregularity due to the grit pull out.

The logical extension of this explanation is that if attricious wear is dominant the surface finish should improve. None of the wheels used in these tests gave this type of wear, but the author has shown in previous tests[17,28] that at very low grinding infeeds the surface finish will improve with grinding time. Infeeds of this type

will give low grinding forces and consequently attricious wear.

Very similar conclusions can be drawn from the profiles of the coarsely dressed wheels presented in Figures 65 and 66.

The results confirm a conclusion reached in section 3.4 from a study of previous work on wheel wear. The influence of grinding time on workpiece surface finish depends on the nature of the wear process occurring on the wheel surface. If the principal wear mechanism is grit fracture or pull out the finish will deteriorate. If attrition predominates the finish will improve. A combination of the two tends to maintain a constant value of surface roughness. The wear mechanism can be influenced by the dressing process and the grinding conditions used.

6.2.3 Retention of dressing parameters on the workpiece surface:

It is noticeable in Figures 63-66 that even when the wheel has sustained considerable radial wear the workpiece profiles still contain features which can be attributed to the dressing process. The effect is more clearly shown in Figures 67 and 68, where a selection of the previous traces are amplified horizontally.

In the primary wear phase, i.e. less than 100 passes, the radial wheel wear is greater than the original peak to valley height on the workpiece surface. However, the influence of the dressing process is still clearly visible. The stable valleys on the wheel, forming the peaks on the workpiece, remain sharply formed. The less stable wheel peaks wear to give flat valleys on the workpiece.

The reason for the different stability on wheel peaks and valleys is discussed in section 5.2.2.

As grinding is continued into the secondary wear phase the workpiece profile becomes more distorted. However, the dressing parameters can still be detected.

The retention of the dressing parameters can be explained by reference to the theory of surface generation discussed in Chapter 4. An individual groove on the workpiece surface which is caused by the dressing parameters is in fact produced by a large number of grits. Each grit makes a contribution until the profile is formed. During the grinding process these grits will wear and if they all wear by attrition a similar form will still be produced on the workpiece.

Grits in the valleys on the wheel surface are relatively stable and will tend to wear by attrition. Consequently the peaks formed on the workpiece will remain sharp. However, the wheel surface peaks will be more susceptible to grit fracture or pull out and so the workpiece valleys will become more distorted as grinding continues.

Due to the variation in bond distribution and strength at different parts of the wheel surface grit pull out will probably occur in a number of places. At these points wheel wear will be greatest and the dressing parameters will not appear on the workpiece surface. The effects of grit pull out can be seen at various parts of the workpiece profiles shown in Figures 67 and 68.

In a paper by Nomura and Tsuzino[46] workpiece surfaces were presented in frequency mode, plotting frequencies detected on the surface against their density of occurrence. For a freshly dressed wheel the frequency due to the dressing traverse rate was dominant. As grinding continued this frequency became less significant and many other, less well defined values were detected. The change was attributed to grit pull out.

Baul et al[41] scanned wheel surfaces with a fibre optic tranducer. During the scan the wheel surface rotated and the tranducer was moved slowly across the wheel. It was found that frequencies corresponding to the dressing diamond traverse rate could be detected, both before and after the wheel was worn. The authors concluded that the history of the wheel is not easily eliminated.

It is clear from these references and the results of this work that the dressing process has an important influence on the surface finish produced throughout the useful life of a grinding wheel. The only way to eliminate the effects of dressing is by grit pull out on a very severe scale, leading to high wheel wear and a loss of wheel geometry. For some rough grinding operations this may be satisfactory, but if reasonable precision is required the acceptable level of wheel wear is likely to retain dressing features on the workpiece surface.

7. WHEEL WEAR IN CROSSFEED SURFACE GRINDING

7.1 Introduction

The development of radial wheel wear with grinding time has been discussed in section 2.2.3 and is illustrated in Figure 2a. A similar type of wear has been shown to apply to plunge cut cylindrical grinding and to traverse cylindrical grinding[8,12-14]. The results obtained in this work are presented through Figures 59-61 and they confirm this wear process.

In crossfeed surface grinding the workpiece is wider than the wheel width and is ground by indexing the wheel, or the workpiece across, at the end of each longditudinal traverse. The indexing movement is termed crossfeed and the crossfeed increment is usually less than the wheel width. Eventually the wheel will have been indexed across the whole width of the workpiece.

For this grinding process a different type of wheel wear has been reported by Purcell[47] and further discussed by Banerjee and Hillier[48,49]. The reported wear mechanism is illustrated in Figure 69 and wear is proposed to occur in two phases.

Phase I is a short period during which an angle is formed on the leading edge of the wheel. The angle is usually formed after the first longditudinal pass of the wheel over the workpiece and, as further increments of crossfeed are applied the angle becomes less steep until, after a short time, it becomes almost constant. It is then termed the approach angle.

Phase II is characterized by a constant approach angle which slowly recedes across the wheel face, towards the trailing edge, as grinding continues. The size of the approach angle is such that the wear band formed presents the number of grits to the workpiece surface which ensures that each grit has a task within its limitations. The wheel continues to grind until the approach angle has receded to a position close to the trailing edge, the grits failing in layers and being pulled out of the bond. When the angle has almost reached the trailing edge the wheel will fail completely due to lack of grit support.

However, in previous tests carried out by the author[17,28] wheel profiles produced in crossfeed surface grinding have indicated a stepped shape. Wear has occurred simultaneously across the whole of the wheel face. These results conflict with the wear theory suggested by Purcell[47].

In this chapter an alternative wear mechanism is proposed for crossfeed surface grinding[50]. The mechanism is shown to be consistent with the type of wheel wear occurring in other grinding processes. Test results are presented to confirm the wear patterns which can be theoretically predicted.

7.2 The Wear Mechanism in Crossfeed Surface Grinding

Figure 70 shows the conditions which are assumed to apply when crossfeed surface grinding. In this case increments of crossfeed are applied in only one direction and, for diagrammatic purposes, the wheel width is assumed to be four times the crossfeed increment per

longditudinal traverse. The wheel is considered as four separate sections, section 1 being termed the leading section and section 4 the trailing section. Each section is of width equal to the cross-feed increment 'f'. The wheel infeed is 'd' and the effects of spindle deflection are not considered.

1st longditudinal traverse:

Section 1

Potential infeed = d

However the wheel is assumed to wear radially by $\Delta_{1\cdot1}$ where $\Delta_{1\cdot1} << d$. A further crossfeed increment is now applied and the second traverse commenced.

2nd longditudinal traverse:

Section 1

Potential infeed = $d - \Delta_{1\cdot1}$

However, the wheel will again sustain radial wear and, if it is assumed that wheel wear is related to infeed, the wear occurring will be $\delta_{1\cdot2}$ where $\delta_{1\cdot2} < \Delta_{1\cdot1}$. Then

Cumulative wheel wear = $\Delta_{1\cdot1} + \delta_{1\cdot2} = \Delta_{1\cdot2}$

Section 2

This section of the wheel is subjected to an infeed of $\Delta_{1\cdot1}$ and will wear by an amount $\Delta_{2\cdot1}$ where $\Delta_{2\cdot1} \ll \Delta_{1\cdot1}$

After a further crossfeed increment the third traverse is carried out

3rd longditudinal traverse:

Section 1

Potential infeed = $d - \Delta_{1\cdot2}$

Wheel wear will be $\delta_{1\cdot3}$ where $\delta_{1\cdot3} < \delta_{1\cdot2}$

Cumulative wheel wear = $\Delta_{1\cdot2} + \delta_{1\cdot3} = \Delta_{1\cdot3}$

Section 2

Potential infeed = $\Delta_{1\cdot2} - \Delta_{2\cdot1}$

Wheel wear will be $\delta_{2\cdot2}$ where $\delta_{2\cdot2} \ll (\Delta_{1\cdot2} - \Delta_{2\cdot1})$

Cumulative wheel wear = $\Delta_{2\cdot1} + \delta_{2\cdot2} = \Delta_{2\cdot2}$

Section 3

Section 3 of the wheel is subjected to an infeed of $\Delta_{2\cdot1}$ and will

consequently wear by an amount $\Delta_{3\cdot1}$ where $\Delta_{3\cdot1} << \Delta_{2\cdot1}$

By similar reasoning, after the 4th traverse:

Cumulative wheel wear

Section 1 = $\Delta_{1\cdot3} + \delta_{1\cdot4} = \Delta_{1\cdot4}$

Section 2 = $\Delta_{2\cdot2} + \delta_{2\cdot3} = \Delta_{2\cdot3}$

Section 3 = $\Delta_{3\cdot1} + \delta_{3\cdot2} = \Delta_{3\cdot2}$

Section 4 = $\Delta_{4\cdot1}$

The above wear mechanism implies that the working surface of a worn wheel will be of stepped form, the width of each step being equal to the crossfeed increment. Maximum and minimum wear will occur on the leading and trailing sections respectively.

If the workpiece is assumed to be of infinite width then at some stage, on the 'n'th traverse, the cumulative wear $\Delta_{1.n}$ on the leading section will be equal to the infeed 'd' and this section will no longer cut. Continued grinding will gradually produce this condition across the whole wheel face so that ultimately, when the wear on the trailing section is equal to the infeed, the wheel will cease to grind. In practice it is unlikely that any workpiece will be wide enough to produce this effect, but nevertheless the workpiece surface will consist of a series of strips, at different heights and of width equal to the crossfeed. It is extremely unlikely that height differences between adjacent strips can be detected, because the wear rate on the trailing section is so slow that any difference is masked by the normal peaks and valleys produced by the grits. However, the gradual accumulation of wear on the trailing section will produce a workpiece which appears to be tapered. A taper is commonly observed on wide workpieces

in practice.

The more usual practical situation involves several transverse passes across the workpiece, infeed being applied at the commencement of each pass. The analysis is more complicated because the wheel and workpiece edges may not be in the same relative position at the start of each pass. The problem is considered later in the discussion and so for the moment it will be assumed that relative positions are constant. If the infeed is the same for each transverse pass it is theoretically impossible for the wear on the leading section to be an infeed increment greater than that on the trailing section. Consequently all sections of the wheel will cut and sustain wear as long as grinding proceeds and the stepped profile will be maintained throughout the life of the wheel.

7.3 Experimental Equipment and Test Procedure

7.3.1 Grinding facilities:

The Jones and Shipman surface grinding machine described in section 4.3.1 was used for these tests.

The grinding wheels were aluminium oxide in a vitrified bond. The wheel specification was 6A 60 I8 V75. The wheel diameter was 7 in. and the maximum width was $\frac{3}{4}$ in. However, the width was varied to give the required ratio of wheel width to crossfeed increment.

Solvac 68, a non-petroleum grinding fluid was used for both wheel dressing and grinding. The application rate was $\frac{3}{4}$ gallon per minute

at a dilution of 100 parts water to 1 part fluid.

7.3.2 Wheel dressing:

The dressing facilities described in section 4.4 were used in these tests.

In order to control the ratio of wheel width to the crossfeed increment the wheel width was varied by dressing a step at one edge of the grinding wheel to control the effective wheel width. The consequent wheel profile is shown in Figure 71. In addition the step was also used as a datum against which radial wheel wear measurements could be made.

Consequently the standardised dressing procedure described in section 4.4.3 was modified to include dressing the step onto the wheel.

1. Using the commercial diamond, dress to remove debris with a diamond traverse rate of 0.005 in. per wheel revolution and an infeed of 0.001 in. per pass.

2. With the same diamond, dress to stabilise the wheel rim and produce a smooth wheel surface. A diamond traverse rate of 0.005 in. per wheel revolution was used with six passes at an infeed of 0.0005 in., six at 0.0002 in. and finally four passes at zero infeed.

3. Dress a step approximately 0.004 in. deep at one edge of the

wheel. This was done by hand with several passes at a low traverse rate and infeed. The step width was arranged to give the correct effective wheel width as shown in Figure 71.

4. Using the special diamond, dress the wheel with one pass at the required traverse rate and infeed.

Two types of dressing were used. A coarsely dressed wheel was produced with a diamond traverse rate of 0.007 in. per wheel revolution and an infeed of 0.001 in. For fine dressing the traverse rate was reduced to 0.002 in.

7.3.3 Wheel wear measurement:

The profile of the worn wheel was produced in the hardened steel blade as discussed in section 4.6.1 and wear was measured with respect to the datum surface dressed onto the wheel.

In the tests reported earlier the Talysurf 4 surface measuring machine was used to record blade profiles. The profiling stylus was moved over the blade using the standard gear box on the machine. The maximum length of traverse with this system is $\frac{1}{2}$ in. and in these tests it was required to measure the full width of the $\frac{3}{4}$ in. wide wheel.

A motorised traversing table with a traversing distance of 6 in. was available for use on the Talysurf 4. This table is designed to be traversed beneath the stationary stylus, enabling recordings to be made of surfaces longer than the gear box stroke length. The single

speed motor on the table gives a horizontal magnification of 4x on the surface profile recorder, compared with 20x or 100x using the standard gear box.

A magnification of 4x was not considered to be adequate for accurate examination of blade surface profiles and consequently the table drive was modified to give a magnification of 10x. The standard motor was replaced by a single speed motor with a reduction gearbox. The motor drove the table via a simple dog clutch, which was manually operated. The drive system is illustrated in Figure 72.

To record the blade profile the blade, in its fixture shown in Figure 29, was placed on a co-ordinate table. The table was mounted on the fixture described in section 4.6.2. For these tests this fixture slotted into the tee slot in the top of the motorised traversing table, which was in turn located in the tee slots in the base of the Talysurf 4. Hence the blade was accurately aligned parallel to the movement of the traversing table and was positioned beneath the stylus by using the co-ordinate table. A general view of the set up is shown in Figure 73.

7.3.4 Workpieces:

The workpiece material was EN24, a 1½% Ni-Cr-Mo tool steel. Each workpiece was oil quenched and tempered to give a hardness of 550 VPN. The ground surface was 6 in. long and 2 in. wide. The material was supplied by the British Iron and Steel Research Association who also provided the chemical composition given in Figure 58.

7.3.5 Test conditions:

A number of parameters were varied in order to assess their influence on wheel wear. They included the dressing process, grinding infeed and table speed, crossfeed increment and ratio of wheel width to crossfeed increment. The conditions are summarised in Figure 74.

7.4 Results and Discussion

7.4.1 Radial wheel wear:

In the first series of tests crossfeed was only applied in one direction across the workpiece and the increments were carefully applied manually to give consistent values. In addition, successive passes across the workpiece were commenced from the same point on the wheel. These conditions were necessary to comply with the assumptions made in the theory of wheel wear.

Figures 75 and 76 show typical series of wheel profiles, taken periodically as grinding proceeds. It is clear that the wheel takes on a stepped form, each step being of width equal to the crossfeed increment. Wear occurs across the whole wheel face, but is greatest at the leading section. The regular roughness pattern, which is initially present due to the dressing process, is quickly removed from the leading sections, but is always identifiable on the trailing sections.

These results confirm one of the basic implications of the proposed wear mechanism; wear will occur in steps across the wheel face.

It is noticeable, particularly in Figures 75b and 76b where the ratio of wheel width to crossfeed increment is only 4 : 1, that the wear is not even across any given section of the wheel. The largest amount of wear occurs at the junctions of adjacent sections and this is considered to be due to instability at the leading edge of the leading section. Grits at this edge are relatively poorly supported, but perhaps more important in these tests, they have been subjected to the forces applied when dressing the step on the wheel. During grinding this edge will tend to break down more rapidly than the rest of the section and leave more metal for the leading edges of subsequent sections to remove. Consequently these edges will also tend to wear more quickly. Because breakdown at the leading edge of one section will cause instability at the adjacent, trailing edge of the preceding section, the scalloped type of wear shown in Figures 75b and 76b is to be expected. The problem is less acute as the ratio of wheel width to crossfeed increment is increased, because more sections are available to remove the metal initially left by the leading section.

The minimum radial wheel wear on each of the sections is related to cross sectional area ground in Figures 77 and 78. These graphs are particularly significant because they show that for each section the form of the wheel wear is similar to that shown in Figure 2a. In the proposed wear theory each section is regarded as being separate and consequently this type of wear curve indicates that the basic wear mechanism in crossfeed surface grinding is the same as that reported for other grinding processes.

7.4.2 The influence of crossfeed increment and wheel width:

Again referring to Figures 77 and 78, it can be seen that as the ratio of wheel width to crossfeed increment is increased the radial wheel wear on each section is considerably reduced. As the number of sections available for grinding increases the proportion of the infeed which is removed in a transverse pass across the workpiece also increases. Consequently, on the next pass, the leading sections will have to remove less metal and will wear at a slower rate. In the early stages of grinding this will not apply because almost the whole of the infeed will be removed by the leading sections, wear on the trailing sections being virtually negligible. The results confirm this point, because at a ground surface area of about 50 in^2 there is little difference between the wear curves for 9 : 1 and 4 : 1 ratios.

Comparison of Figures 77 and 78 shows that for the same wheel width to crossfeed increment ratio an increase in the crossfeed increment gives a reduction in wheel wear. Further confirmation of this effect was obtained from a test with a larger crossfeed increment of 0.170 in. The results for this test are shown in Figure 79 and in Figure 80 they are compared with the results obtained with crossfeed increments of 0.030 in. and 0.070 in.

The reduction in wheel wear is considered to be due to the scalloped effect, discussed above in section 7.4.1, which appears on the surface. At a low crossfeed increment breakdown at the leading and trailing edges of a wheel section are likely to converge, so that the wear measured at the centre of the section is greater than would have occurred due to simple radial wear. Figure 76b shows the pronounced

scalloping obtained with a crossfeed increment of 0.030 in. As the crossfeed increment is increased convergence is less likely to occur, so that the measured radial wheel wear will be reduced. The influence of crossfeed increment on scalloping can be clearly seen by comparing Figures 75b, 76b and 79.

In practice maximum grinding wheel width is fixed by the machine dimensions, so that any increase in crossfeed increment can only be obtained at the expense of a decrease in the ratio of wheel width to crossfeed increment. These changes give opposite effects on radial wheel wear, but in these tests lowest wear was achieved by using a high ratio of wheel width to crossfeed increment. However, further tests, using wider wheels to give greater flexibility in the choice of crossfeed increment and ratio, may reveal an optimum combination.

7.4.3 The influence of wheel dressing:

The results obtained in the plunge cut grinding tests and discussed in section 6.2.1 show that as the traverse rate of the dressing diamond is decreased radial wheel wear is also decreased. Consequently if the wear mechanism in crossfeed surface grinding is similar to that occurring in other grinding processes then the same pattern should emerge.

A typical series of wheel traces for a finely dressed wheel is shown in Figure 81 and in Figure 82 the measured radial wheel wear for coarse and fine wheels are compared. There is a very significant reduction in the wear rate on all sections of the wheel when

fine dressing is used.

7.4.4 The influence of other grinding conditions:

Both the workpiece speed and the infeed during grinding were varied. The recorded radial wheel wear on the various wheel sections are tabulated in Figure 83 and it can be seen that a reduction in either parameter gave a reduction in wheel wear.

For the conditions used in these tests the average maximum undeformed chip thickness 't_{max}' is given by the approximate expression[51]

$$t_{max} = \left\{ \frac{4v}{VCr} \sqrt{\frac{d}{D}} \right\}^{\frac{1}{2}}$$

where v = workpiece speed

V = wheel speed

C = number of grits per unit area on the wheel rim

r = ratio of mean chip width to chip thickness

d = infeed

D = wheel diameter

Hence, for a given wheel speed, a reduction in either workpiece speed or infeed will give a lower average maximum chip thickness and a consequent decrease in the maximum force acting on each grit. Grits will be less likely to fracture or be dislodged from the bond under these lower force conditions and so the wear will be reduced.

The actual magnitudes of the reductions in wheel wear are interesting.

A change in the infeed from 0.001 in. to 0.0005 in. constitutes a 50% reduction in metal removal rate. After the same amount of metal has been removed the wear on the leading section of the wheel used at a low infeed is 30% less than that occurring at the higher infeed. Changing the table speed from 56 feet per minute to 40 feet per minute gives a 30% change in metal removal rate, whereas the reduction in wheel wear is only 6%.

In a C.I.R.P. co-operative research programme reported by Snoeys and Decneut[52] results were presented to show the relationship between wheel wear and metal removal rate. For the conditions used in the tests discussed here the relationship should be roughly linear[52]. Consequently the above results are surprising and were rechecked. Similar data was obtained and clearly further work is necessary to clarify the discrepancy between these results and those obtained by Snoeys and Decneut[52].

7.4.5 Crossfeeding in both directions:

For normal applications in which several transverse passes are being taken across a workpiece it is usual to apply crossfeed increments in both directions. Thus the trailing wheel section on one pass becomes the leading wheel section on the next. In this situation both wheel edges will sustain similar amounts of radial wear and the central part of the wheel will wear relatively slowly. The effect is confirmed in Figure 84.

7.4.6 Variable crossfeed increments:

All the results presented above have been obtained for conditions in which the crossfeed increments were precisely controlled and each transverse pass was commenced at the same point on the wheel. However, in the production grinding situation crossfeed increments are applied automatically and successive passes are commenced from random positions. On the machine used, a hydraulically operated ratchet and pawl mechanism was available for automatic crossfeeding.

A test was carried out using this mechanism and without controlling the starting point for each transverse pass. The actual crossfeed increments were recorded throughout the test. The average increment was 0.070 in. with a standard deviation of 0.005 in. The workpiece profiles obtained are shown in Figure 85.

Comparison of these results with those presented in Figure 75a indicates that in the early stages of grinding fairly well defined steps are present, particularly on the leading wheel sections. However, as grinding continues and the height difference between adjacent steps becomes smaller, the steps are less well defined and it may be argued that there is an angle on the wheel. However, the wear mechanism has not changed. Steps are still being formed, but due to the lack of control over traverse position and crossfeed increments the number of steps increases and consequently they are not so obvious.

7.4.7 The wear mechanism:

These results have clearly shown that the wear mechanism proposed in

section 7.2 is correct. In a recent paper on traverse cylindrical grinding Pekelharing et al[53] published a similar theory to explain wheel wear in this process. A model was developed which enabled the influence of certain of the grinding parameters to be predicted. The theoretical predictions are much the same as those presented in this work for crossfeed surface grinding.

Workpiece profiles are not given in the papers published by Purcell[47] and Banerjee and Hillier[48,49]. Consequently it is not possible to decide from their tests whether or not the wheel is wearing over the whole of its width. The initial rapid breakdown shown in Phase I of Figure 69 is similar to that shown on the leading edge of the leading section of wheels used in this work. However, it is not possible to detect a stable approach angle on any of the workpiece profiles presented in this report.

8. WORKPIECE SURFACE GENERATION IN CROSSFEED SURFACE GRINDING

8.1 The Generation of the Workpiece Surface

It has been shown in Chapter 4 that when a single point diamond is used to dress a grinding wheel the parameters used in the dressing process can be detected on the workpiece surface produced by the wheel. The features of the dressing process are generated by the combination of a number of wheel profiles. Each wheel profile will probably contain some points which are coincident with the locus of the dressing diamond and these points will appear on the workpiece surface.

Another important feature of these points is that they will be arranged helically around the wheel periphery, due to the helical path of the dressing diamond relative to the wheel. In plunge cut surface grinding the helix can influence the roughness of the workpiece surface if the speed ratio between the wheel surface and the workpiece is changed and this is discussed in section 5.3.

When the crossfeed increment in a surface grinding operation is less than half the wheel width, each part of the workpiece surface is traversed at least twice by the wheel. If the height difference between any two adjacent sections on the wheel is less than the effective peak to valley height on the wheel the workpiece surface will be formed by a combination of the grooves produced by these sections. If the rotational position of the wheel on the second traverse is precisely the same as it was on the first traverse the

grooves will be in phase and will not change the surface profile. However, this is very unlikely to occur. It is probable that there will be a phase difference and a consequent reduction in the peak to valley height on the workpiece. The effect is illustrated in Figure 86.

A series of grinding tests were carried out to verify this point. Commencing from one edge of the workpiece a number of longditudinal passes were carried out, applying an increment of crossfeed at the end of each pass. The number of passes used was equal to the ratio of the wheel width to the crossfeed increment. At this stage the section of the workpiece adjacent to the edge had been traversed by each wheel pass, whereas the section farthest away from the edge had only been traversed once. The consequent workpiece profile was measured on the Talysurf 4.

The results for a coarsely dressed wheel with a ratio of wheel width to crossfeed increment of 9 : 1 are shown in Figure 87. Similar results for a finely dressed wheel are given in Figure 88. It can be seen that as the number of wheel traverses across any one section of the workpiece is increased the roughness is reduced particularly for a relatively low number of traverses.

In Figure 89 the above results and two other tests are presented at a lower horizontal magnification enabling the whole of the ground workpiece surface to be illustrated in one trace. In addition to showing the change in surface roughness, these results also show that the stepped profile appears on the wheel after only a few traverses. These profiles confirm the theoretical prediction discussed in section 7.2.

8.2 Variation in Surface Roughness across the Workpiece

Consider a wheel with a wheel width to crossfeed increment ratio of 4 : 1. When the workpiece surface has been ground it will consist of a series of strips, of width equal to the crossfeed. The surface profile on each strip will be formed by four consecutive passes of the wheel along the workpiece. The strip adjacent to the first edge will be formed by passes 1,2,3 and 4, whereas the next strip will consist of passes 2,3,4 and 5. Consequently each strip will have three passes in common with the adjacent strips and one different pass, so that the roughness of adjacent strips will vary.

In previous work[17,28] the author has measured the surface roughness of the strips formed on a workpiece by crossfeed surface grinding. The results are given in Figures 90 and 91 and they confirm the anticipated roughness variation.

8.3 The Influence of Wheel Wear on Surface Finish

It is clear from the blade profiles shown in Figures 75 and 76 that as grinding continues the leading wheel sections are worn away quite quickly. Although these sections continue to remove metal they do not contribute to the final workpiece surface, because the radial wheel wear is greater than the peak to valley height on the workpiece. Hence there will be a reduction in the number of wheel sections available to cause out of phase peaks and valleys on the workpiece and the roughness will tend to increase. However, the trailing sections, which are forming the workpiece surface, will also wear. The infeed on these sections is very low and so the wear

mechanism will probably be predominantly attricious. In section 6.2.2 it is concluded that if attricious wear is occurring the surface roughness of the workpiece will probably improve. In Figures 75a, 76a and 79 it can be seen that the blade profile produced by the wheel does become less rough on the trailing sections as grinding proceeds and this will tend to improve the roughness of the workpiece surface.

Consequently there are two factors affecting the workpiece surface roughness and, depending upon the relative significance of these factors, the roughness will either deteriorate, improve or remain substantially constant.

The workpiece surface roughness was measured during the wheel wear tests discussed in Chapter 7 and some of the results are presented in Figure 92. Curve A shows that for a coarsely dressed wheel at a crossfeed increment of 0.070 in., the dominant feature is peak wear on the trailing sections so that workpiece roughness gradually improves as grinding continues. Pahlitzsch and Appun[29] obtained a similar result for a coarsely dressed wheel in traverse cylindrical grinding.

If a finely dressed wheel is used under these conditions curve B is obtained, indicating an increase in roughness during the early stages of grinding. The increase in roughness can be explained by reference to Figure 82. In the early stages of grinding both coarse and fine wheels wear at similar rates on the leading sections. The grinding forces are high and the wheels wear rapidly. Consequently the number of sections available to influence the workpiece surface reduces at

about the same rate. However, on the trailing sections very little wear occurs on the finely dressed wheel because it is very stable. Hence wear on the leading sections has more influence than peak wear on the trailing sections. The lower values of roughness can be expected due to the fine dressing.

If the crossfeed increment is reduced to 0.030 in. the roughness measured after a limited grinding time is lower than that achieved with a crossfeed increment of 0.070 in. due to the increase in the wear rate associated with lower crossfeed increments. Wear rate is discussed in section 7.4.2. Differences in the later stages of grinding between curves A and C are not considered to be significant.

When the wheel width is reduced to give only a 4 : 1 ratio of wheel width to crossfeed increment the roughness is increased. An increase can be expected, for the reasons given in section 8.1. Another problem at this low ratio is the scalloping effect discussed in section 7.4.1. Because only four sections are available for grinding, the final workpiece surface is produced almost entirely by the trailing wheel section, particularly in the later stages of grinding, when the wheel has sustained considerable wheel wear. Any scalloped effect appearing on this trailing section will be transferred to the workpiece and this effect is clearly shown in Figure 93. In practice waviness of this magnitude would almost certainly be unacceptable and the wheel would be redressed.

8.4 Retention of Dressing Features on the Workpiece Surface

It has already been shown in Chapter 6 that the workpiece surface

produced by a grinding wheel is strongly influenced by the dressing parameters used. In section 6.2.3 results were presented to show that even after considerable radial wheel wear dressing features can still be detected on the workpiece.

In crossfeed surface grinding the workpiece surface is formed by the trailing sections of the wheel. These sections operate with low infeeds and so they wear relatively slowly, as shown in Figures 77 and 78. Consequently the dressing parameters will be retained for long grinding times and this can be seen on the blade profiles in Figures 75a and 76a.

These results confirm the important influence of wheel dressing on the workpiece surface and also show that the dressing process is particularly significant in crossfeed surface grinding. Dressing parameters continue to appear on the workpiece after considerable grinding times.

9. FUTURE WORK

9.1 Workpiece Surface Generation

In this work it has been shown that the wheel profile envelope is closely related to the workpiece profile produced by the wheel. However, there are some discrepancies and these have been explained by considering the wheel indexing system between profiles. The wider the indexing interval, the more chance there will be that high points on grits will be missed.

Verification of this effect can be obtained by significantly reducing the indexing interval between samples. It would not be possible to handle the very large increase in data with the existing computer programme. The programme would have to be modified to operate in stages, developing several profile envelopes, which could be combined together at a later stage.

If the cutting action on the workpiece surface is ideal the wheel profile envelope should precisely conform to the workpiece profile. In this respect the profile envelope is an ideal profile. However, in tests with single grits and pyramidal diamonds[54-58] it has been shown that with the high negative rake angles on abrasive grits transverse plastic deformation is also probable. Plastic deformation will influence the shape of the workpiece profile.

It is possible that a comparison between a precise wheel profile envelope and the workpiece profile produced will give some indication of the magnitude of the plastic flow which occurs on the workpiece

surface.

9.2 Wheel Dressing

The wheel dressing operation has been shown to be an extremely important factor in the grinding process. The operation influences both the rate and nature of the wheel wear and also the surface roughness produced on the workpiece and the influence is maintained for long grinding periods. The dressing diamond traverse rate, its shape and also the infeed are significant individual parameters, but it is also important to consider their combined effects. Failure to do so results in the contradictory recommendations made by Pacitti[15] and Fisher[27].

A comprehensive study of the combined influence of these parameters on wheel wear and surface finish would be valuable. In such an investigation the test conditions should be representative of industrial practice. The sharply pointed pyramidal diamond used in the tests reported here was necessary because of the fundamental nature of the objectives. However, a sharp point is not a very practical shape because of the high wear rate on the point.

In any future work on wheel dressing it will be important to have facilities available for higher wheel speeds than those used in these tests.

9.3 Crossfeed Surface Grinding

It has been shown that the radial wheel wear and the surface finish

produced in this process are dependent upon the crossfeed increment and also the ratio of wheel width to crossfeed increment. In these tests these parameters were varied independently by altering the wheel width. However, in the practical situation the maximum wheel width is fixed by the dimensions of the grinding machine. From these tests both high crossfeed increments and high ratios are desirable, but for a maximum width one parameter can only be increased at the expense of a reduction in the other. Grinding time is also important, because, for the same infeed, a reduction in the crossfeed increment gives a proportional increase in grinding time. It is possible, depending on the workpiece requirements, that grinding time can be kept constant by increasing either the infeed or the work speed, but these parameters have also been shown to influence wear rate. Wheel speed is also a significant factor because of its influence on wheel wear and surface roughness and should be varied in future work on the process.

It can be seen therefore that it is not enough to simply analyse the influence of any one of the above parameters. They must all be investigated simultaneously to develop the best economic solution in a particular situation.

10. CONCLUSIONS

1. When a dressing diamond is traversed across a grinding wheel it causes breaking and splintering of the material on the wheel rim.

2. There will be some points on the wheel surface which are coincident with the diamond locus.

3. An individual wheel profile in the dressing direction does not show regular features of the type appearing on the work-piece produced by the wheel.

4. Each axial wheel profile taken around the wheel periphery is many times rougher than the workpiece surface.

5. As the number of profiles used to generate the profile envelope is increased the roughness of the envelope is reduced.

6. The workpiece surface is generated by the combination of points coincident with the dressing diamond locus.

7. The error between the wheel profile envelope and the workpiece profile is reduced as the number of wheel profiles used to generate the envelope is increased.

8. The differences between the wheel profile envelope and the workpiece profile are due to the failure to record all the high points on the rim of the wheel.

9. When a grinding wheel is dressed by a single point diamond the wheel produces a workpiece profile which is closely related to the theoretical profile obtained by considering the locus of the dressing diamond.

10. The valleys produced on the wheel by the diamond are more stable than the peaks and consequently the workpiece peaks are sharp, whereas the valleys tend to be flatter than the theoretical profile.

11. As the speed ratio between the wheel and the workpiece is increased the workpiece roughness is reduced due to the helical nature of the wheel surface.

12. In plunge cut surface grinding radial wheel wear occurs in two phases, a primary phase of rapid wear and a secondary, longer phase during which wheel wear rate is slower and more consistent.

13. Primary wheel wear is influenced by the dressing process and the grinding conditions.

14. Secondary wheel wear is also influenced by the dressing process and the grinding conditions.

15. The influence of wheel wear on the surface finish depends on the nature of the wear process. If the principal wear mechanism is fracture wear the finish will deteriorate. If attrition predominates the finish will improve. A combination of the two

tends to cause a constant value of surface finish.

16. Dressing features are retained on the workpiece surface after considerable radial wheel wear. The peaks remain sharp, but the valleys become flatter.

17. If severe grit pull out occurs the dressing features will disappear.

18. Acceptable levels of wheel wear in precision grinding operations are likely to maintain dressing features on the workpiece surface.

19. If the magnitude and position of the crossfeed increments in surface grinding are constant the wheel will develop a stepped profile, each section having a width equal to the crossfeed increment.

20. Wear occurs simultaneously across the whole wheel width, but wear on the leading sections is greater than on the trailing sections.

21. At low ratios of wheel width to crossfeed increments the wear on each section may give a scalloped effect.

22. The radial wheel wear on each section has primary and secondary phases, similar to those obtained in plunge cut surface grinding.

23. Wheel wear is reduced if the ratio of wheel width to crossfeed increment is increased.

24. For the range of crossfeed increments used an increase in the increment, while maintaining the same ratio to wheel width, gives a reduction in wheel wear rate.

25. Wear rate is dependent on the dressing process, a finely dressed wheel wearing more slowly than a wheel which has been coarsely dressed.

26. A reduction in either the infeed or the workpiece speed during grinding reduces the wear rate.

27. If crossfeeding is provided in both directions across the workpiece the wheel wears quickly at both edges and relatively slowly in the middle.

28. If the crossfeed increments are not precisely controlled and occur in random positions across the wheel face the steps on the wheel are less pronounced and the wheel surface will be tapered.

29. In crossfeed surface grinding, as the number of traverses across any one section of the workpiece is increased the roughness tends to decrease.

30. The workpiece surface consists of a series of strips, of width equal to the crossfeed increment and each strip

potentially has a different surface roughness.

31. Surface roughness changes with grinding time, the actual direction of the change depending on the relative significance of wear on the leading and trailing sections.

32. The scalloped shape produced at low wheel width to crossfeed increment ratios can cause severe secondary waviness on the workpiece surface.

33. Dressing parameters will continue to appear on the workpiece surface for long grinding times in crossfeed surface grinding.

REFERENCES

1. WETTON A.G.
A review of published fundamental research on the grinding of metals.
M.T.I.R.A. Research Report No. 38, December 1970.

2. PEKLENIK J.
Testing the grade of grinding wheels.
Microtecnic, v 14, 1960.

3. KALISZER H.
Pneumatic method of testing grinding wheels.
Proc. 3rd M.T.D.R. Conference, 1962.

4. PETERS J., SNOEYS, R. and DECNEUT A.
Sonic testing of grinding wheels.
Proc. 9th M.T.D.R. Conference, 1968.

5. HAHN R.S. and PRICE R.L.
A non-destructive method of measuring local hardness variations in grinding wheels.
Annals C.I.R.P. v XVI, 1968.

6. SHAW M.C.
The grinding of metals.
Inst. of Mech. Engrs., Conference on Technology of Engineering Manufacture, 1958.

7. HAHN R.S.

Effect of wheel - work conformity in precision grinding.

Trans. A.S.M.E., v 77 1955.

8. KRABACHER E.J.

Factors influencing the performance of grinding wheels.

Trans. A.S.M.E., Series B, August, 1959.

9. MALKIN S. and COOK N.H.

The wear of grinding wheels. Part 1 - Attricious wear.

Trans. A.S.M.E., Series B, November, 1971.

10. MALKIN S. and COOK N.H.

The wear of grinding wheels. Part 2 - Fracture wear.

Trans. A.S.M.E., Series B, November, 1971.

11. YOSHIKAWA H. and SATA T.

Study on wear of grinding wheels.

Trans. A.S.M.E., Series B, 1963.

12. KOLOC J.

On the wear of grinding wheels.

Microtecnic, v XIII, n 1, 1959.

13. GRISBROOK H., HOLLIER R.H. and VARLEY P.G.

Related patterns of grinding forces, wheel wear and surface finish.

Int. J. Prod. Res., v 1, 1962

14. PATTINSON E.J. and CHISHOLM A.J.W.
The effect of dressing techniques on grinding wheel wear.
Int. Conf. on Manufacturing Technology, Ann Arbor, Michigan, 1967.

15. PACITTI V. and RUBENSTEIN C.
The influence of dressing depth of cut on the performance of a single point diamond dressed alumina grinding wheel.
Int. J. Mach. Tool Des. Res., v 12, 1972.

16. KORNBERGER Z. and KOZIARSKI A.
Cutting characteristics of grinding wheels dressed by different methods.
Machinery and production engineering, v 110, 31 March 1971.

17. VICKERSTAFF T.J.
On the significance of the wheel dressing operation in the grinding process.
University of Nottingham, 1970, MSc thesis.

18. LINDSAY R.P.
Dressing and its effect on grinding performance.
A.S.T.M.E., Creative Manufacturing Seminars, Paper MR69-568, 1969

19. SATO K.
On the surface roughness in grinding.
Jnl. Japan Soc. Prec. Engg. 1950

20. YANG C.T. and SHAW M.C.
The grinding of titanium alloys.
Trans. A.S.M.E., v 77, 1955.

21. ORIOKA T.
On the grinding geometry for the random spacing of abrasive grains on wheel surfaces.
Reports of the Faculty of Engg., Yamanashi University, Japan, v 109 n 8, July, 1957.

22. FARMER D.A., BRECKER J.N., NAKAYAMA K. and SHAW M.C.
Study of the finish produced in surface grinding.
Int. Conf. on Metrology, I.Mech.E., Oxford, April, 1968.

23. YOSHIKAWA H. and SATA T.
Simulated grinding process by Monte Carlo method.
Annals C.I.R.P., v XVI, 1968.

24. MERLIN J.
Getting the best out of your single point diamond dresser.
Cutting Tool Engineering, June, 1967.

25. SELBY J.S.
Dressing abrasive grinding wheels with diamond tools.
De Beers Industrial Diamond Division, London.

26. HAHN R.S.
The relation between grinding conditions and thermal damage in the workpiece.
Trans. A.S.M.E., Series B, 1960.

27. FISHER R.C.
The twelve diamond dressing variables.
Cutting Tool Engineering, April, 1973.

28. VICKERSTAFF T.J.
Diamond dressing - its effect on work surface roughness.
Industrial Diamond Review, July, 1970.

29. PAHLITZSCH G. and APPUN J.
Effect of truing conditions on circular grinding.
Industrial Diamond Review, v 14, September/October, 1954.

30. PAHLITZSCH G. and THOEING W.
New research into the truing process in grinding.
Industrial Diamond Review, v 19, May/June/July, 1959.

31. THORN A.R.
The effect of grinding wheel speed on the life of single-point diamond dressing tools.
M.T.I.R.A. report to Advisory Panel on Grinding Machines.

32. McKEE R.E., MOORE R.S. and BOSTON O.W.
Experimental study of cylindrical grinding.
Trans. A.S.M.E. November, 1947.

33. KACZMAREK J. and KORNBERGER Z.
Cutting capability of grinding wheels, its symptoms and stability.
Annals C.I.R.P., v XXI, 1972.

34. VICKERSTAFF T.J. and HENDER M.
Wheel wear and surface finish in cylindrical grinding.
University of Aston in Birmingham, June 1971.

35. LINDBERG P.
Experiments on grinding.
College International pour l'etude scientifique des techniques de production mechanique, April 1956.

36. HAHN R.S. and LINDSAY R.P.
The influence of process variables on material removal, surface integrity, surface finish and vibration in grinding.
10th M.T.D.R. Conf., Manchester, 1969.

37. HAHN R.S. and LINDSAY R.P.
Principles of grinding. Part II, the metal removal parameter.
Machinery (NY), August, 1971.

38. HAHN R.S. and LINDSAY R.P.
On the basic relationships between grinding parameters.
Annals C.I.R.P. v XVIV, 1971.

39. BHATEJA C.P., CHISHOLM A.W.J. and PATTINSON E.J.
The influence of grinding wheel wear and dressing on the quality of ground surfaces.
Proc. Int. Grinding Conf. Pittsburgh, 1972.

40. MALKIN S. and ANDERSON B.
Active grains and dressing particles in grinding.
Proc. Int. Grinding Conf. Pittsburgh, 1972.

41. BAUL R.M., GRAHAM D. and SCOTT W.
Characterization of the working surface of abrasive wheels.
Tribology, August, 1972.

42. OPITZ H., ERNST W. and MEYER K.F.
Grinding at high cutting speeds.
6th M.T.D.R. Conference, 1965.

43. GUHRING K.
Leistungssteigerung der schleipverfahren durch hohe schnittgeschwindigkeiten.
Industrie -Anzeiger, v 89, n 32, April 1967.

44. What is gained by high speed grinding.
Metalworking Production, 20 November, 1968.

45. HOARE S.W.
Applications of high speed grinding.
M.T.I.R.A. Seminar, 17 May 1972.

46. NOMURA M. and TSUZINO T.
A consideration of the grinding process.
Bull. Japan Soc. Prec. Engg. v 4, n 3, 1970.

47. PURCELL J.

A note on an investigation of the surface grinding process.

Note No. 38, The College of Aeronautics, Cranfield, 1956.

48. HILLIER M.J.

On a three dimensional model of the surface grinding process.

Int. J. Mach. Tool Des. Res. v 6, 1966.

49. BANERJEE J.K. and HILLIER M.J.

Wheel wear pattern in surface grinding.

The Tool and Manufacturing Engineer, February 1969.

50. VICKERSTAFF T.J.

Wheel wear and surface roughness in crossfeed surface grinding.

Int. J. Mach. Tool Des. Res. v 13, 1973.

51. REICHENBACH G.S., MAYER J.E., KALPAKCIOGLU S. and SHAW M.C.

The role of chip thickness in grinding.

Trans. A.S.M.E., v 78, 1956.

52. SNOEYS R. and DECNEUT A.

Review of results of the co-operative research program of the CIRP grinding group.

Annal C.I.R.P. v XVIV, 1971.

53. PEKELHARING A.J., VERKERK J. and BEUKERING F.C.V.

A model to describe wheel wear in cylindrical grinding.

Proc. Int. Grinding Conf. Pittsburgh, 1972.

54. GRISBROOK H., MORAN H. and SHEPHERD D.
Metal removal by a single abrasive grit.
Iron and Steel Inst. Conf. Machinability, London, 1965.

55. RUBENSTEIN C., GROSZMAN E.K. and KOENIGSBERGER F.
Force measurements during cutting tests with single point tools simulating the action of a single abrasive grit.
Proc. Int. Industrial Diamond Conference, Oxford, 1966.

56. SASAKI T. and OKAMURA K.
The cutting mechanism of abrasive grit.
Bull. J.S.M.E., v 3, n 12, 1960.

57. WETTON A.G.
A review of theories of metal removal in grinding.
Jnl. Mech. Eng. Science, v 11, n 4, 1969.

58. GORMLY M., FISHER R.G. and MATHIAS W.K.
From art to science in grinding.
Grinding and Finishing, 1961.

APPENDIX I

I.1 List of Definitions used in the Computer Programme

DATA 1	-	Punched paper tape input of wheel profiles.
DATA 2	-	Punched paper tape input of workpiece profile.
EVCO	-	Individual value of a wheel profile.
RAXEVCO	-	Individual value in zero standardised matrix of maximum values.
NROWS	-	Numbers of columns used to generate the RAXEVCO matrix.
RCO	-	Scale adjusted and zero standardised individual value on the workpiece profile.
RCR	-	Initially an individual value on the workpiece profile, but finally used as the error between RAXEVCO and RCO.
NDATA	-	Number of wheel profiles sampled.
NTEST	-	Number of columns in the RAXEVCO matrix.
NITV	-	Number of comparisons made between columns of RAXEVCO and RCO.
SCALE	-	Magnification used in recording the wheel profiles divided by the magnification used in recording the workpiece profile.
EINT	-	Interval distance between adjacent points on a wheel profile.
RINT	-	Interval distance between adjacent points on the workpiece profile.
IMAX 1	-	Length of individual columns in the EVCO matrix.
IMAX 2	-	Length of shortest column in the EVCO matrix.

RMAX 2 - Total number of recorded points on the workpiece profile.

EDIST - Distance along the wheel profile from the first recorded point.

RDIST - Number of points on the workpiece profile in the distance EDIST.

RHT - Height on the workpiece profile at distance EDIST from the start of the profile.

TSQ - Sum of squares of errors between RAXEVCO and RCO.

TER - Sum of errors between RAXEVCO and RCO.

TMAX - Maximum error between RAXEVCO and RCO.

TMIN - Minimum error between RAXEVCO and RCO.

RMEAN - Mean of errors between RAXEVCO and RCO.

VAR - Variance of errors between RAXEVCO and RCO.

SD - Standard deviation of errors between RAXEVCO and RCO.

RANGE - Range of errors between RAXEVCO and RCO.

I.2 Flowchart for the Computer Programme

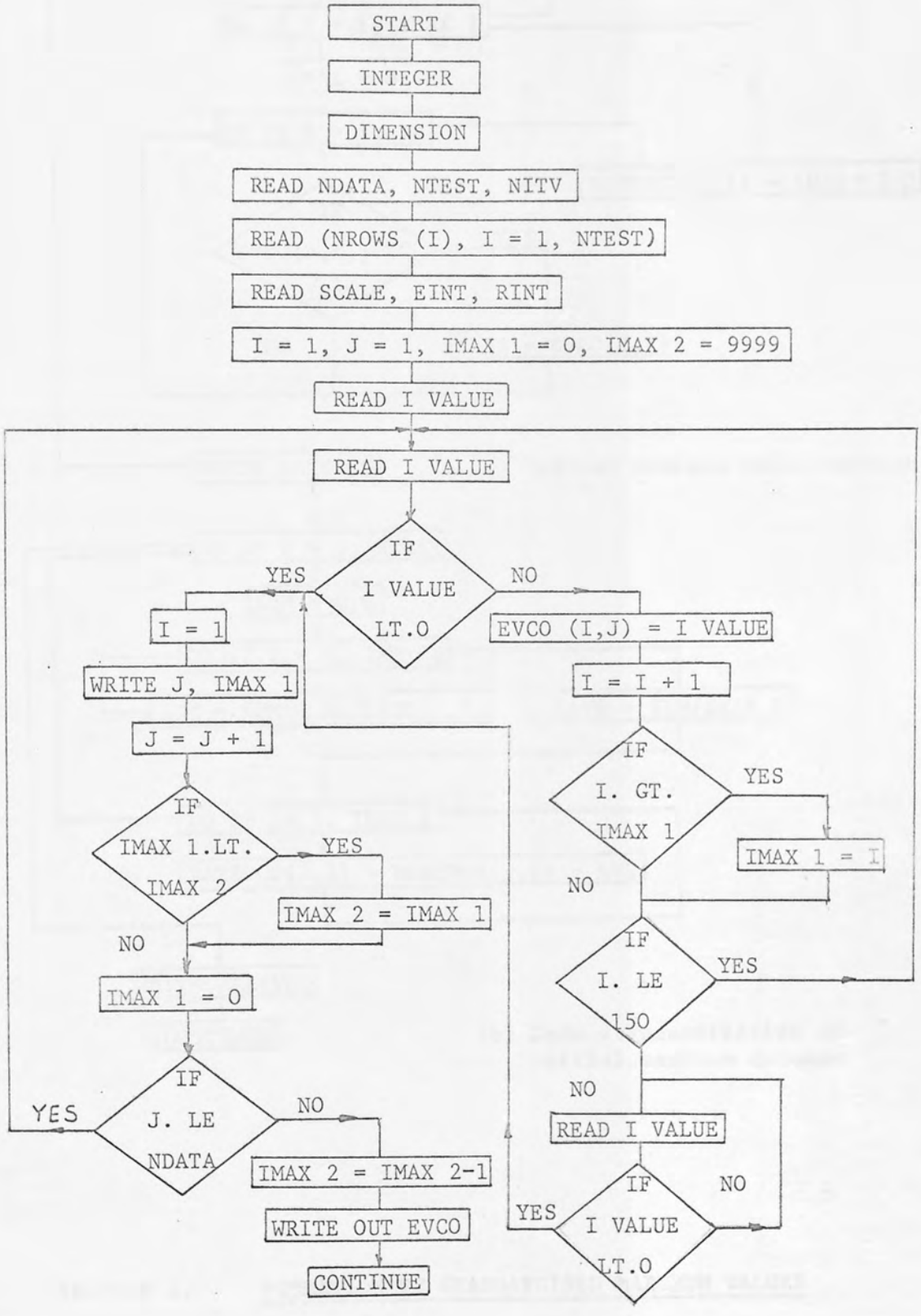

SECTION 1. INPUT OF WHEEL PROFILES INTO EVCO MATRIX

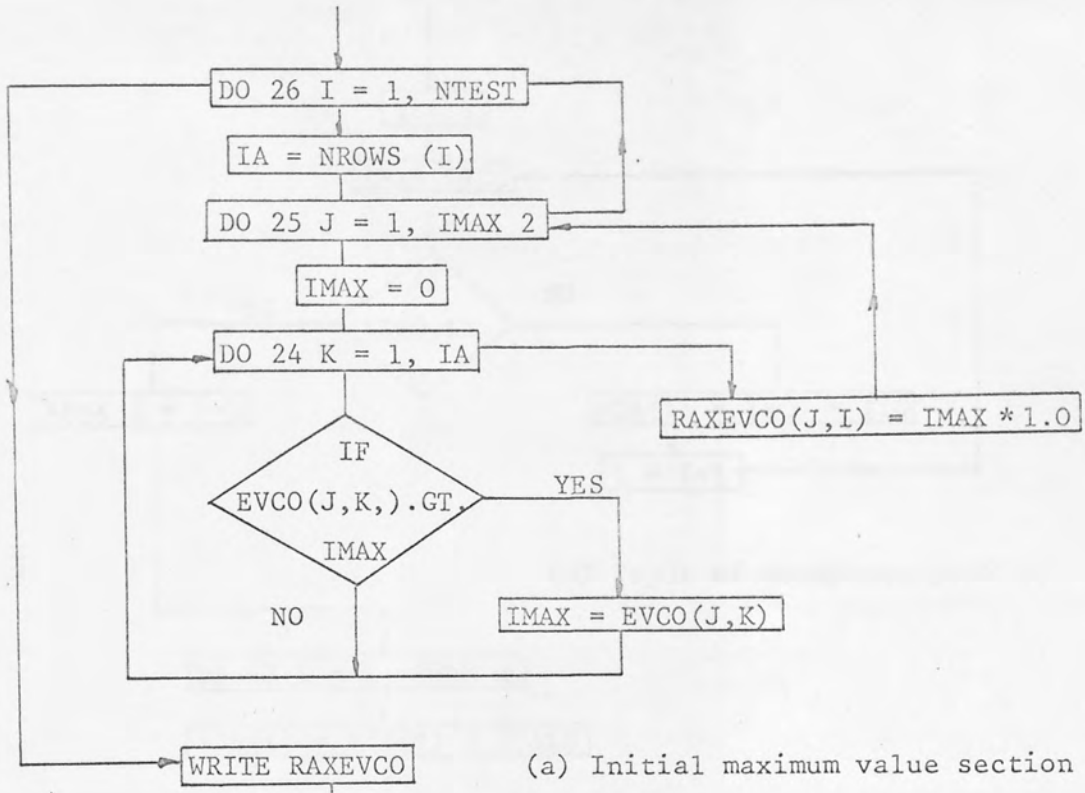

(a) Initial maximum value section

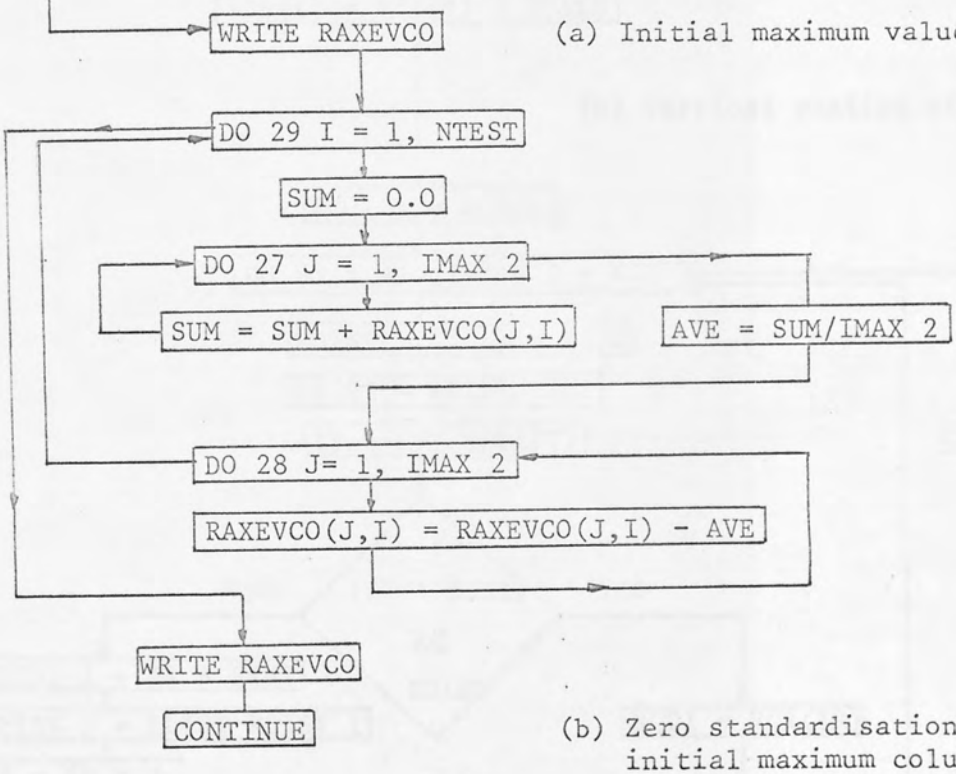

(b) Zero standardisation of initial maximum columns

SECTION 2. FORMATION OF STANDARDISED MAXIMUM VALUES

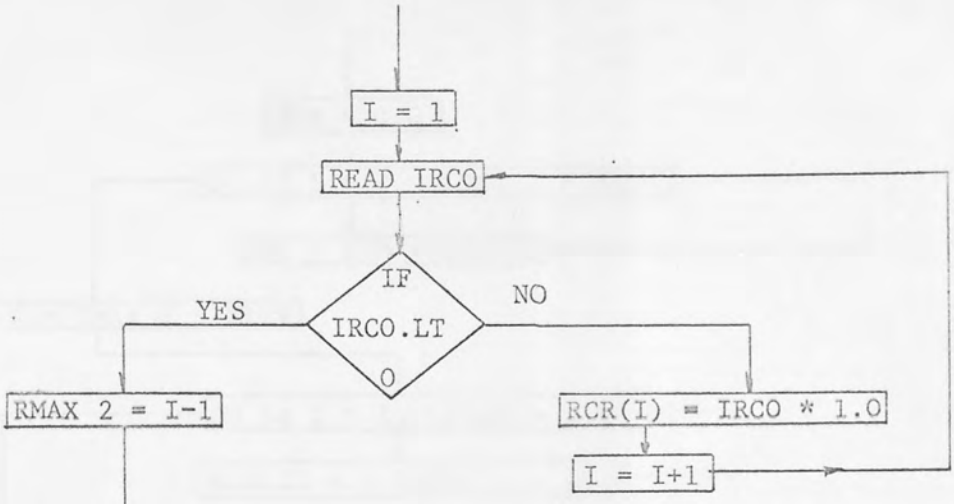

(a) Input of workpiece profile

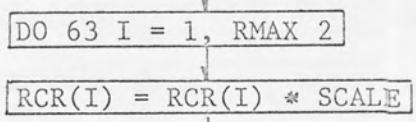

(b) Vertical scaling of workpiece profile

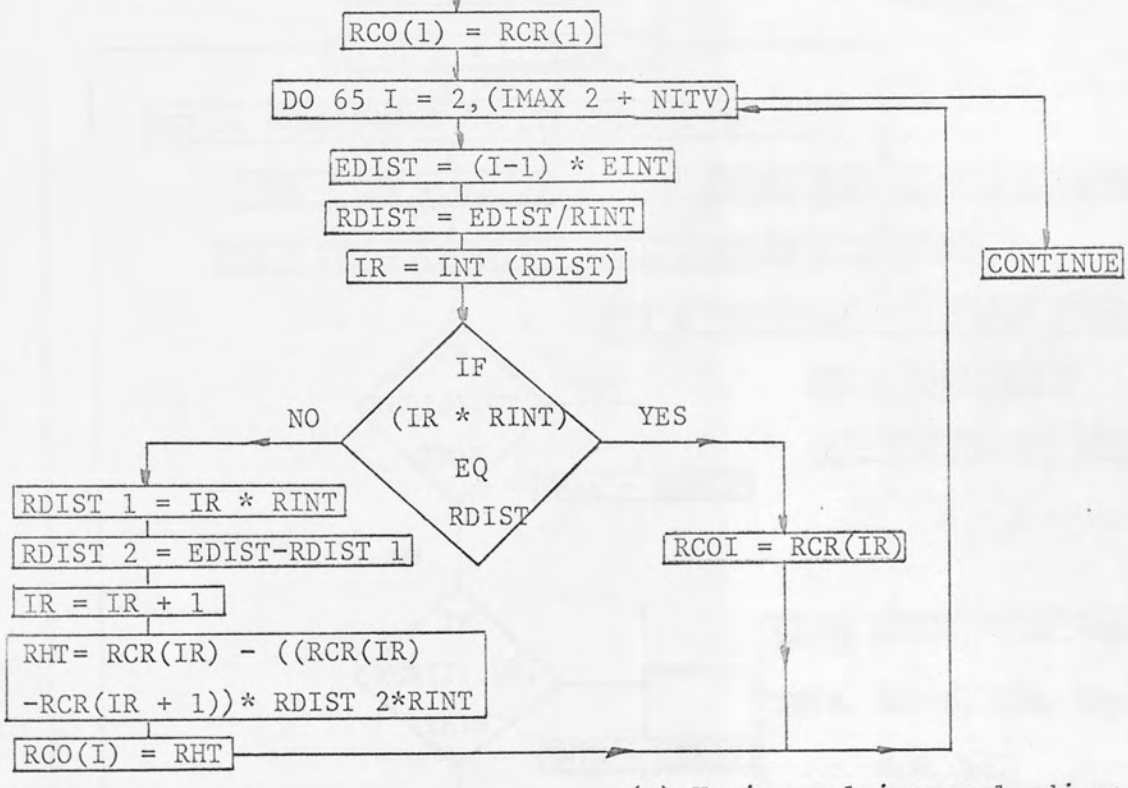

(c) Horizontal interval adjustment to match wheel profiles

SECTION 3. INPUT AND SCALING OF WORKPIECE PROFILE

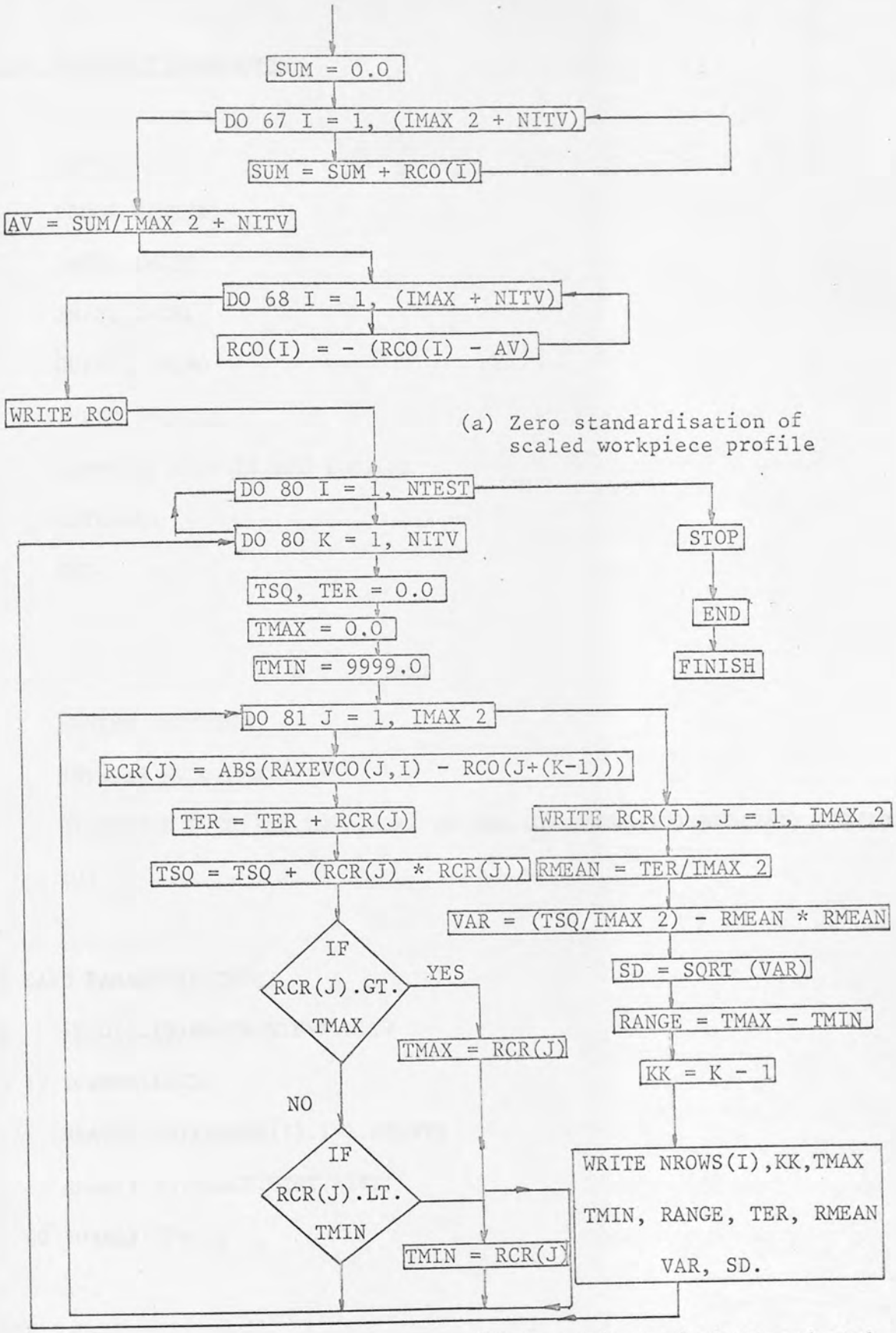

(a) Zero standardisation of scaled workpiece profile

(b) Comparison of wheel and workpiece profiles

SECTION 4. COMPARISON OF WHEEL AND WORKPIECE PROFILES

I.3 Computer Programme

```
      LIST
      PROGRAM(FXXX)
      INPUT 1=CRO
      INPUT 2=CR1
      OUTPUT 3=LPO
      INPUT 4=CR2
      COMPRESS INTEGER AND LOGICAL
      EXTENDED
      END


      MASTER GRINDING
      INTEGER EVCO.RMAX2
      DIMENSION EVCO(150.200).RAXEVCO(150.10).NROWS(10).RCO(261).RCR(100
      10)
C
C CARD PARAMETER INPUT
C     READ(1.19)NDATA.NTEST.NITV
   19 FORMAT(10I3)
      READ(1.19)(NROWS(I).I=1.NTEST)
      READ(1.20)SCALE.EINT.RINT
   20 FORMAT(3F6.2)
      I=1
      J=1
      IMAX1=0
      IMAX2=9999
```

```
C
C INPUT OF EVCO FROM DATA1
C     READ(2.22)IVALUE
   21 READ(2.22)IVALUE
   22 FORMAT(IO)
      IF(IVALUE.LT.0)GO TO 23
      EVCO(I.J)=IVALUE
      I=I+1
      IF(I.GT.IMAX1)IMAX1=I
      IF(I.LE.150)GO TO 21
   18 READ(2.22)IVALUE
      IF(IVALUE)23.18.18
   23 I=1
      WRITE(3.90)J.IMAX1
   90 FORMAT(10X.14.10X.14)
      J=J+1
      IF(IMAX1.LT.IMAX2)IMAX2=IMAX1
      IMAX1=0
      IF(J.LE.NDATA)GO TO 21
      IMAX2=IMAX2-1
C
C WRITE OUT OF EVCO
C
      NCNT=NDATA
      IH=-19
      IJ=0
   50 IH=IH+20
      IJ=IJ+20
      IF(NCNT.LT.20)IJ=NCNT
```

```
      NCNT=NCNT-20
      WRITE(3.51)((IK).IK=IH.IJ)
   51 FORMAT(1H1.///.53X.13H EVCO LISTING.//.9X.20(2X.13))
      DO 53 I=1.IMAX2
      WRITE(3.52)(I).(EVCO(I.J).J=IH.IJ)
   52 FORMAT(2X.13.5X.20(2X.13))
   53 CONTINUE
      IF(NCNT.GT.0)GO TO 50
C
C CREATION OF RAXEVCO - INITIAL MAXIMUMS
C     DO 26 I=1.NTEST
      IA=NROWS(I)
      DO 25 J=1.IMAX2
      IMAX=0
      DO 24 K=1.IA
      IF(EVCO(J.K).GT.IMAX)IMAX=EVCO(J.K)
   24 CONTINUE
      RAXEVCO(J.I)=IMAX * 1.0
   25 CONTINUE
   26 CONTINUE
      WRITE(3.30)
      WRITE(3.31)(NROWS(I).I=1.NTEST)
      DO 97 I=1.IMAX2
      WRITE(3.32)(I).(RAXEVCO(I.J).J=1.NTEST)
   97 CONTINUE
C
C        - ZERO STANDARDISATION
C
      DO 29 I=1.NTEST
```

```
      SUM=0.0
      DO 27 J=1.IMAX2
   27 SUM=SUM+RAXEVCO(J.I)
      AVE=SUM/IMAX2
      DO 28 J=1.IMAX2
   28 RAXEVCO(J.I)=RAXEVCO(J.I)-AVE
   29 CONTINUE
C
C WRITE OUT OF RAXEVCO
C
      WRITE(3.30)
   30 FORMAT(1H1.///.9X.40H GRINDING TEST: MAXIMUM VALUE ANALYSIS.//.1
     17X.24H MAXIMUM VALUE PRINTOUTS.//.1X.36H  ROW                NUMBER
     1OF COLUMN)
      WRITE(3.31)(NROWS(I).I=1.NTEST)
   31 FORMAT(1X.9HNUMBER    .10(13.4X)./)
      DO 33 I=1.IMAX2
      WRITE(3.32)(I).(RAXEVCO(I.J).J=1.NTEST)
   32 FORMAT(1X.I3.3X.10(1X.F6.1))
   33 CONTINUE
C
C INPUT OF RAZOR BLADE TRACE INTO RCR
C
      I=1
   60 READ(4.22)IRCO
      IF(IRCO.LT.0)GO TO 62
      RCR(I)=IRCO*1.0
      I=I+1
      GO TO 60
```

```
  62 RMAX2=I-1
C
C VERTICAL SCALING OF RCR
C
      DO 63 I=1.RMAX2
  63 RCR(I)=RCR(I)*SCALE
C
C RCR INTERVAL ADJUSTMENT TO CREATE RCO
C
      RCO(1)=RCR(1)
      DO 65 I=2.(IMAX2+NITV)
      EDIST=(I-1)*EINT
      RDIST=EDIST/RINT
      IR=INT(RDIST)
      IF((IR*RINT).EQ.RDIST)GO TO 64
      RDIST1=IR*RINT
      RDIST2=EDIST-RDIST1
      IR=IR+1
      RHT=RCR(IR)-((RCR(IR)-RCR(IR+1))*(RDIST2/RINT))
      RCO(I)=RHT
      GO TO 65
  64 RCO(I)=RCR(IR)
  65 CONTINUE
C
C ZERO ADJUSTMENT
C
      SUM=0.0
      DO 67 I=1.(IMAX2+NITV)
  67 SUM=SUM+RCO(I)
```

```
      AV=SUM/(IMAX2+NITV)
      DO 68 I=1.(IMAX2+NITV)
   68 RCO(I)=-(RCO(I)-AV)
C
C PRINT OUT OF RCO TRACE
C
      WRITE(3.69)
   69 FORMAT(1HO.//////.10X.10H RCO TRACE.//////)
      DO 70 I=1.(IMAX2+10)
   70 WRITE(3.71)I.RCO(I)
   71 FORMAT(10X.I3.10X.F6.1)
C
C START OF COMPARISON SECTION
C
      DO 80 I=1.NTEST
      DO 80 K=1.NITV
      TSQ.TER=0.0
      TMAX=0.0
      TMIN=9999.0
      DO 81 J=1.IMAX2
      RCR(J)=ABS(RAXEVCO(J.I)-RCO(J+(K-1)))
      TER=TER+RCR(J)
      TSQ=TSQ+(RCR(J)*RCR(J))
      IF(RCR(J).GT.TMAX)TMAX=RCR(J)
      IF(RCR(J).LT.TMIN)TMIN=RCR(J)
   81 CONTINUE
      WRITE(3.83)(RCR(J).J=1.IMAX2)
   83 FORMAT(15(1X.F6.1))
      RMEAN=TER/IMAX2
```

```
      VAR=(TSQ/IMAX2)-(RMEAN*RMEAN)
      SD=SQRT(VAR)
      RANGE=TMAX-TMIN
      KK=K-1
      WRITE(3.84)NROWS(I).KK.TMAX.TMIN..RANGE.TER.RMEAN.VAR.SD
   84 FORMAT(///.30X.26H NUMBER OF ROWS IN TEST = .I4./.33X.23H RAZOR TR
     1ACE POSITION = .I4.///.10X.17H MAXIMUM ERROR = .F6.1.10X.17H MINIM
     1UM ERROR = .F6.1.10X.18H RANGE OF ERROR = .F6.1.//.5X.15H TOTAL E
     1RROR = .F8.1. 5X.14H MEAN ERROR = .F6.1. 5X.21H VARIANCE OF ERROR
     1= .F6.1. 5X.21H STD.DEV. OF ERROR = .F6.3.///)
   80 CONTINUE
      STOP
      END
```

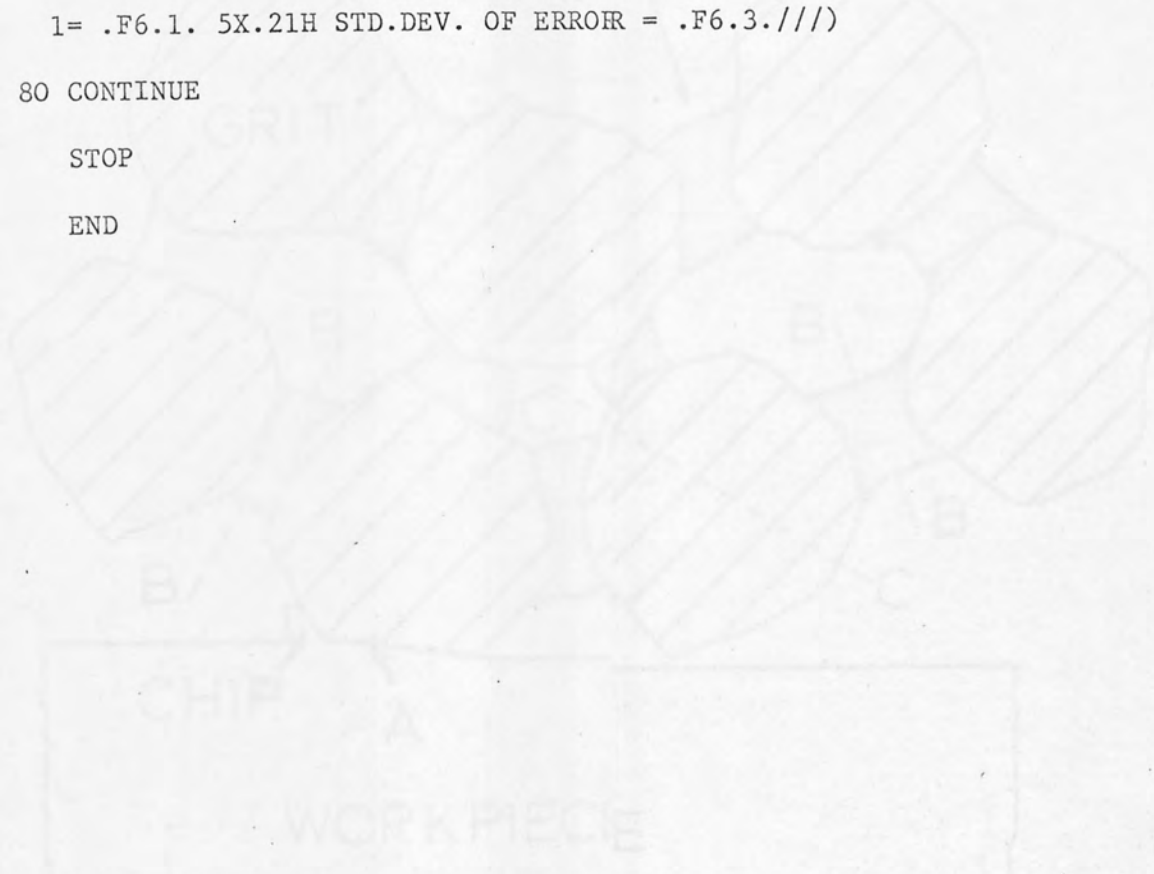

Grinding wheel construction and wear processes

Fig.1

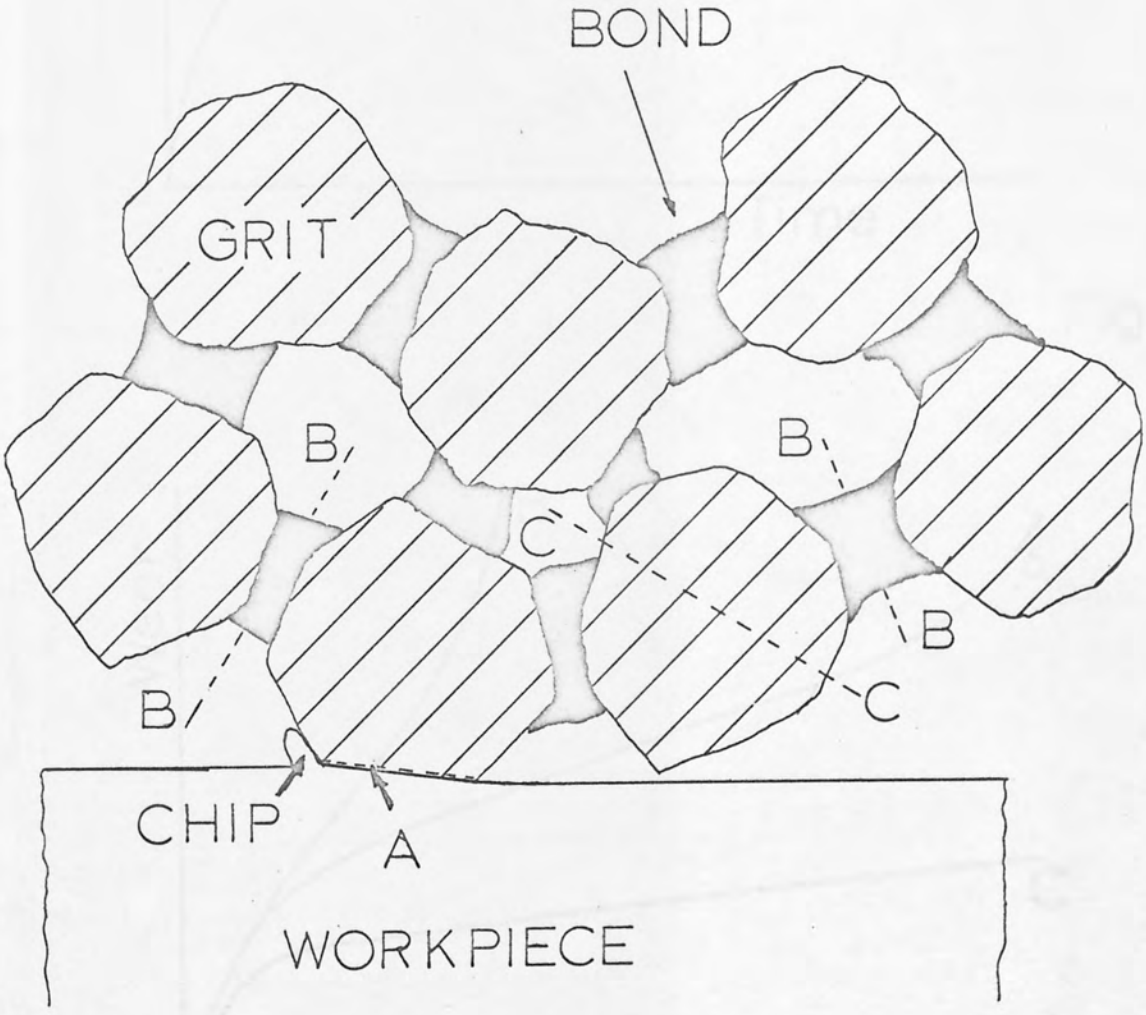

Grinding wheel construction and wear processes

Fig.1

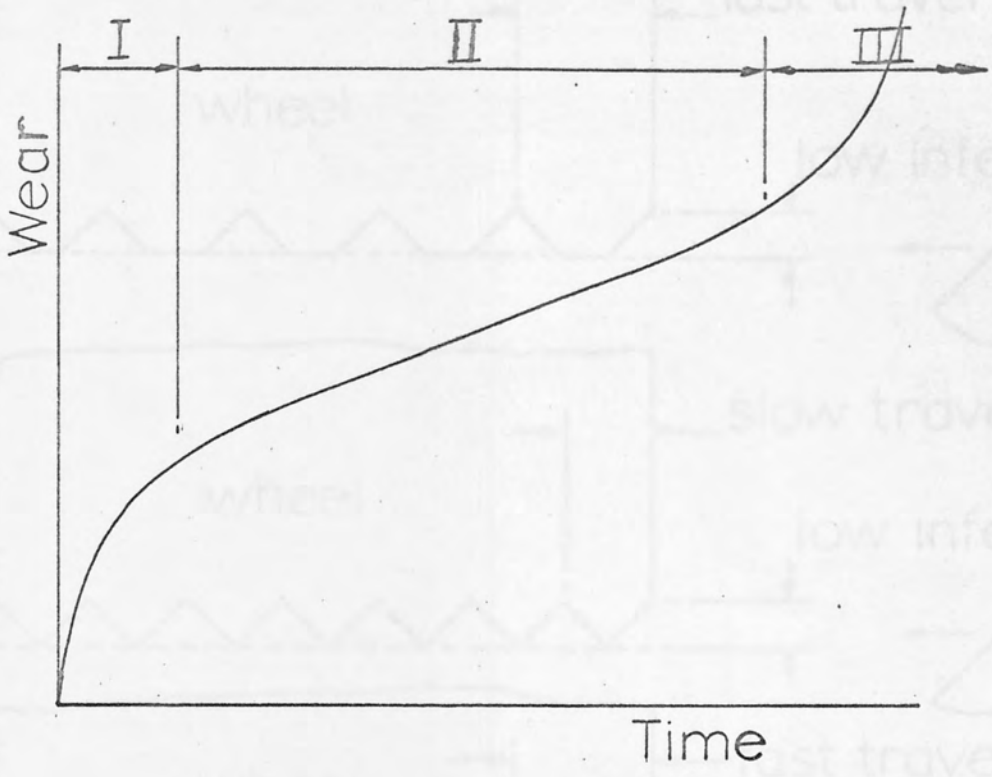

Fig.2a

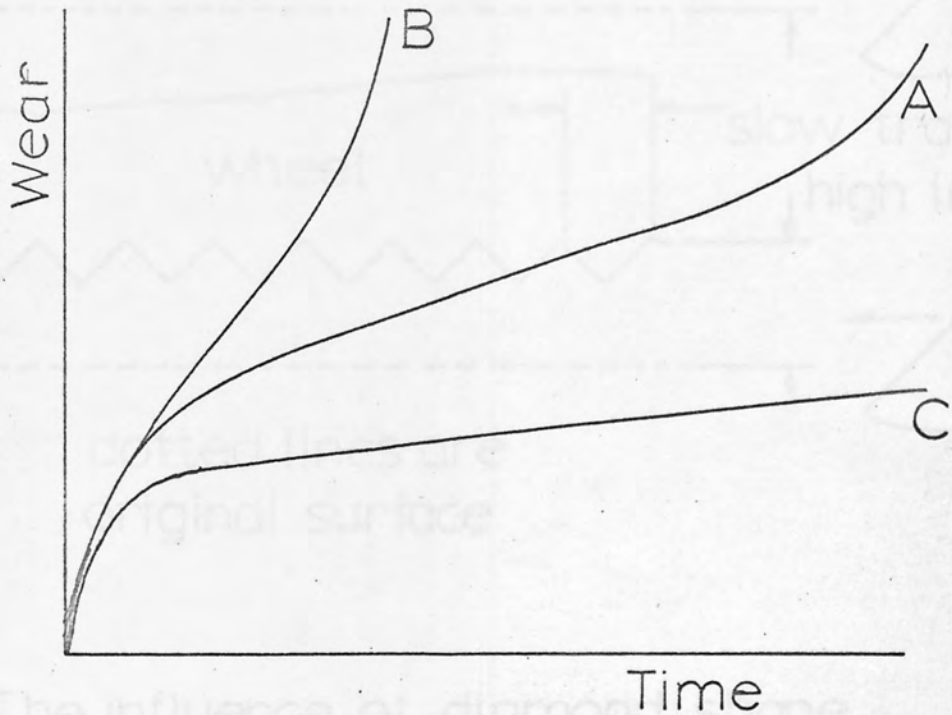

Patterns of wheel wear with time

Fig.2b

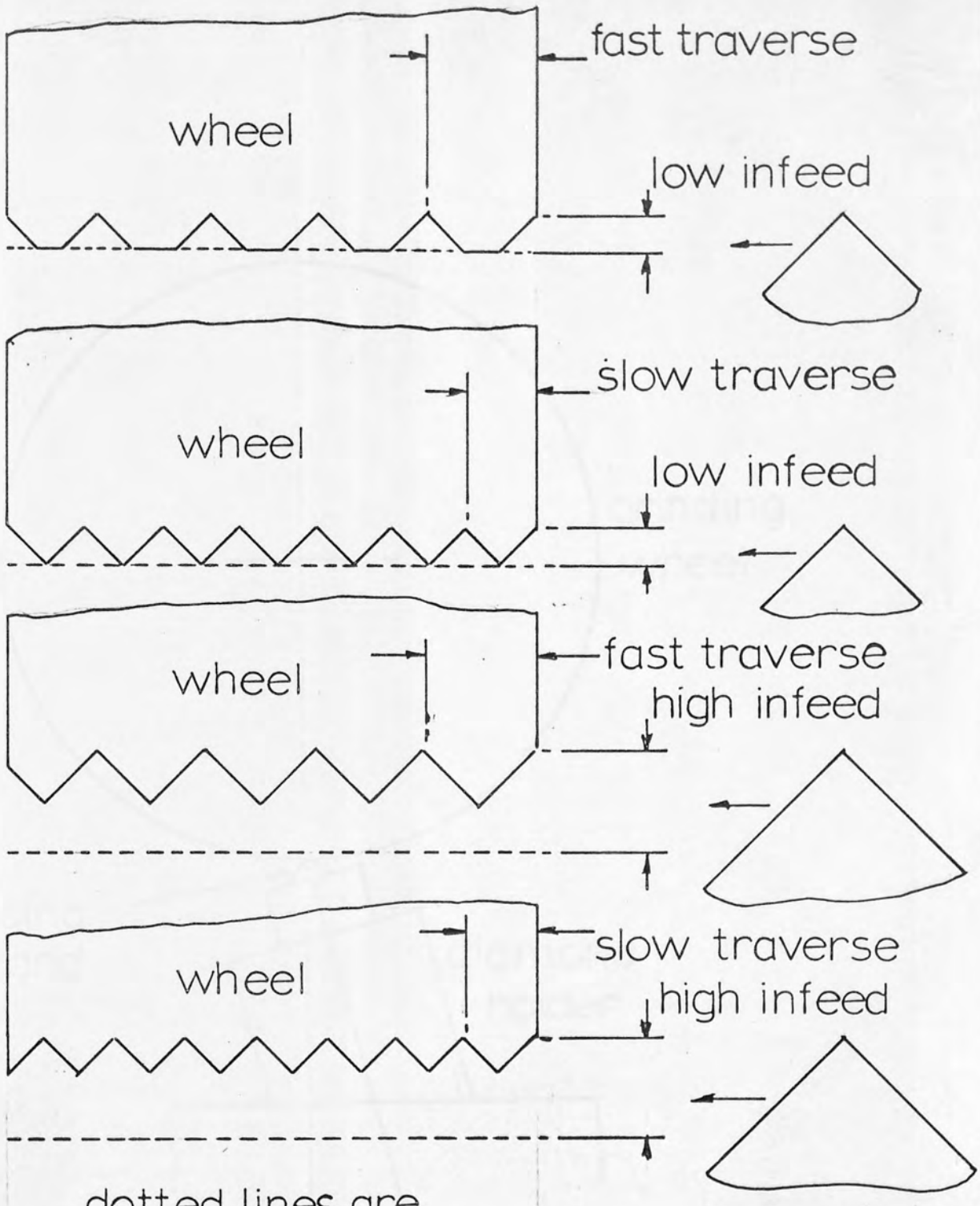

The influence of diamond shape, traverse rate and infeed on the wheel surface

Fig.3

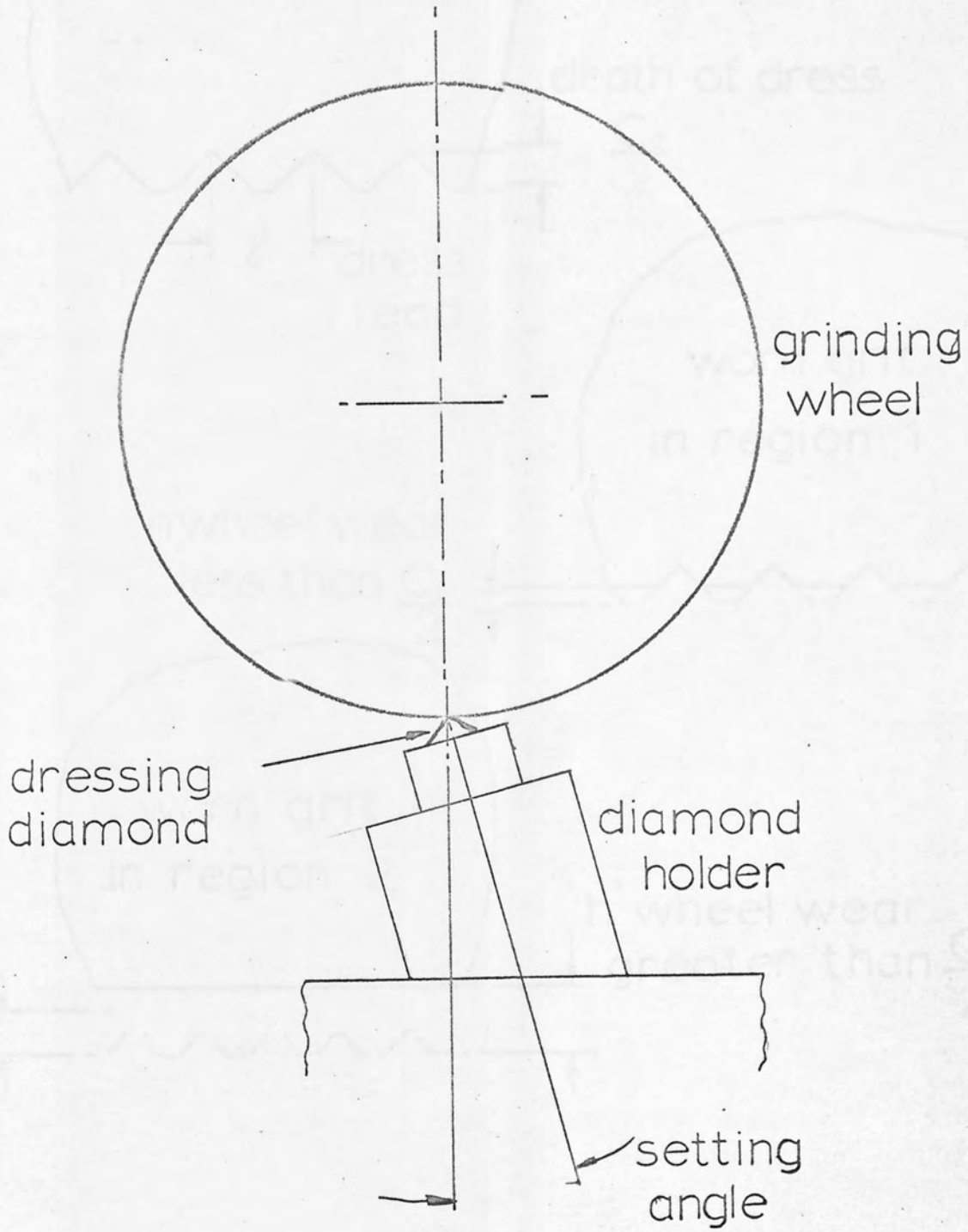

Diamond setting angle

Fig. 4

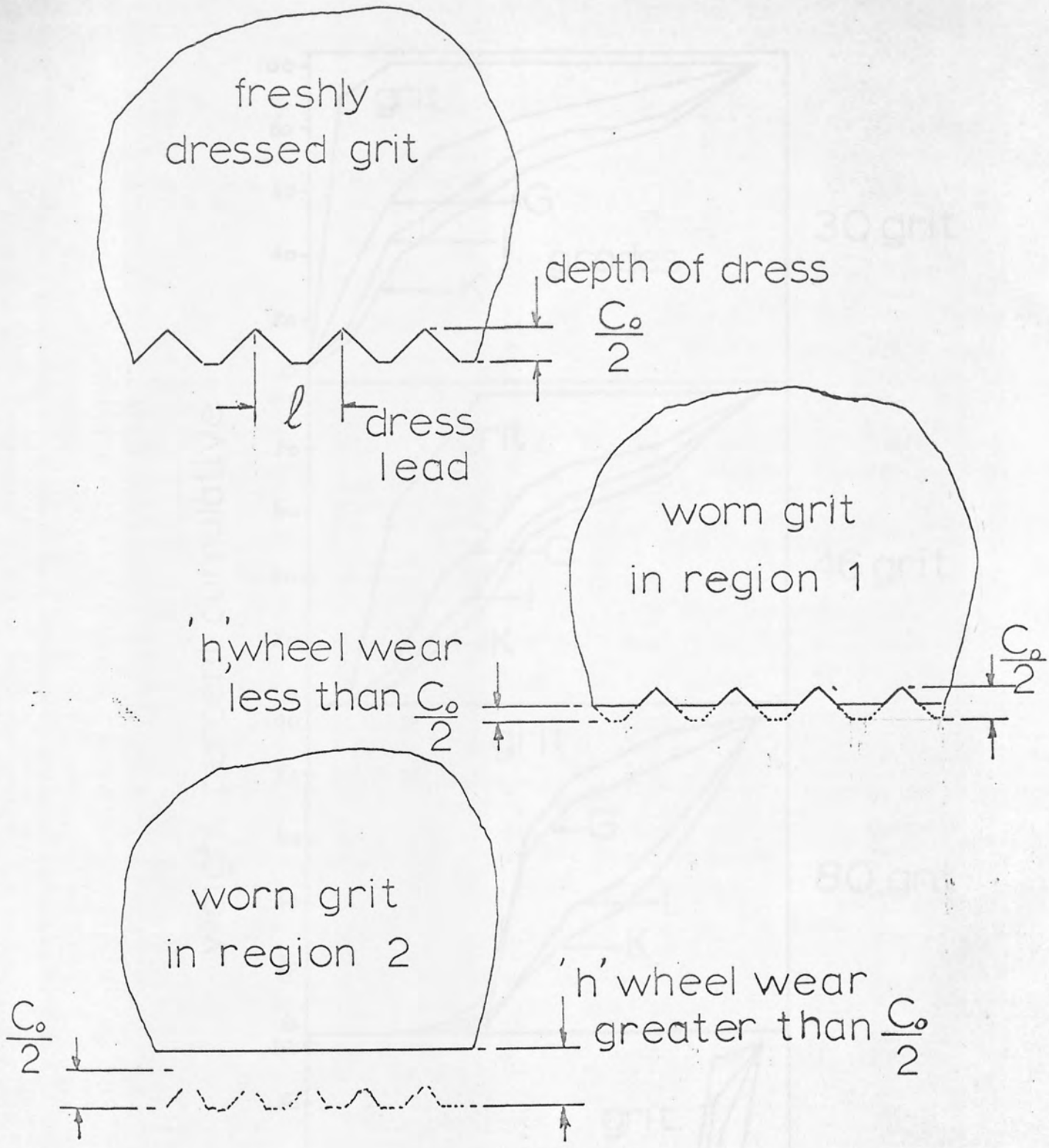

Wear on the grits

Lindsay ref. 18

Fig.5

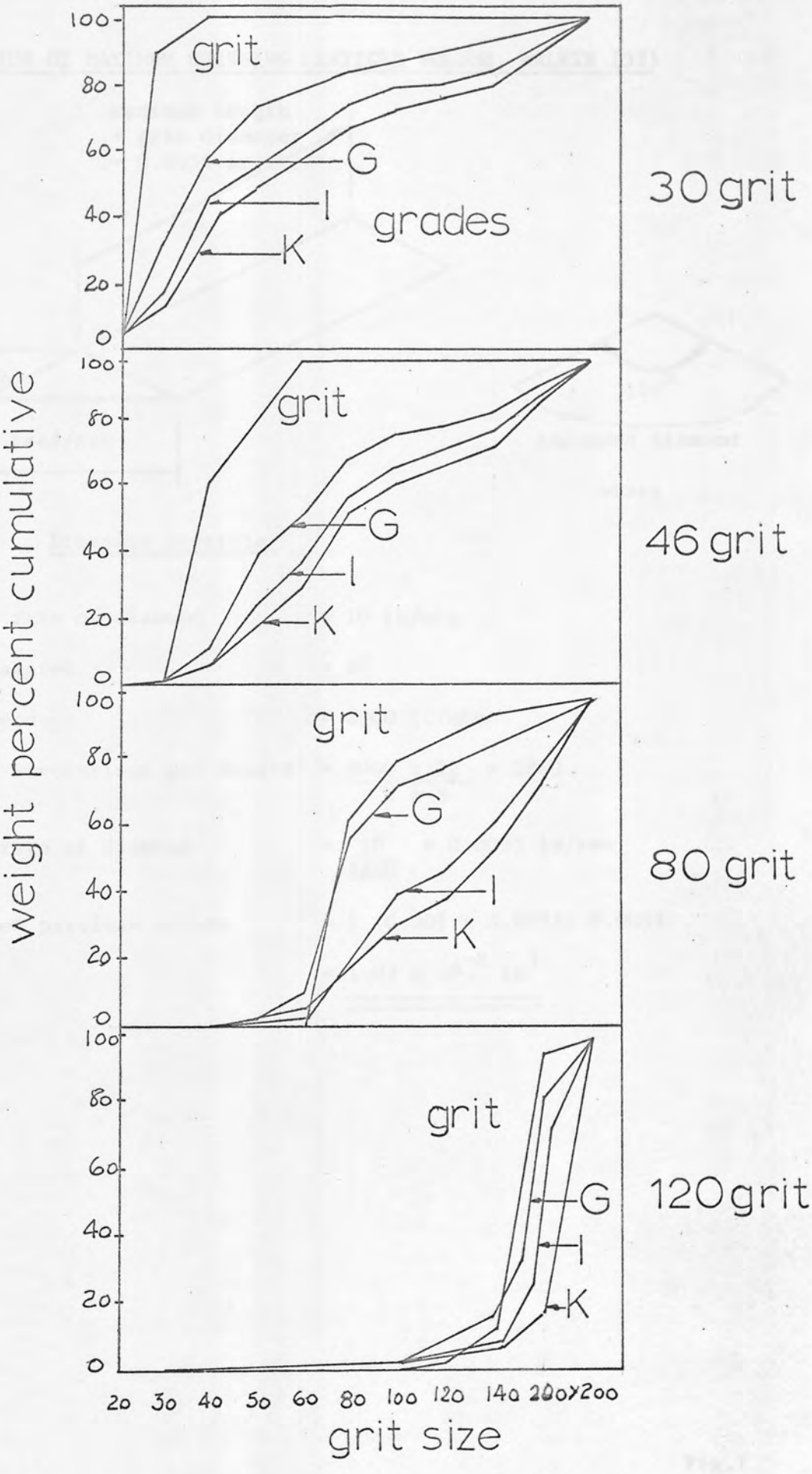

Dressing particle size distribution

Malkin ref. 40 Fig.6

CALCULATION OF MAXIMUM DRESSING PARTICLE VOLUME . MALKIN (32)

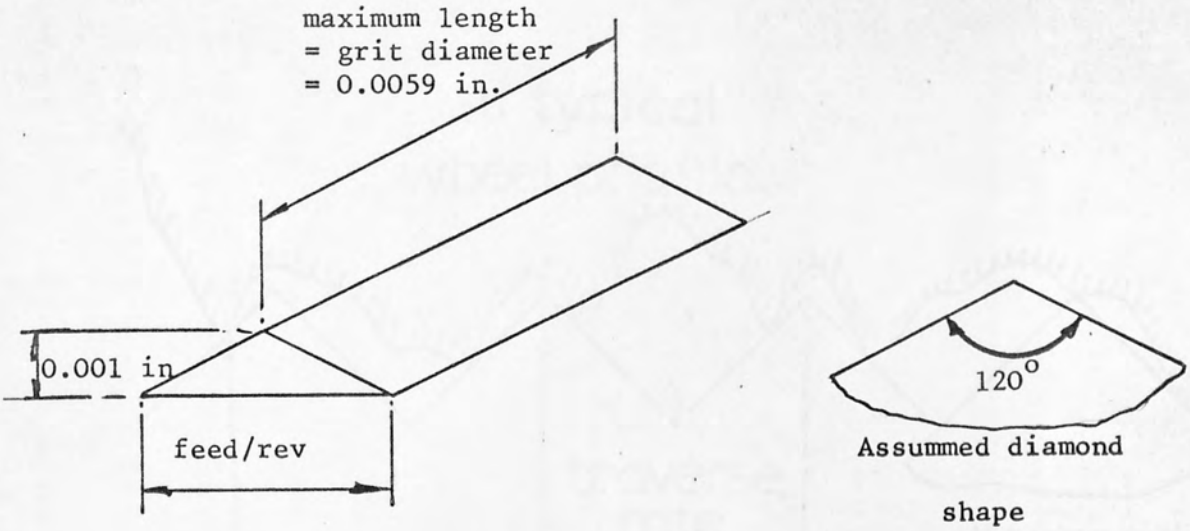

Dressing particle

Traverse rate of diamond = 10 in/min

Wheel diameter = 8"

Wheel speed = 6000 ft/min

Wheel revolutions per minute $= \frac{6000 \times 12}{\pi \times 8} = 2860$

Feed rate of diamond $= \frac{10}{2860} = 0.0035$ in/rev

Maximum particle volume $= \frac{1}{2} (0.001 \times 0.0035)\ 0.0059$

$= 1.03 \times 10^{-8}\ in^3$

Fig.7

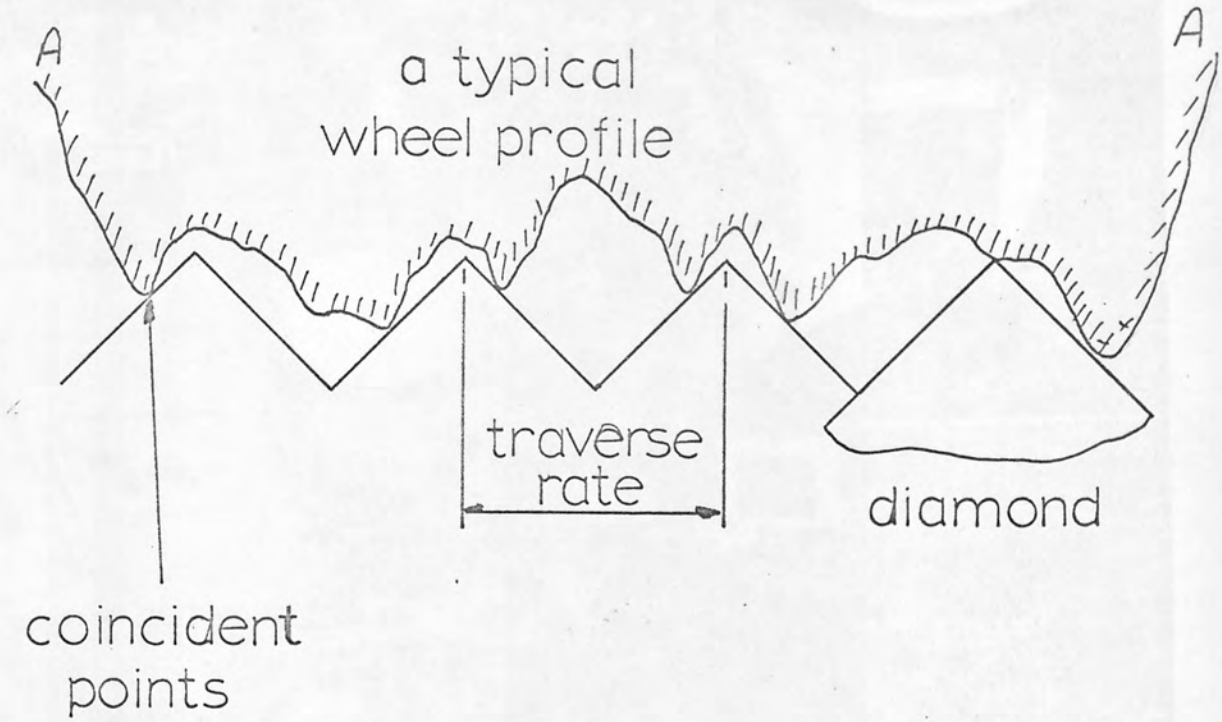

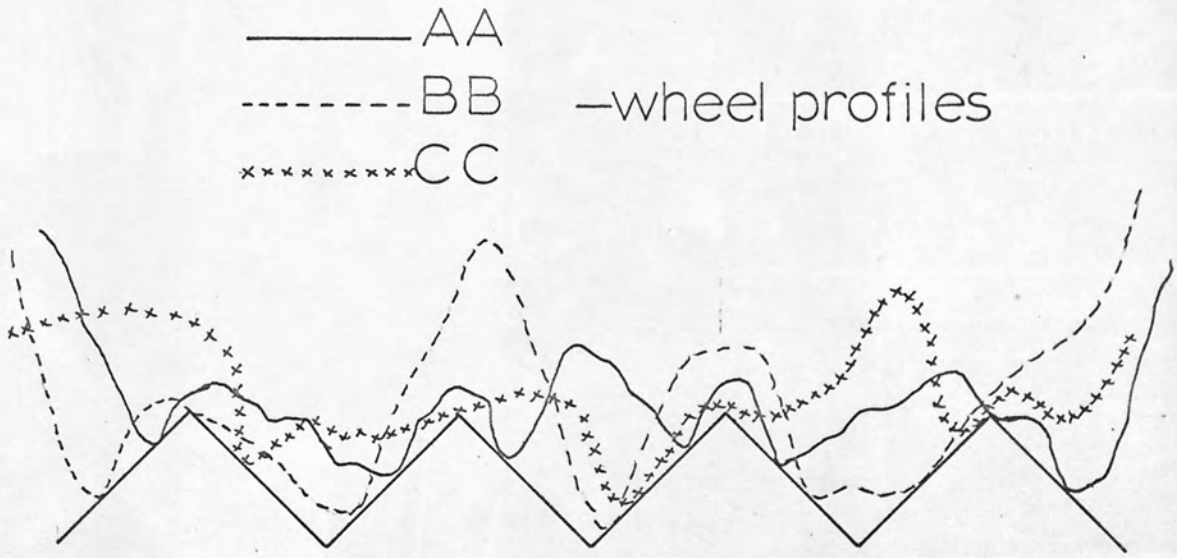

Workpiece surface generation

Fig.8

Fig.9

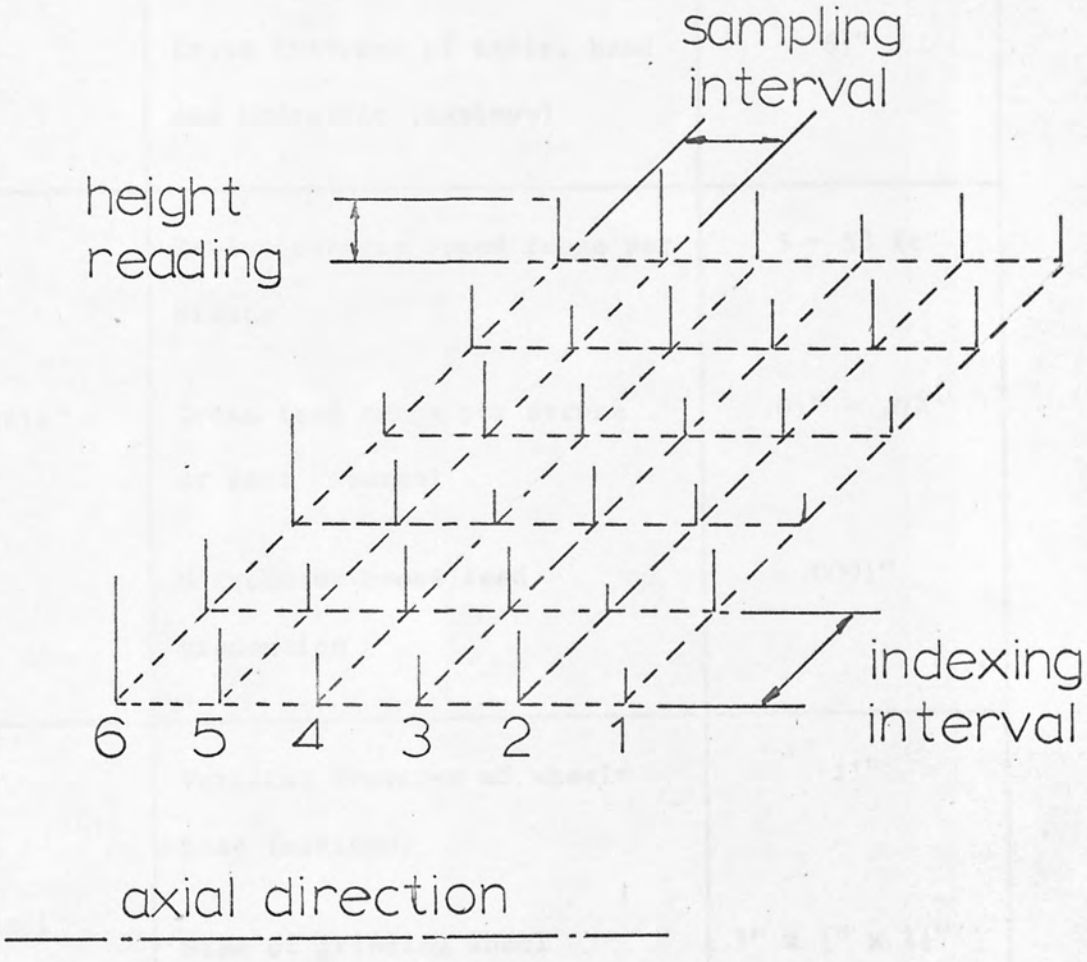

Network of wheel profiles

Fig.10

Capacity	Working surface of table	18" x 6"
	Longditudinal traverse of table, hand and hydraulic (maximum)	19"
	Cross traverse of table, hand and hydraulic (maximum)	$6\frac{3}{4}$"
Table	Table traverse speed range per minute	5 - 55 ft
	Cross feed range per stroke at each reversal	.01" - .07"
	Micrometer cross feed graduation	.0001"
Wheel head	Vertical traverse of wheel-head (maximum)	11"
	Size of grinding wheel	7" x $\frac{1}{2}$" x $1\frac{1}{4}$"
	Speed of wheel	2800 rpm
	Wheelhead motor	1 HP

Grinding machine specification

Fig.11

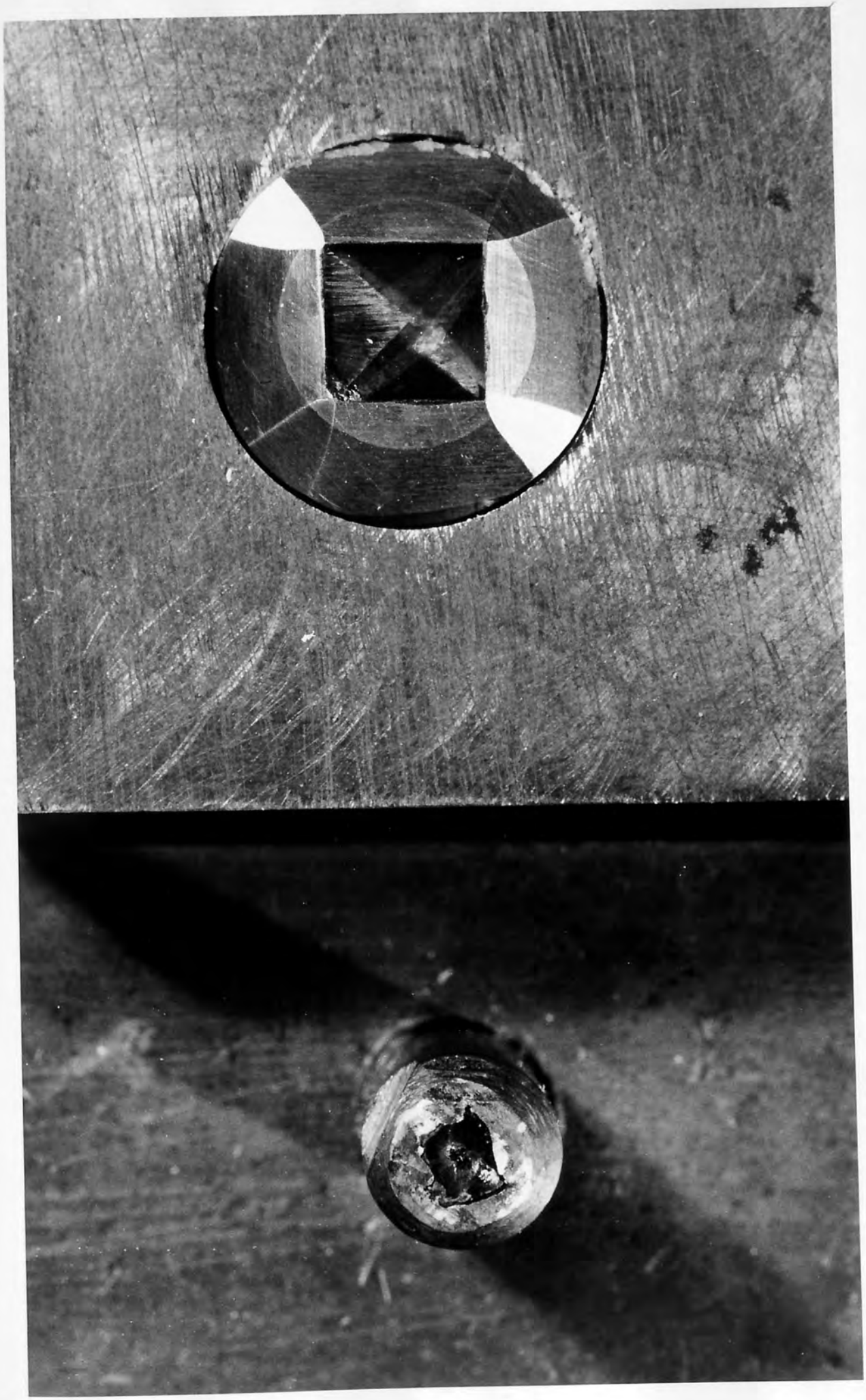

Fig.12

Fig.13

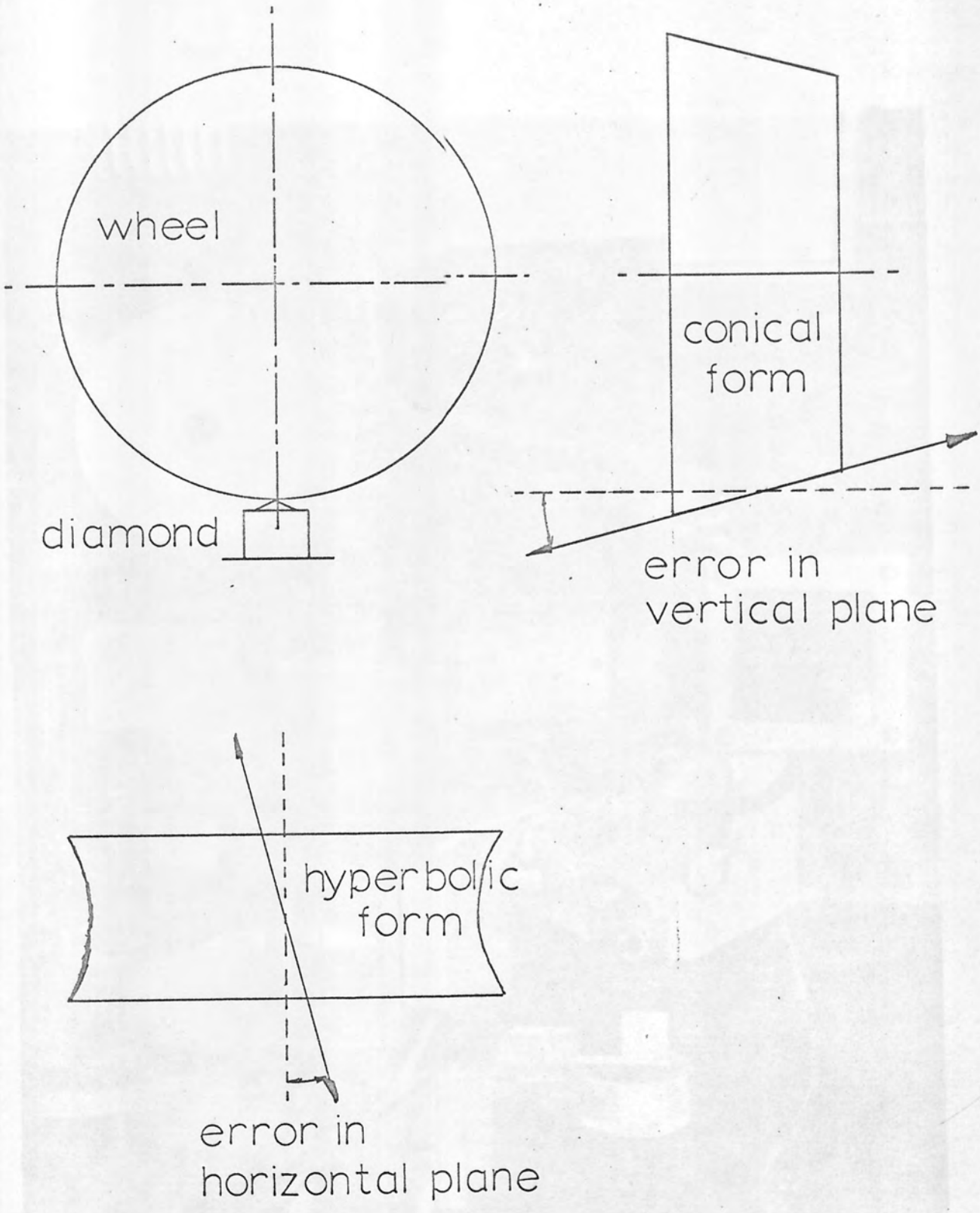

Errors in wheel form

Fig.14

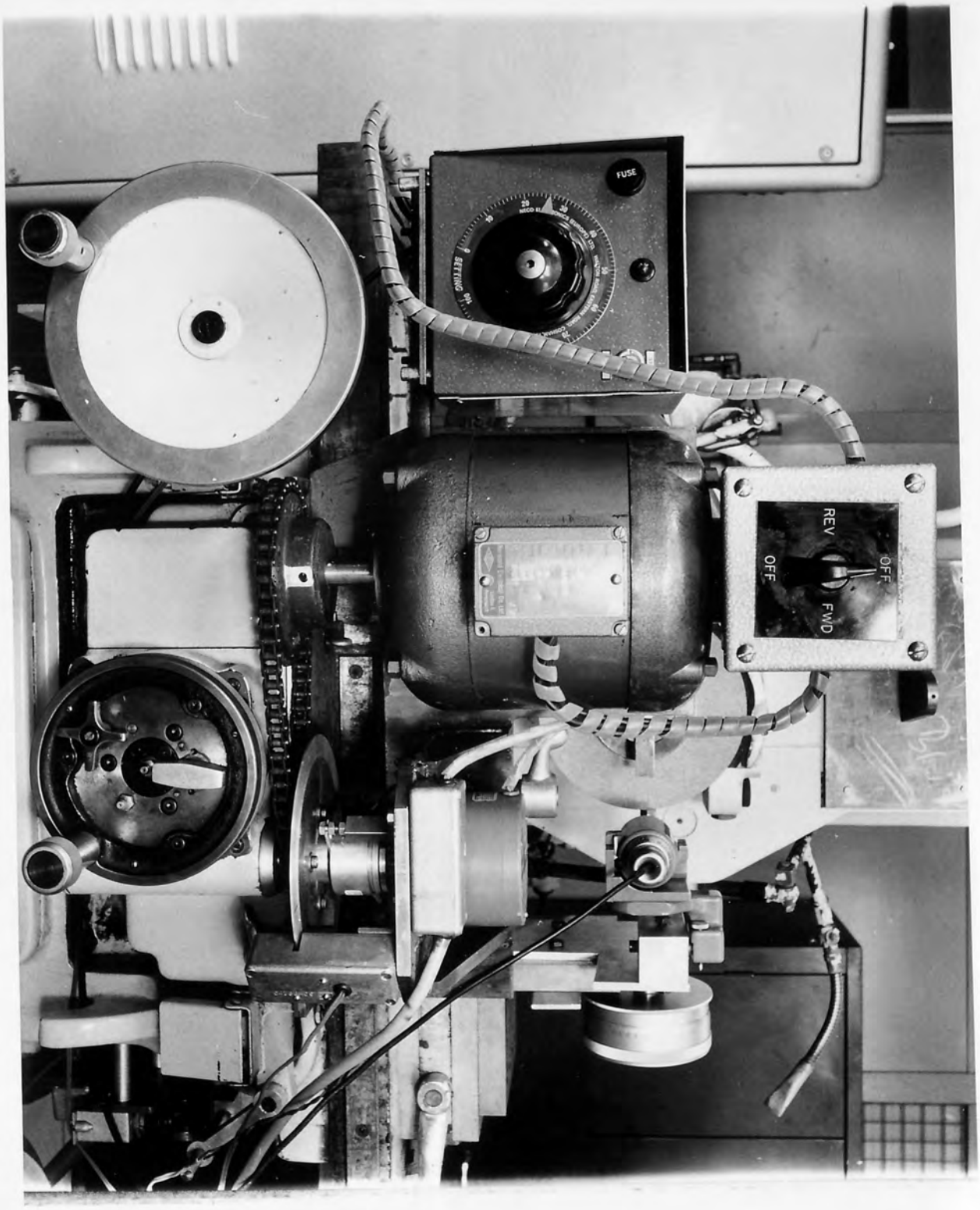

Fig.15

MACHINE TABLE FINE FEED SHAFT SPEEDS

Dressing motor - controllable speed range

= 200 - 2000 revs/min

Gear ratio from motor to fine feed shaft = 3.8 : 1

Fine feed shaft speeds = 760 - 7600 revs/min

MACHINE TABLE CROSS TRAVERSE SPEEDS

Cross traverse per revolution of the

fine feed shaft = .005 in.

Cross traverse speeds = 3.8 - 38.0 in/min

DRESSING DIAMOND TRAVERSE RATES

Grinding wheel speed = 2800 revs/min

Maximum dressing traverse rate = $\frac{38.0}{2800}$ = 0.0136 in/rev

Minimum dressing traverse rate = $\frac{3.8}{2800}$ = 0.0014 in/rev

Available diamond dressing traverse speeds

Fig.16

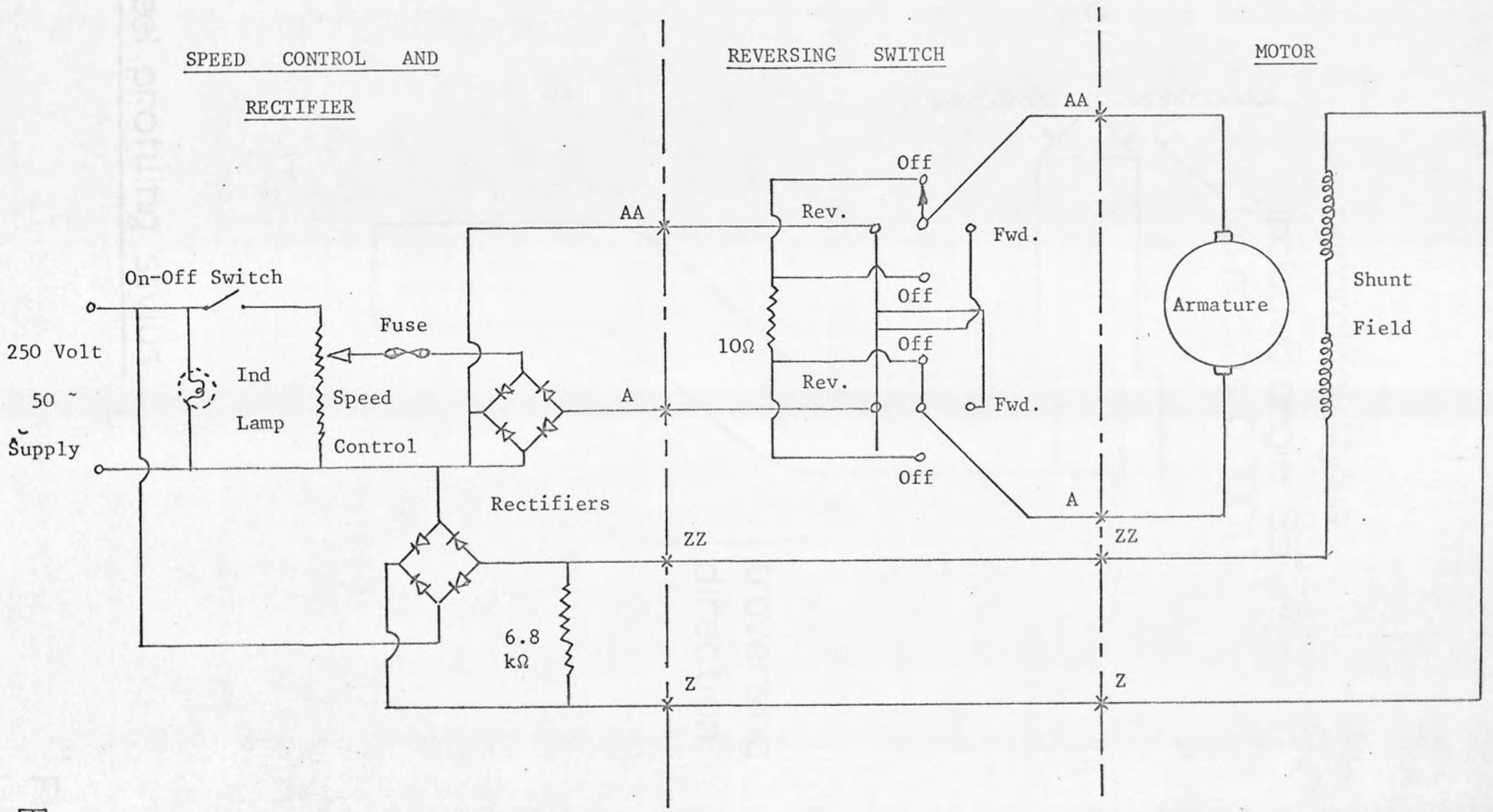

Fig. 17

WIRING DIAGRAM FOR SPEED CONTROL, REVERSING SWITCH AND MOTOR

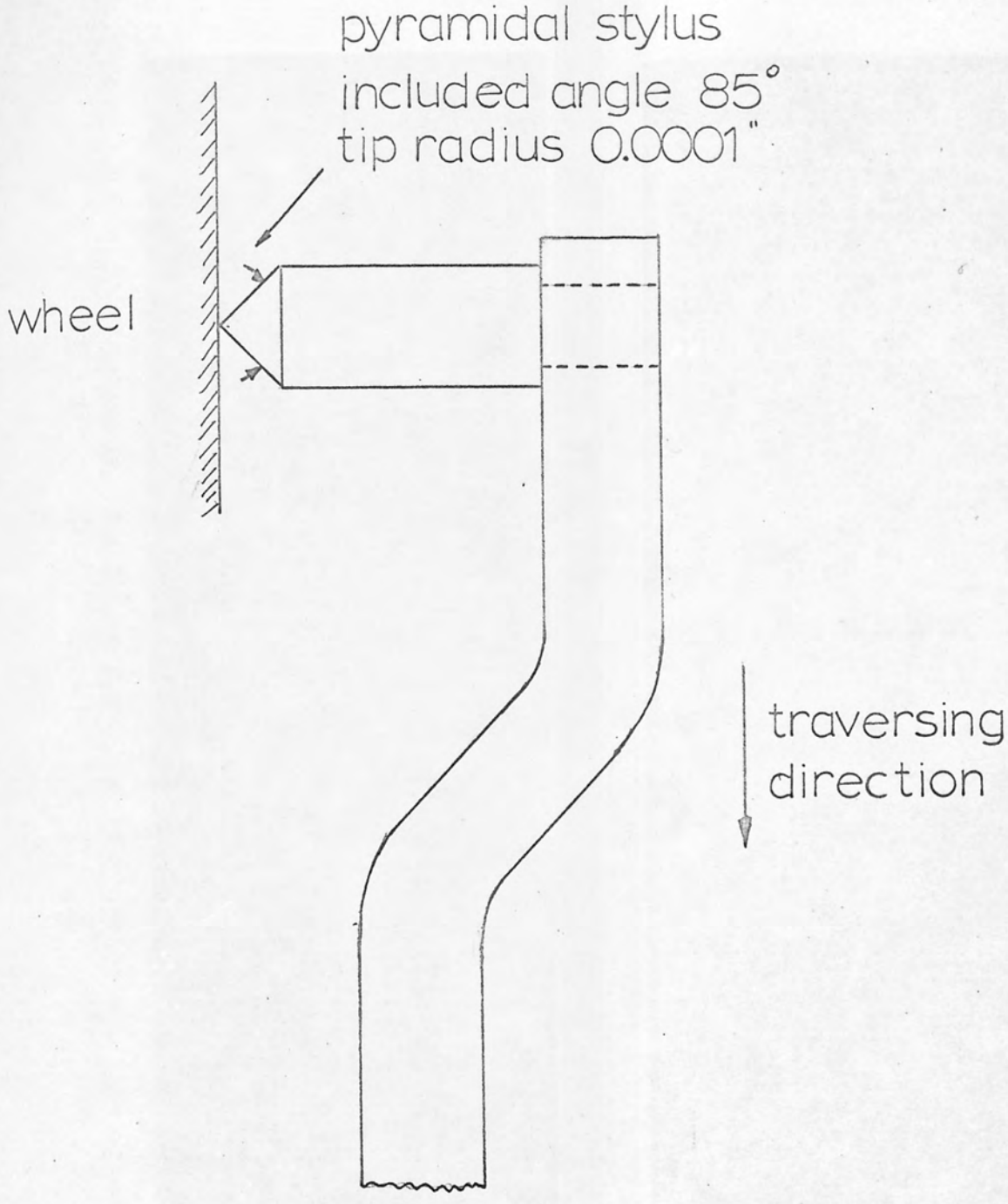

Wheel profiling stylus

Fig.18

Typical wheel and workpiece profiles

Fig.19

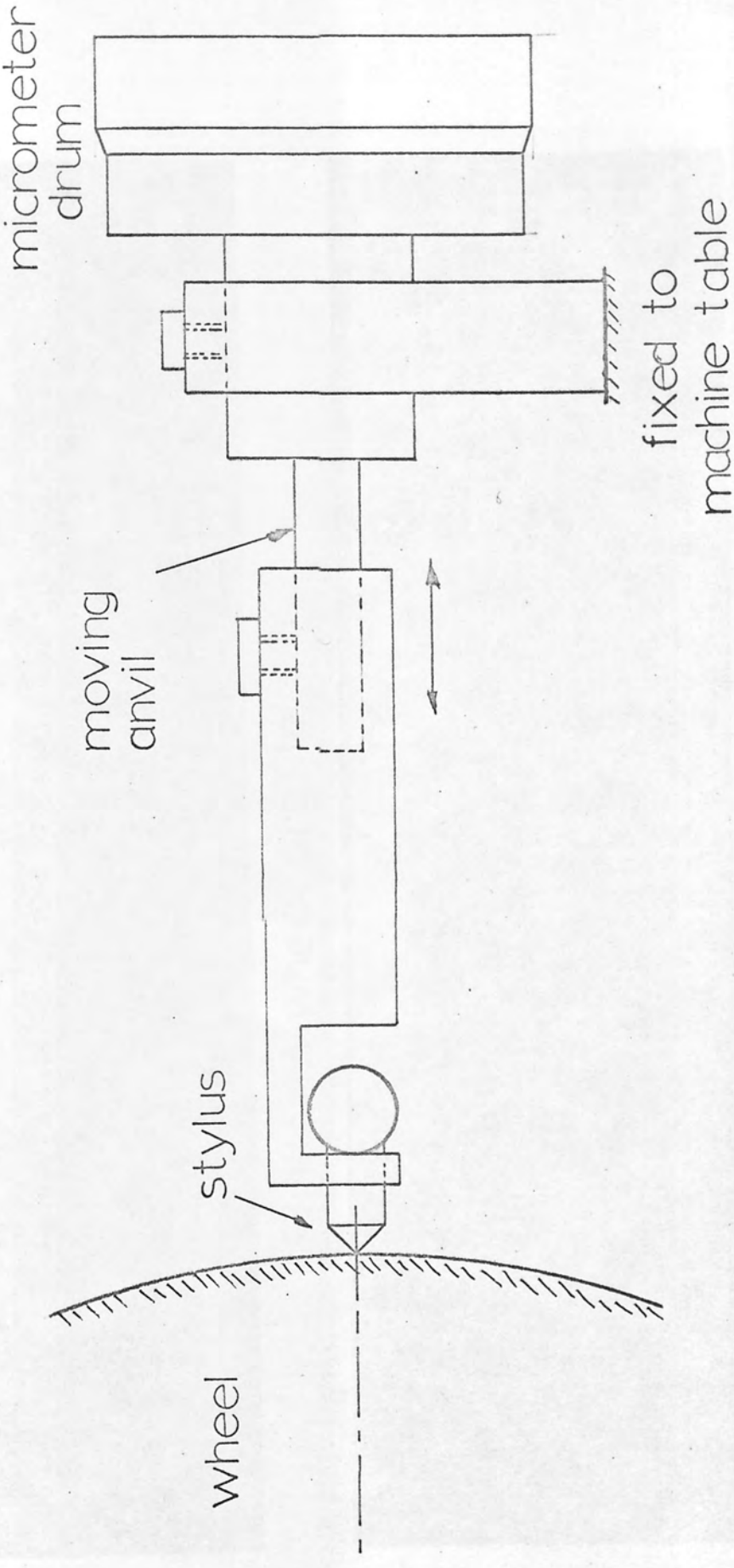

Profiling stylus cut-off system

Fig. 20

Full-form and cut-off wheel profiles

Fig. 21

Fig.22

'M' SERIES SLO-SYN STEPPING MOTOR

Motor type : M091 - FD09

Supplier : Superior Electric Nederland N.V.

Step angle	1.8^{o}
Total steps per revolution	200
Time for single step (m.sec.)	3.1
Nominal rated torque (oz.in.)	110

Stepping motor specification

Fig.23

Machine table drive system

Fig. 24

PROFILING STYLUS TRAVERSE SPEEDS

A number of pulse frequencies were available to drive the motor (Fig.26).

Total number of motor steps per revolution = 200

Considering a pulse frequency of 40 Hz

Motor revolutions per second = $\frac{40}{200}$ = 0.2

Machine table traverse per revolution of the fine feed shaft = 0.005 in

Profiling stylus traverse speed = 0.2 x 0.005

= 0.001 in/sec

Pulse frequency (Hz)	Traverse speed (in/sec)
40	0.0010
100	0.0025
200	0.0050
500	0.0125
500 Reverse	0.0125

Profiling stylus traverse speeds

Fig.25

Stepping motor drive system

Fig. 26

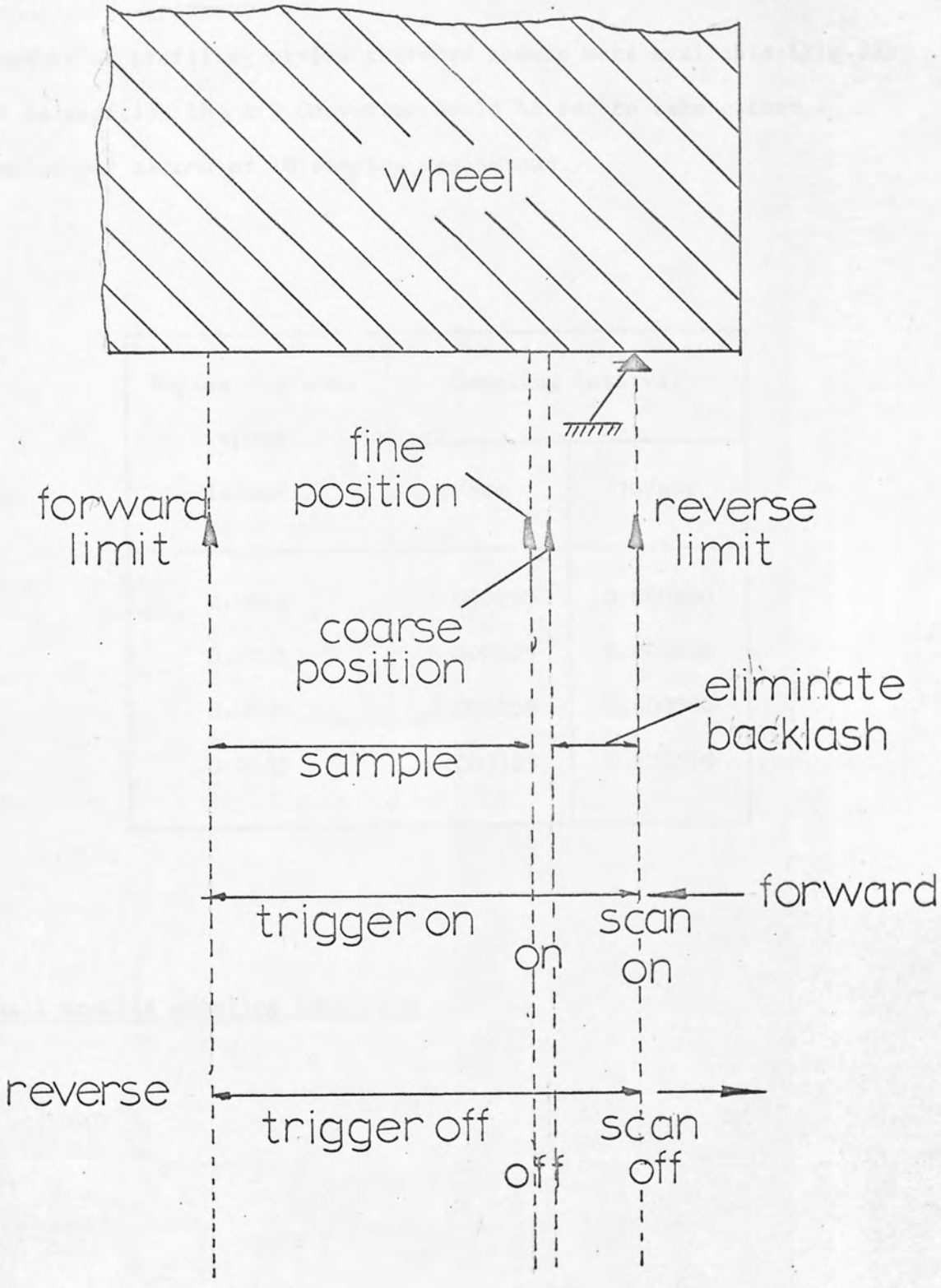

Functions - stylus traversing system

Fig. 27

WHEEL PROFILE SAMPLING INTERVALS

A number of profiling stylus traverse speeds were available (Fig.25) and in addition the A-D Converter could be set to take either 4 samples per second or 10 samples per second.

Stylus traverse speed in/sec	Sampling interval	
	4/sec	10/sec
0.0010	0.000250	0.000100
0.0025	0.000625	0.000250
0.0050	0.001250	0.000500
0.0125	0.003125	0.001250

Wheel profile sampling intervals

Fig.28

Fig.29

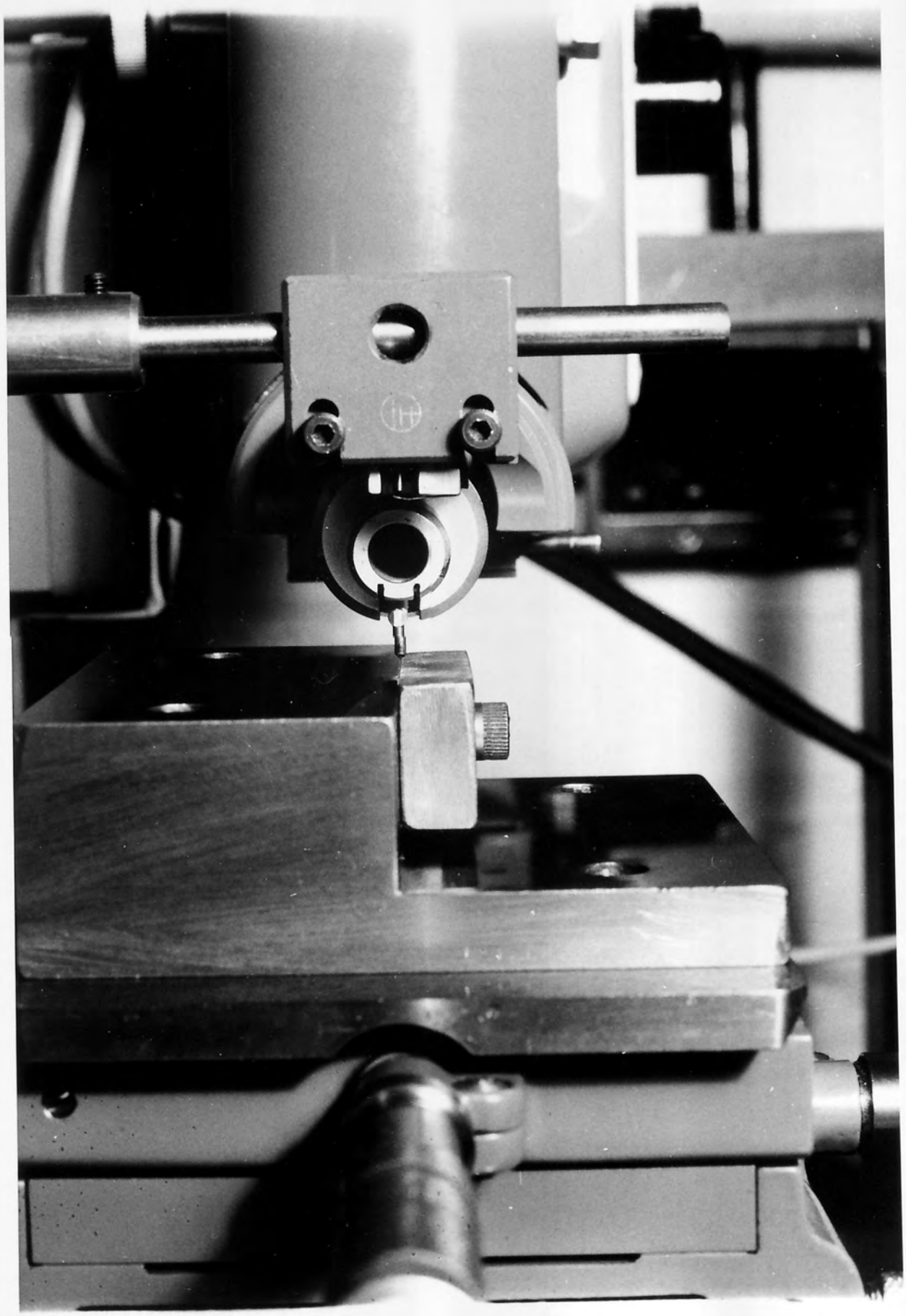

Fig.30

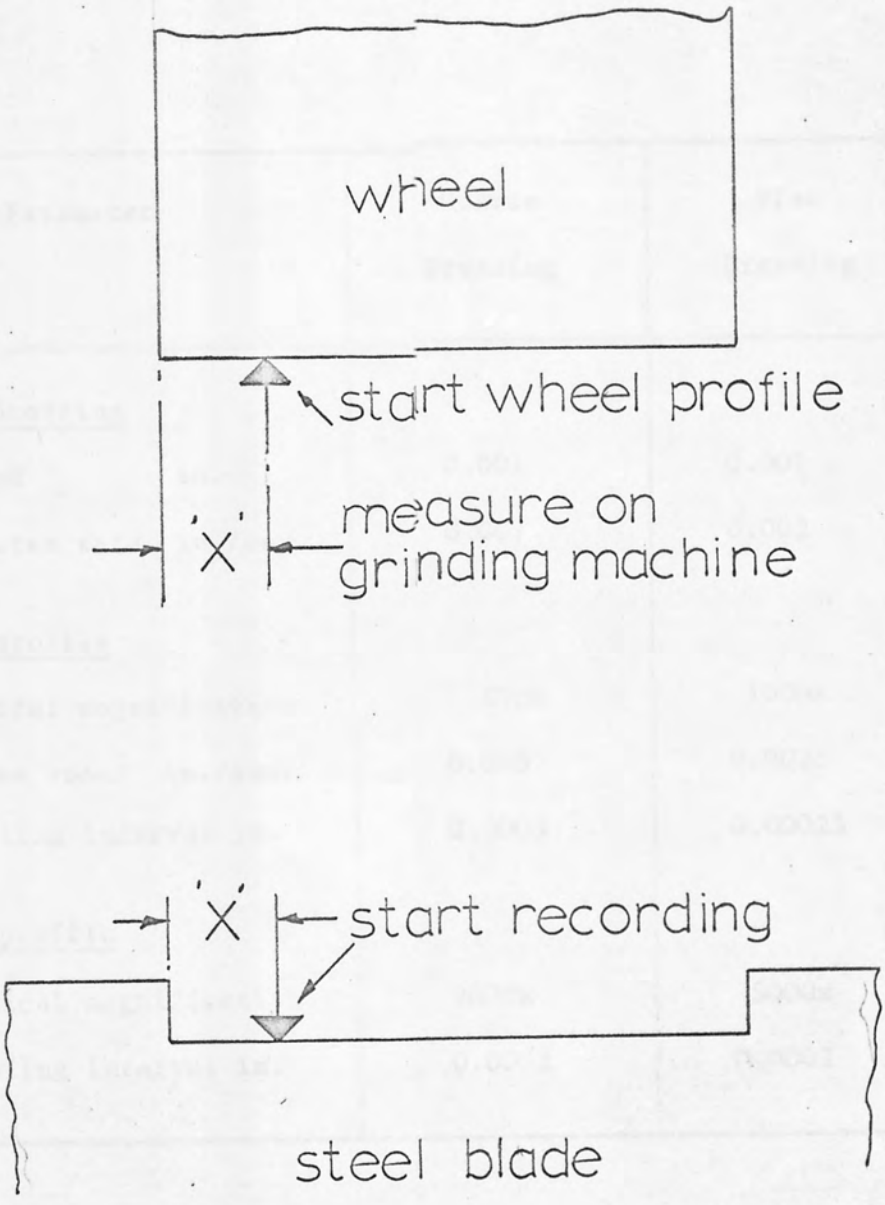

Technique to ensure wheel and workpiece profiles start from the same point

Fig. 31.

Parameter	Coarse Dressing	Fine Dressing
Wheel dressing		
Infeed in.	0.001	0.001
Traverse rate in./rev.	0.007	0.002
Wheel profile		
Vertical magnification	500x	1000x
Stylus speed in./sec.	0.005	0.0025
Sampling interval in.	0.0005	0.00025
Blade profile		
Vertical magnification	2000x	5000x
Sampling interval in.	0.0002	0.0002

Test conditions for comparison of wheel and workpiece profiles

Fig.32

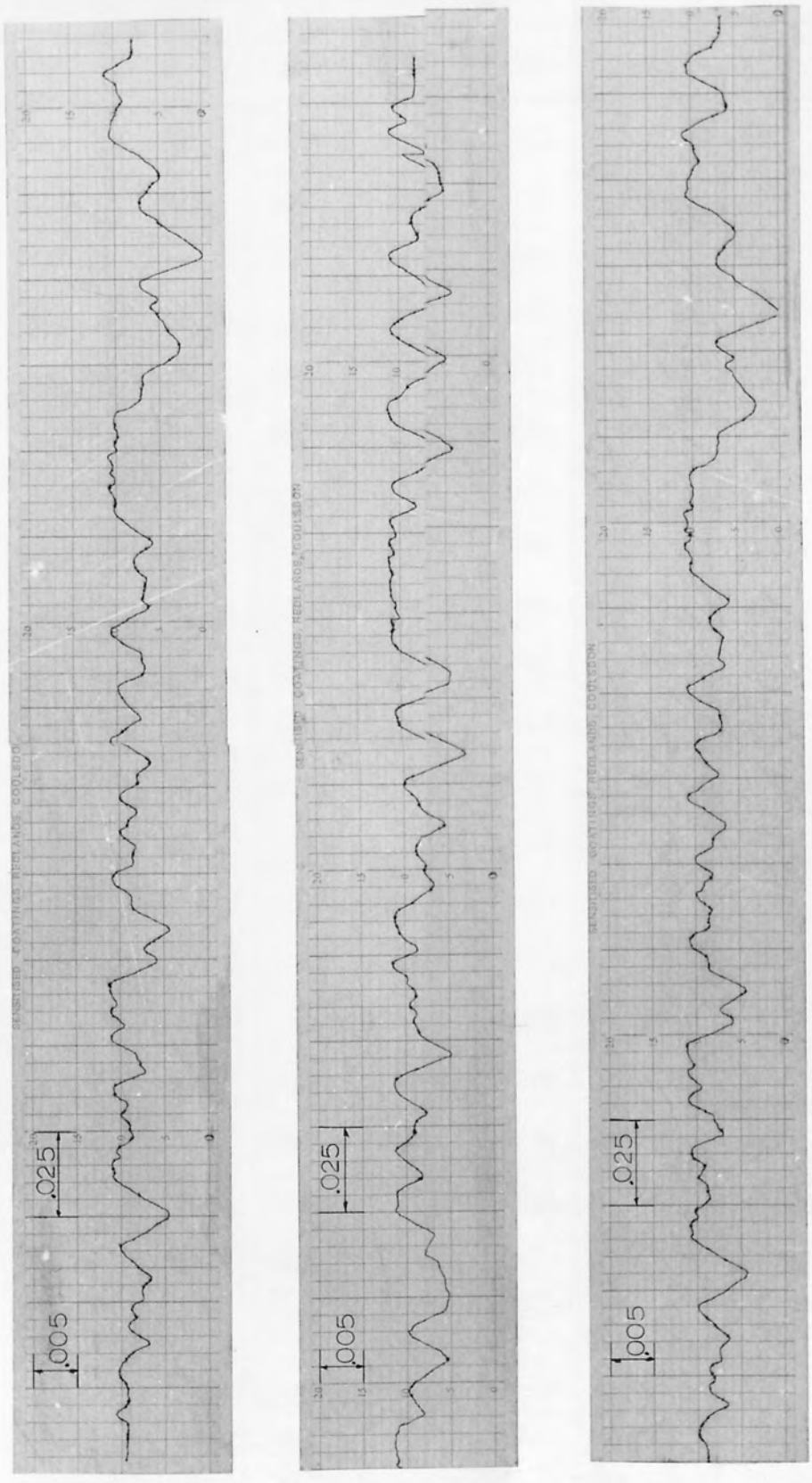

Typical wheel profiles

Fig. 33

ROW NO	NUMBER OF COLUMNS FROM EVCO MATRIX							
	20	40	60	80	100	120	140----	200
1	624	624	624	707	707	721	721	721
2	480	480	480	658	658	658	691	735
3	410	410	410	654	654	686	686	710
4	362	438	438	610	610	694	694	720
5	380	528	528	610	610	654	654	723
6	406	602	602	610	610	610	623	697
7	440	615	615	615	615	615	635	681
8	430	626	626	626	626	626	626	639
9	402	670	670	670	670	670	670	670
10	346	687	687	687	687	687	687	687
11	398	684	684	684	684	684	684	684
12	450	670	670	670	670	670	670	670
13	390	660	660	660	660	660	660	660
14	454	670	670	670	670	670	670	670
15	520	673	673	673	673	673	687	687
16	543	673	673	673	673	673	697	697
17	605	608	608	608	608	669	669	669
18	638	638	638	638	638	638	638	639
19	629	629	629	629	641	641	641	669
20	599	599	599	599	622	630	630	637
.....								
150	568	568	670	670	670	670	670	732

RAXEVCO matrix - coarsely dressed wheel

Fig.34

ROW NO	NUMBER OF COLUMNS FROM EVCO MATRIX							
	20	40	60	80	100	120	140------	---200
1	680	680	700	700	700	700	700	700
2	700	700	700	700	700	700	701	701
3	602	602	602	700	700	700	700	727
4	540	540	540	711	711	711	711	740
5	520	520	520	720	720	720	720	740
6	527	527	527	700	707	707	707	710
7	543	543	543	600	700	700	700	723
8	640	640	640	640	650	650	650	701
9	647	647	647	647	700	700	700	700
10	700	707	707	707	721	721	721	721
11	700	800	800	800	800	800	800	800
12	720	740	740	740	740	740	740	740
13	700	721	721	721	740	740	740	740
14	713	713	713	713	740	740	740	740
15	717	717	717	717	720	720	720	720
16	700	700	700	700	700	700	700	703
17	700	711	711	711	711	720	720	750
18	703	743	743	743	743	743	743	800
19	700	743	743	743	743	743	743	807
20	700	740	740	740	740	753	753	807
.....								
150	700	700	700	700	700	700	700	700

RAXEVCO matrix - finely dressed wheel

Fig.35

Wheel and workpiece profile comparison
Coarse dressing

Fig 36.

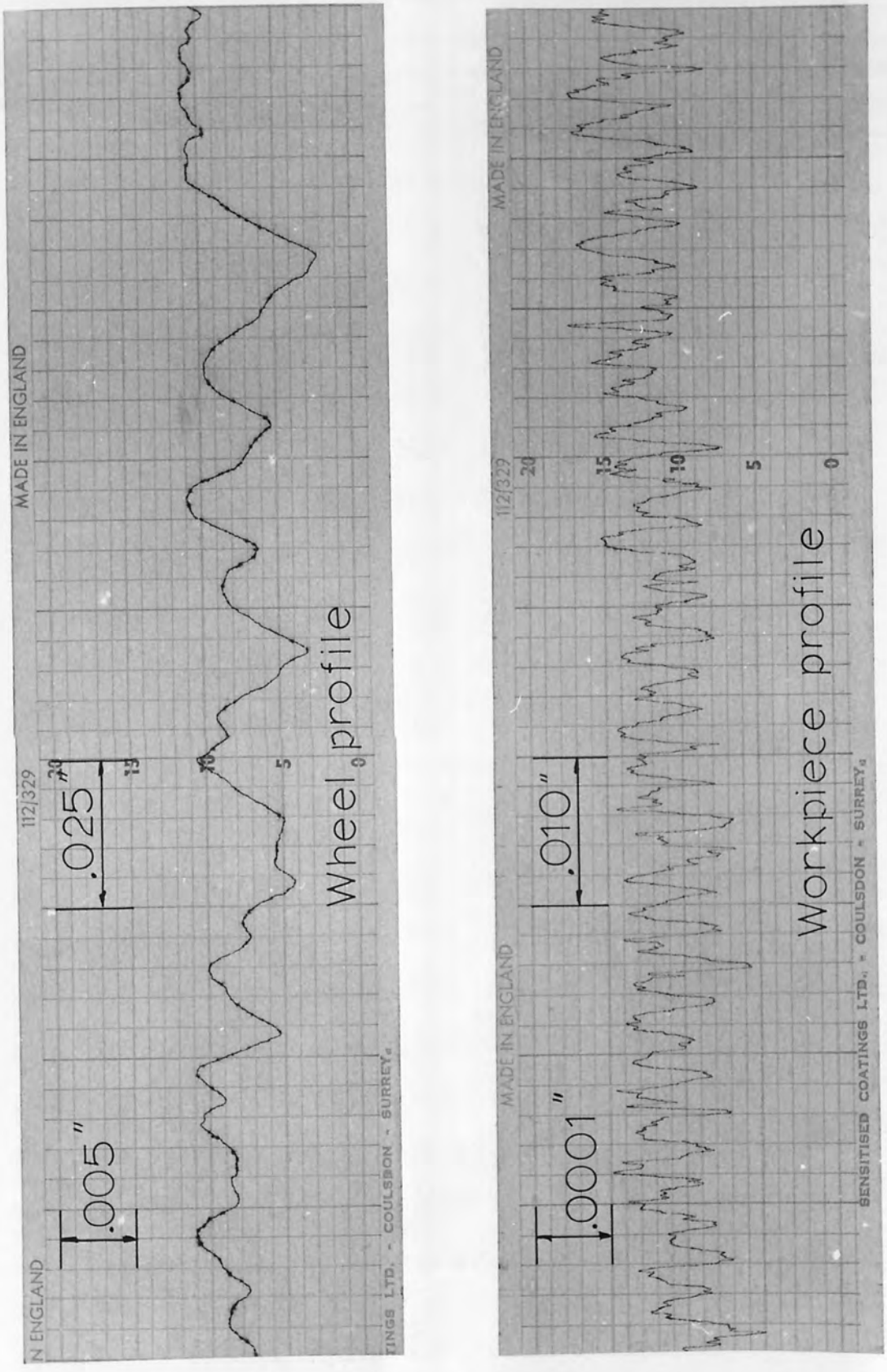

Wheel and workpiece profile comparison

Fine dressing

Fig 37

ROW NO	NUMBER OF COLUMNS FROM EVCO MATRIX									
	20	40	60	80	100	120	140	160	180	200
0	104.0	54.5	46.4	37.8	37.3	34.1	33.4	30.9	29.1	28.8
1	103.3	51.6	43.6	34.8	34.2	31.2	31.1	28.6	27.0	27.0
2	102.4	48.6	40.6	31.3	30.8	28.5	28.4	26.1	24.2	24.2
3	101.2	46.1	37.7	27.2	26.1	25.1	25.4	24.1	22.2	22.3
4	100.4	44.2	35.8	25.5	25.3	24.5	24.0	23.3	21.8	21.6
5	99.7	44.0	36.0	26.4	26.2	25.9	24.8	24.8	23.4	22.6
6	99.5	45.0	37.6	28.9	28.7	28.8	28.0	28.3	26.9	25.8
7	99.2	47.6	40.6	32.1	32.0	32.5	31.8	31.6	30.0	28.9
8	99.2	50.4	43.4	35.6	35.5	35.2	34.5	33.8	32.1	31.0
9	99.7	53.2	46.2	39.4	38.9	37.2	36.5	35.7	34.0	33.1
10	100.5	54.8	48.0	41.6	41.0	38.5	37.2	36.4	34.4	33.5
11	101.1	55.9	49.0	42.5	41.9	38.4	37.0	35.8	33.9	33.1
12	101.6	56.1	49.5	42.1	41.5	37.9	36.0	34.3	32.6	32.2
13	101.6	55.4	48.8	39.9	39.3	35.3	33.8	32.1	30.3	30.1
14	101.5	53.4	46.3	37.8	37.3	33.2	31.7	29.5	27.7	27.6
15	101.0	50.7	43.3	34.7	34.1	30.3	29.3	26.6	25.0	25.3
16	100.5	47.2	39.9	31.4	30.8	27.5	26.7	24.4	22.8	23.1
17	100.2	45.0	37.4	28.7	28.2	24.9	24.0	22.6	21.0	21.0
18	99.6	43.8	36.4	26.6	26.0	23.8	22.8	21.5	20.1	19.8
19	99.5	43.4	35.7	26.3	25.9	25.0	23.7	23.0	22.0	21.5

Mean errors for each comparison of wheel and workpiece profiles - coarsely dressed wheel

Fig.38

ROW NO	NUMBER OF COLUMNS FROM EVCO MATRIX									
	20	40	60	80	100	120	140	160	180	200
0	83.6	45.1	41.4	35.3	32.8	31.4	30.3	30.3	29.7	30.2
1	84.6	46.2	42.0	35.9	33.8	32.9	31.8	31.8	31.2	31.2
2	85.5	47.1	43.3	37.7	36.0	35.0	33.9	33.9	33.3	32.6
3	86.3	49.9	43.8	38.3	36.6	35.7	34.5	34.5	33.8	33.1
4	86.2	48.7	44.8	38.9	37.0	36.0	34.9	34.9	34.1	33.5
5	85.1	48.4	44.2	38.2	36.1	34.7	33.9	33.9	33.4	33.1
6	84.1	48.2	44.0	38.0	35.4	33.9	33.1	33.1	32.6	32.9
7	82.5	47.0	43.0	36.8	34.7	33.0	32.3	32.3	32.0	32.3
8	81.7	45.6	41.6	35.2	33.1	31.3	30.1	30.1	29.6	30.0
9	80.9	45.9	42.0	35.4	33.4	31.5	30.4	30.4	29.8	30.1
10	80.9	45.5	41.9	36.2	34.0	32.4	31.3	31.3	30.6	30.8
11	81.7	45.5	42.1	36.6	34.6	33.5	32.3	32.3	31.8	31.3
12	82.2	47.8	44.2	38.2	36.1	35.5	34.2	34.2	33.6	33.5
13	82.2	48.7	45.4	39.7	38.1	37.1	36.0	36.0	35.3	35.0
14	82.0	49.2	45.7	40.1	38.0	36.9	35.9	35.9	35.3	35.1
15	81.4	49.6	46.3	40.5	38.2	36.7	35.5	35.5	35.0	35.2
16	81.2	48.7	45.0	39.2	36.8	35.3	34.5	34.5	34.2	34.9
17	81.4	46.4	42.6	36.8	34.9	33.4	32.4	32.4	32.1	33.1
18	82.2	46.1	42.3	36.3	34.3	32.9	31.8	31.8	31.3	32.1
19	82.7	46.9	43.1	37.0	35.4	34.0	32.9	32.9	32.3	33.0

Mean errors for each comparison of wheel and workpiece profiles - finely dressed wheel

Fig.39

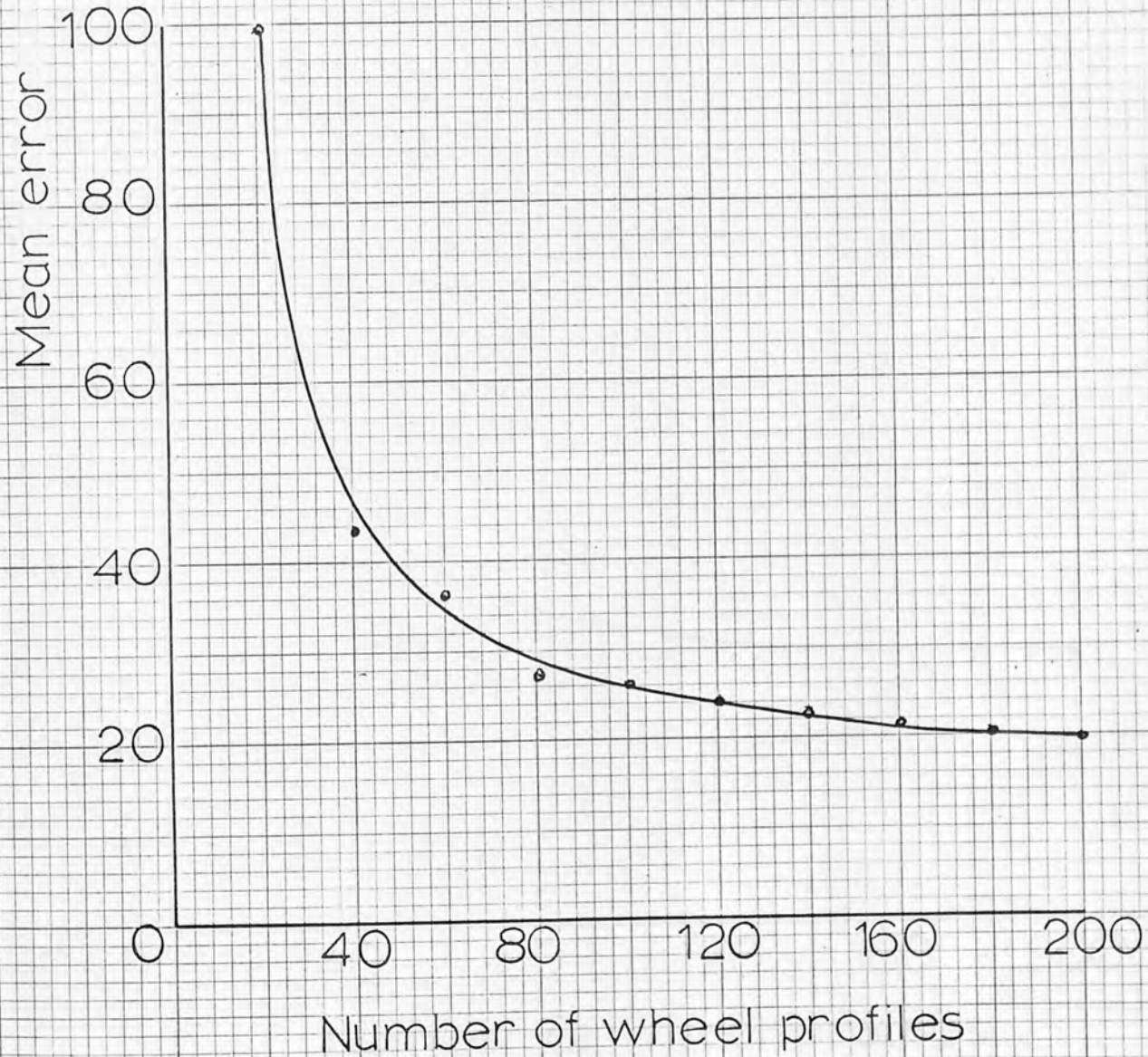

Mean errors between wheel and workpiece profiles - Coarse dress

Fig. 40.

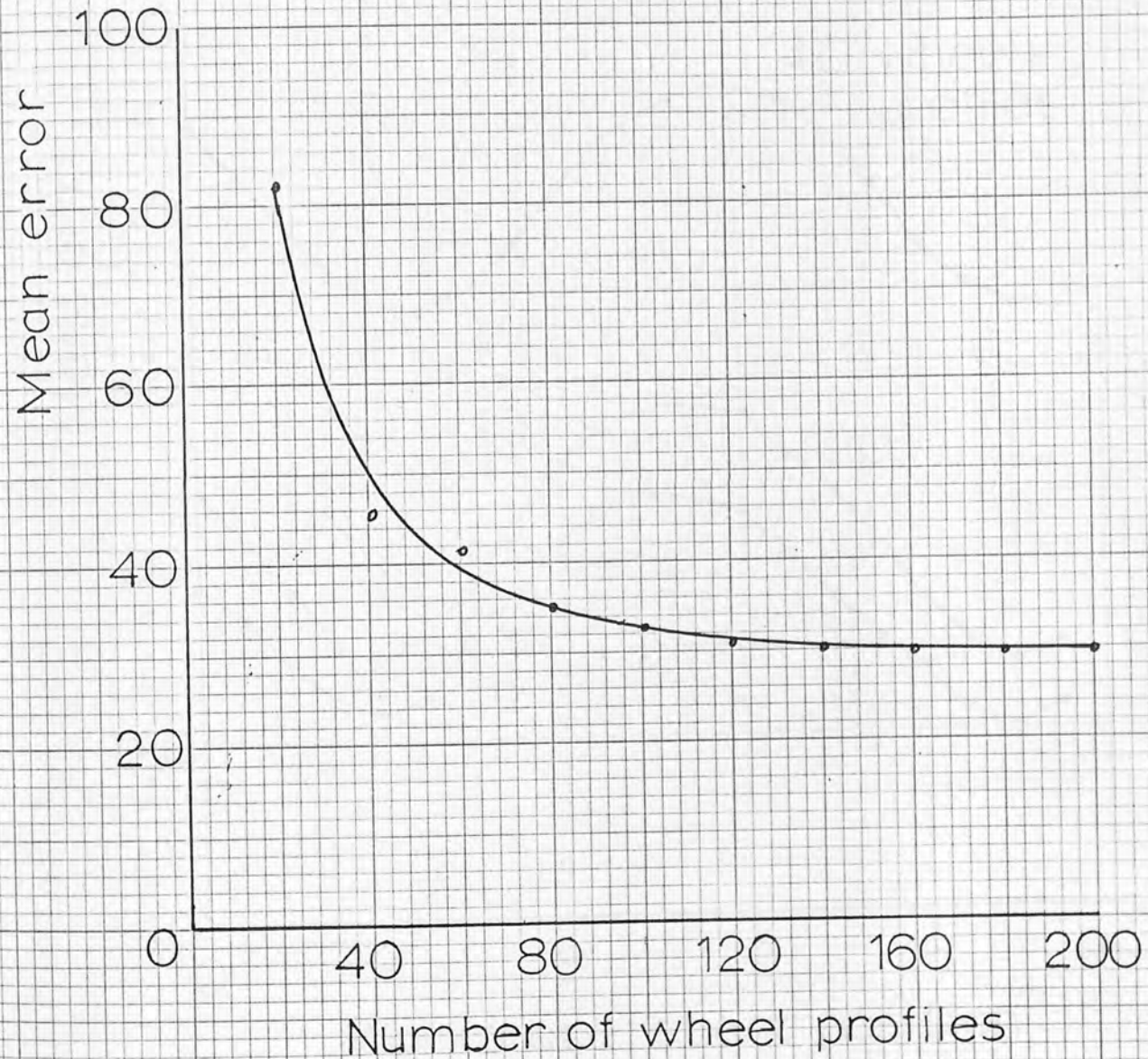

Mean errors between wheel and workpiece profiles - Fine dress

Fig. 41.

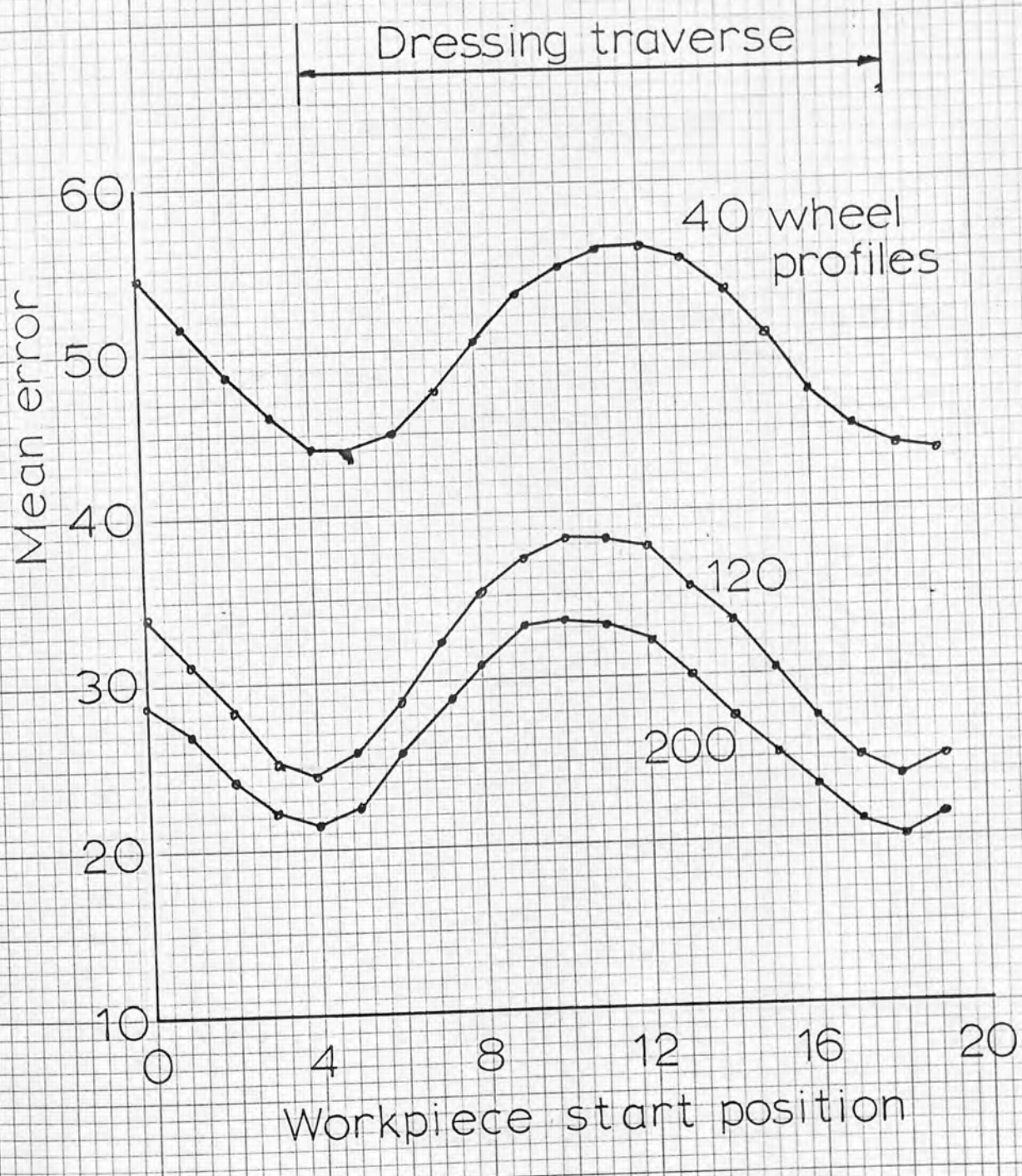

Mean error for different workpiece start positions - Coarse dress

Fig.42.

Mean error for different workpiece start positions - Fine dress

Fig. 43.

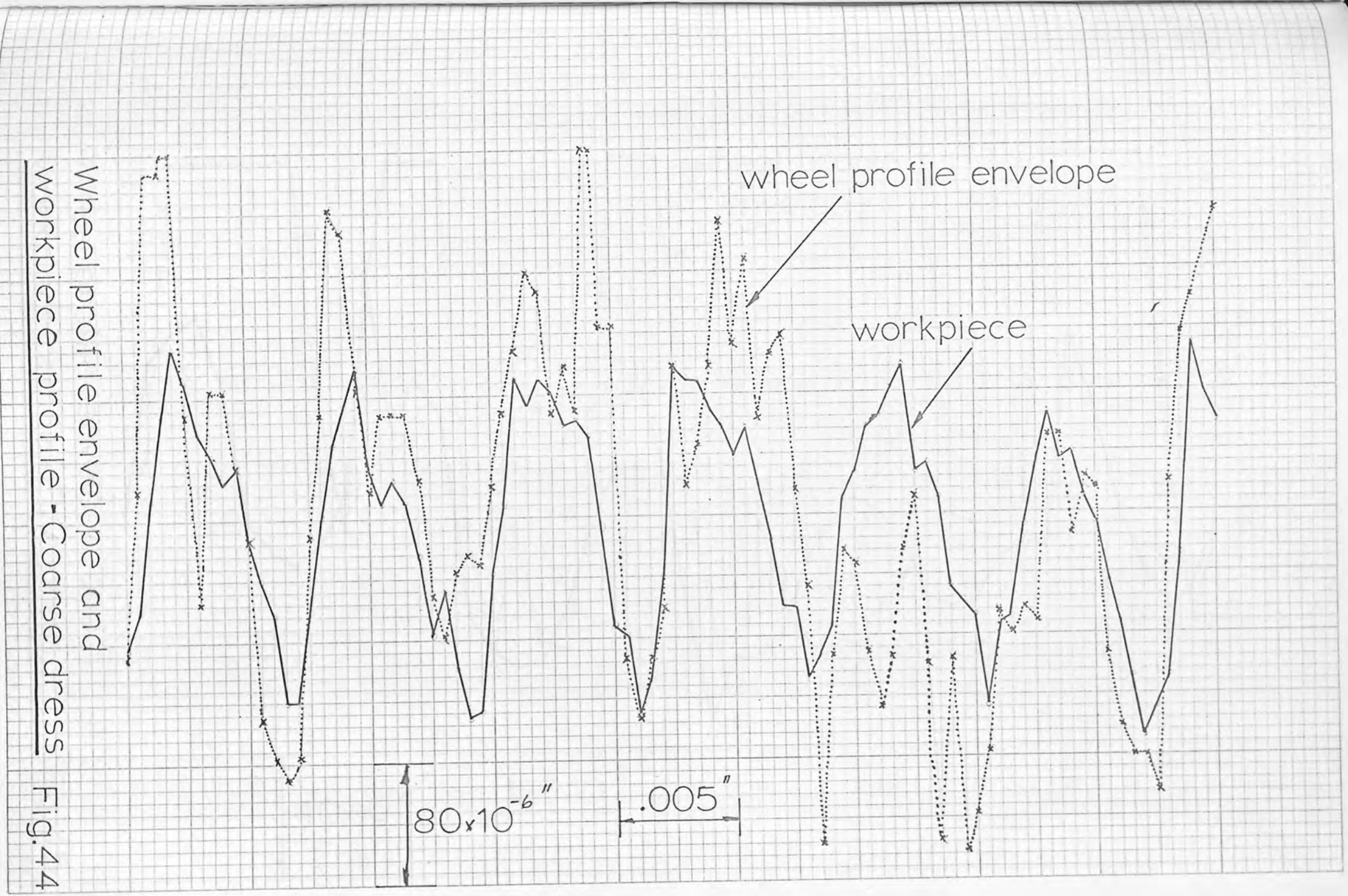

Wheel profile envelope and workpiece profile - Coarse dress

Fig.44

Wheel profile envelope and workpiece profile - Fine dress

Fig. 45

PARAMETER CALCULATED	COARSE DRESSING		
	Digital Value	Actual Value in.	% of peak to valley on workpiece
Maximum error	57.8	235×10^{-6}	59
Minimum error	0.2	0.8×10^{-6}	0
Range of error	57.6	231×10^{-6}	58
Total error	2968.1		
Mean error	19.8	80×10^{-6}	20
Standard deviation	14.8	59×10^{-6}	15
Variance	218.1		

PARAMETER CALCULATED	FINE DRESSING		
	Digital Value	Actual Value in.	% of peak to valley on workpiece
Maximum error	134.0	268×10^{-6}	165
Minimum error	0.4	0.8×10^{-6}	0
Range of error	133.6	268×10^{-6}	168
Total error	4441.5		
Mean error	29.6	60×10^{-6}	37
Standard deviation	23.1	46×10^{-6}	29
Variance	534.3		

Comparison parameters calculated for wheel and workpiece profiles

Fig.46

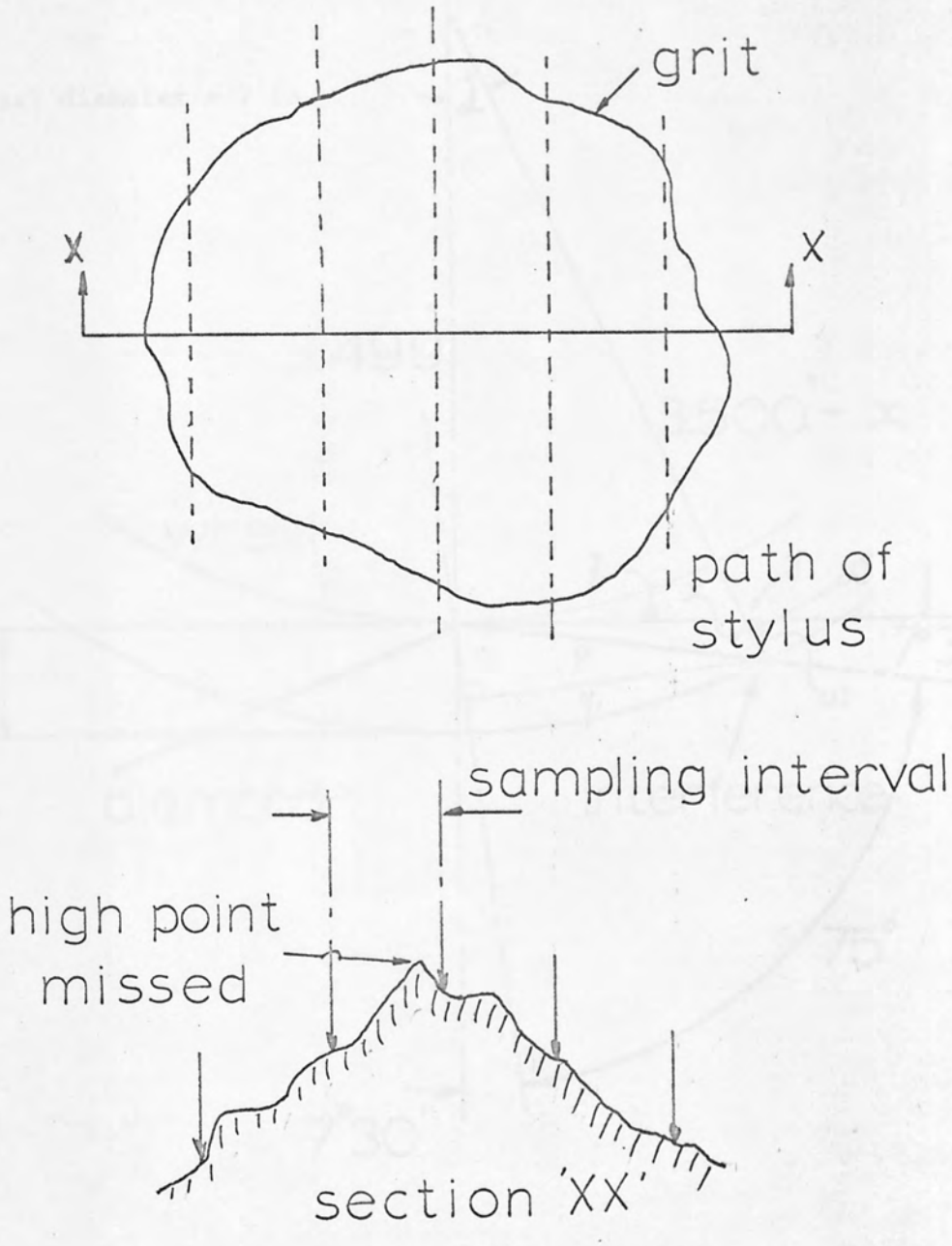

Profiling stylus failing to record a high point on a grit

Fig.47.

EFFECTIVE DIAMOND ANGLE

Assumed wheel diameter = 7 in.

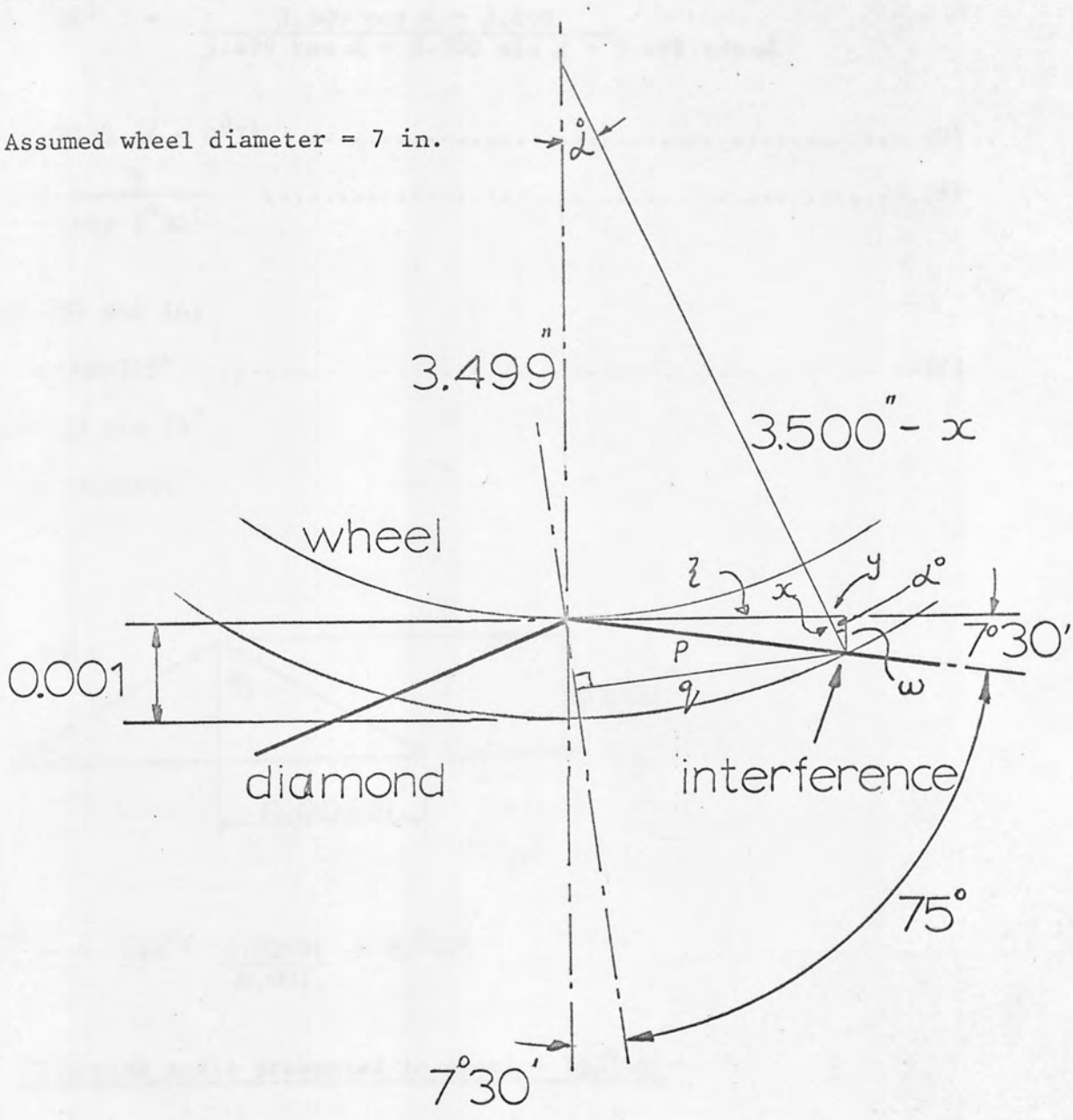

Calculation

$y = x \sin\alpha$ $\qquad x = 3.500 - \frac{3.499}{\cos\alpha}$

$$y = \left\{3.500 - \frac{3.499}{\cos\alpha}\right\} \sin\alpha = 3.500 \sin\alpha - 3.499 \tan\alpha \quad \text{.....(1)}$$

$$\omega = \frac{y}{\tan\alpha} = 3.500 \cos\alpha - 3.499 \quad \text{.....(2)}$$

$$\zeta = 3.499 \tan\alpha \quad \text{.....(3)}$$

$$\tan 10^\circ = \frac{\omega}{\zeta + y} \quad \text{.....(4)}$$

Fig.48
(cont.)

and by substitution of (1), (2) and (3) in (4)

$$\tan 7^{\circ}30' = \frac{3.500 \cos \alpha - 3.499}{3.499 \tan \alpha + 3.500 \sin \alpha - 3.499 \tan \alpha}$$

From which $\alpha = 0^{\circ}7'$ .....(5)

$$\rho = \frac{z}{\cos 7^{\circ}30'}$$ .....(6)

From (3) and (6)

$\rho = 0.00715"$ .....(7)

$q = \rho \sin 75^{\circ}$

$= 0.00691"$

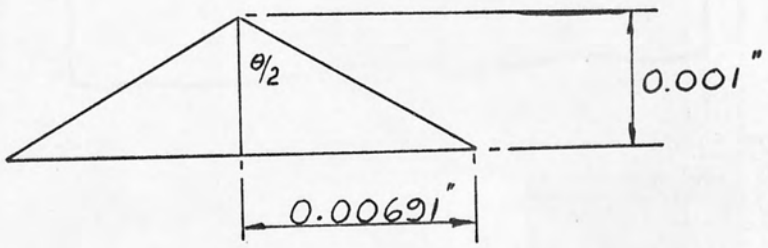

$$\theta/2 = \tan^{-1} \frac{0.00691}{0.001} = 81^{\circ}47'$$

Effective angle presented to wheel = $163^{\circ}34'$

Fig.48

THEORETICAL WORKPIECE PROFILES

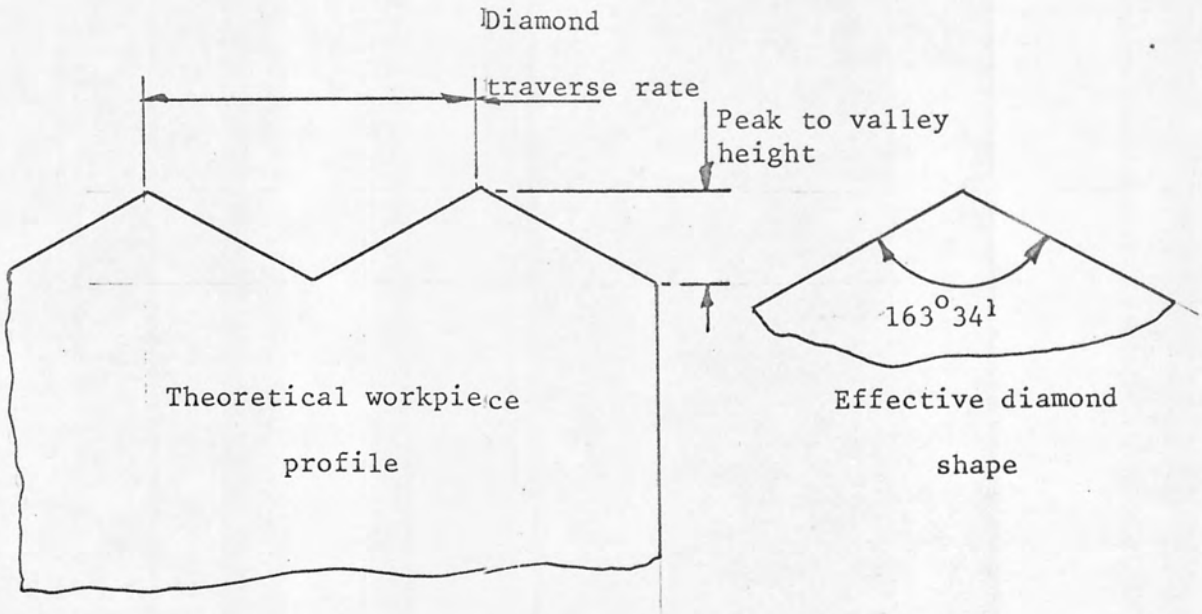

Diamond traverse rate = 0.002 in/rev. Infeed = 0.001 in.

Peak to valley height = $\frac{0.002}{2 \tan 81^{\circ}47'}$ = 0.000145 in

Diamond traverse rate = 0.007 in/rev. Infeed = 0.001 in

Peak to valley height = $\frac{0.007}{2 \tan 81^{\circ}47'}$ = 0.000506 in.

Calculation of theoretical workpiece profiles

Fig.49

Comparison of actual and theoretical workpiece profiles

Fig.50.

Comparison of actual and theoretical workpiece profiles

Fig. 51.

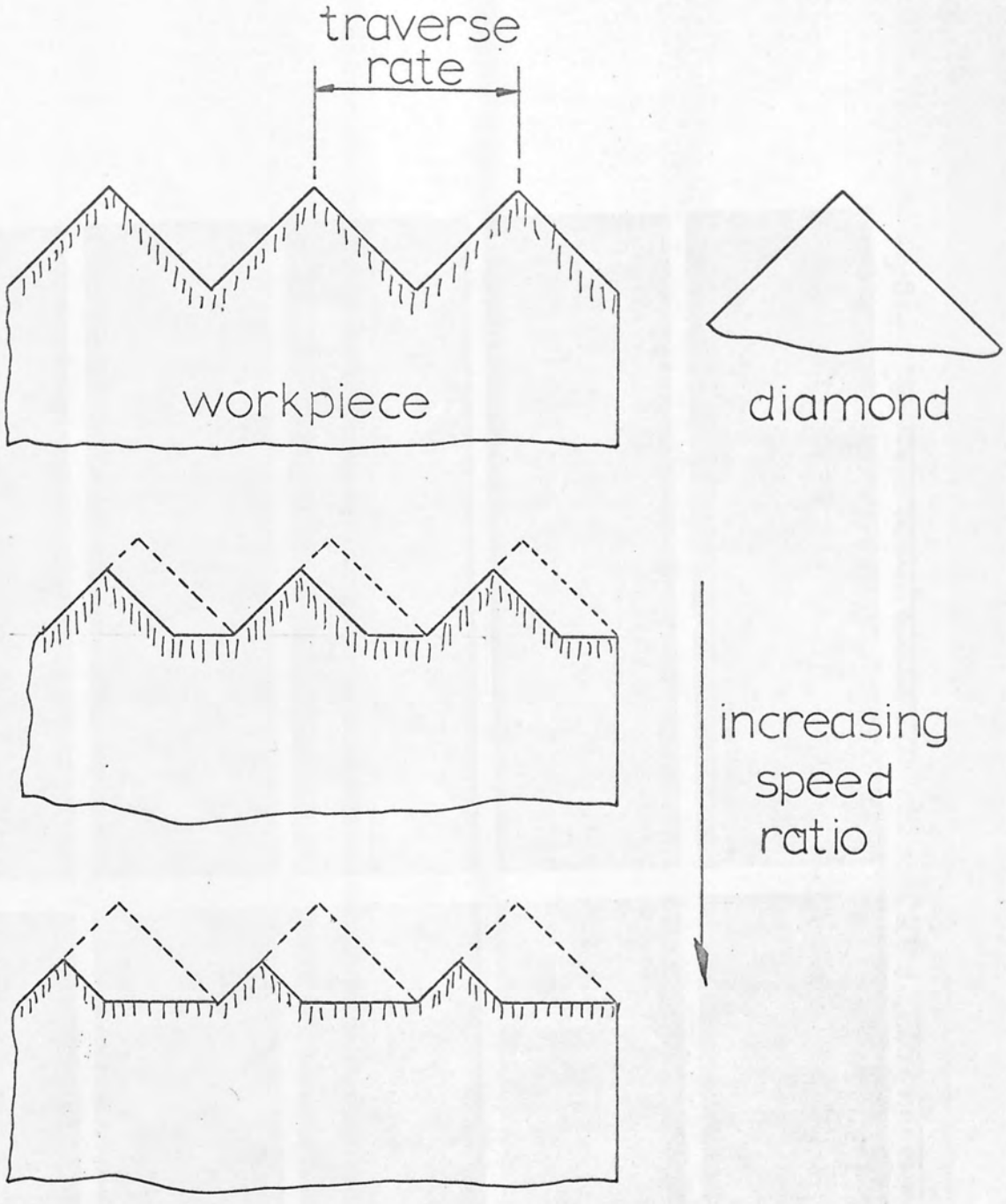

Theoretical workpiece profiles
at different speed ratios

Fig.52.

Coarse dressing traverse rate =.007" Fig.53

Fine dressing traverse rate =.002" Fig.54

Speed ratio test results

Fig. 53. & 54.

SPEED RATIO TESTS

For each speed ratio between the wheel and the workpiece the surface roughness of the workpiece was measured in μin C.L.A. Two dressing conditions were used, fine dress at 0.002 in per revolution and coarse dress at 0.007 in per revolution. In both cases the diamond infeed was 0.001 in.

Speed Ratio	Surface roughness μin CLA	
	Fine dress	Coarse dress
100 : 1	120	39.6
120 : 1	108	36.0
210 : 1	80	30.0
270 : 1	56	27.6
350 : 1	45	25.2
1000 : 1	32	18.8

Influence of speed ratio on surface roughness

Fig.55

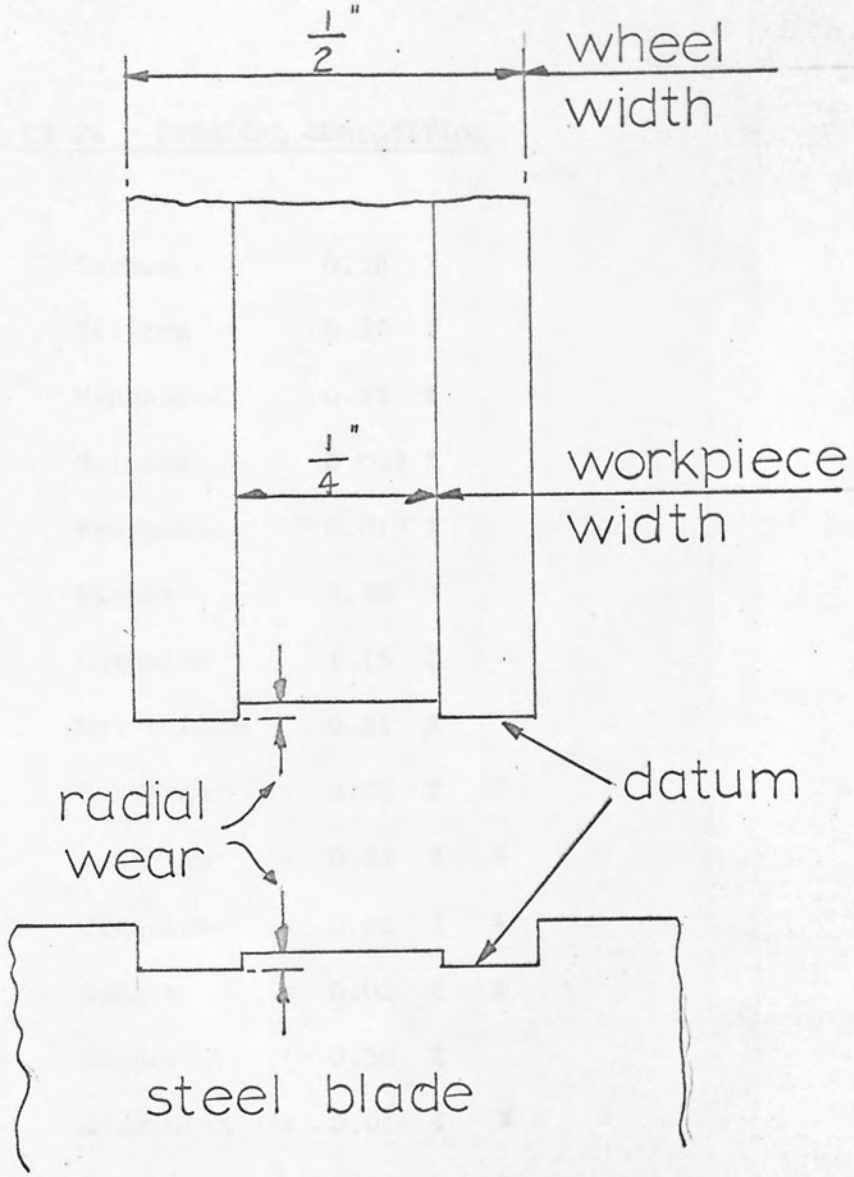

Radial wheel wear measurement

Fig.56

EN 24 - CHEMICAL COMPOSITION

Carbon		0.38 %	
Silicon		0.25 %	
Manganese		0.61 %	
Sulphur		0.022 %	
Phosporus		0.017 %	
Nickel		1.50 %	
Chromium		1.16 %	
Molybdenum		0.31 %	
Tungsten	<	0.02 %	*
Vanadium	<	0.03 %	*
Titanium	<	0.02 %	*
Cobalt	<	0.02 %	*
Copper		0.30 %	
Aluminium	<	0.01 %	*
Tin	<	0.02 %	*
Lead	<	0.05 %	*

* Denotes spectographic result

Oil quench from 850°C. Temper at 200°C for one hour

Chemical composition of workpiece material

Fig.57

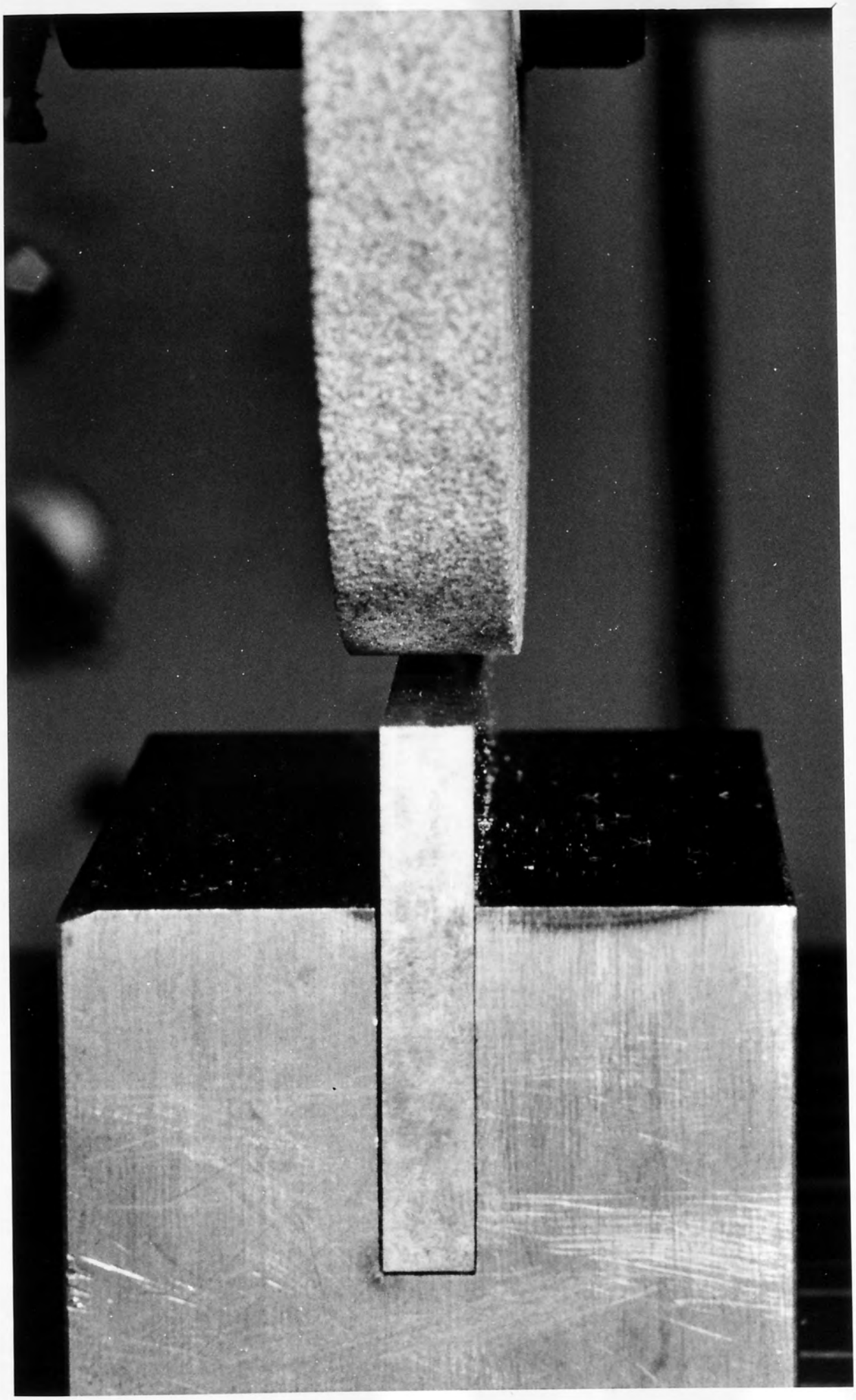

Fig.58

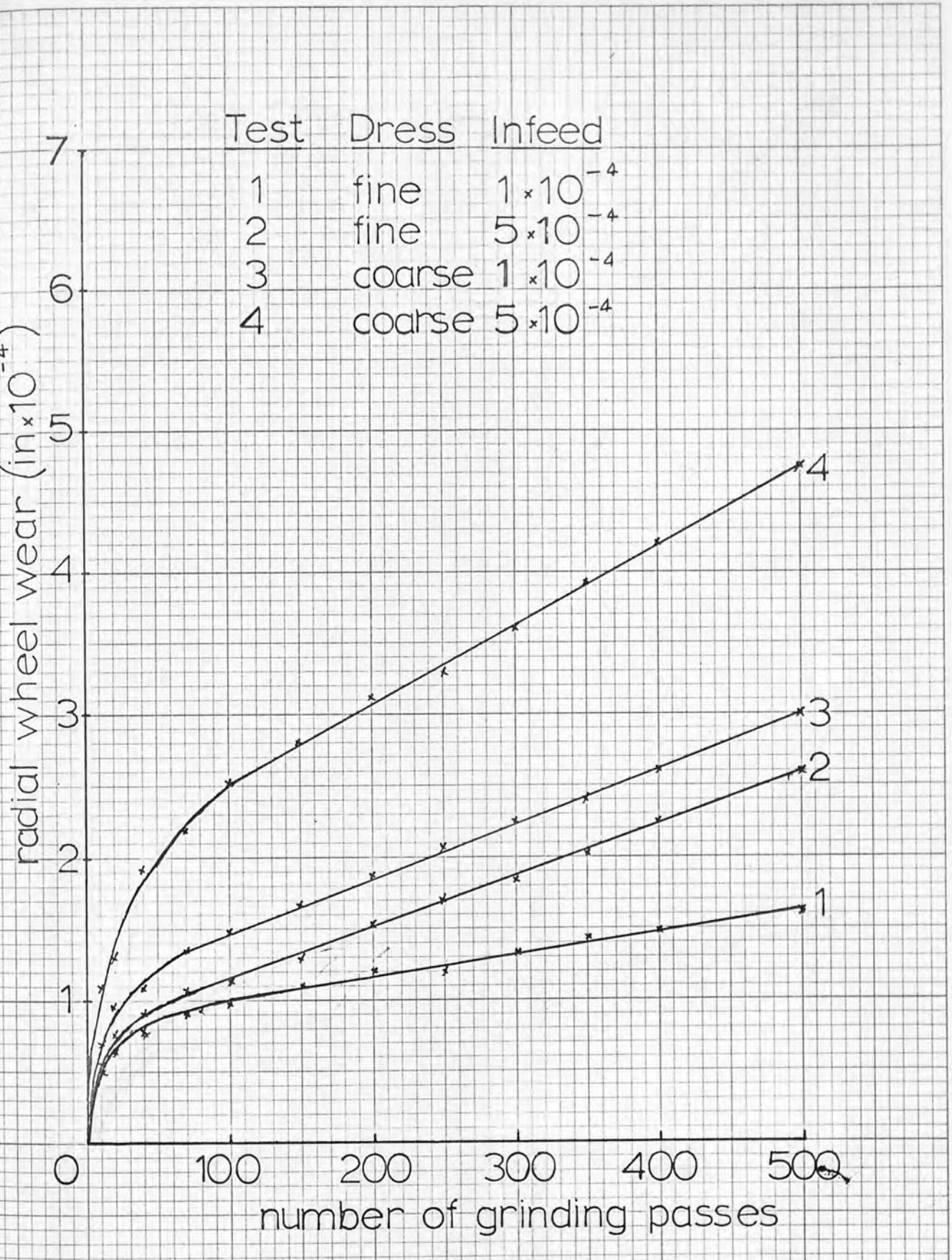

Plunge grind wear tests - G wheel

Fig.59.

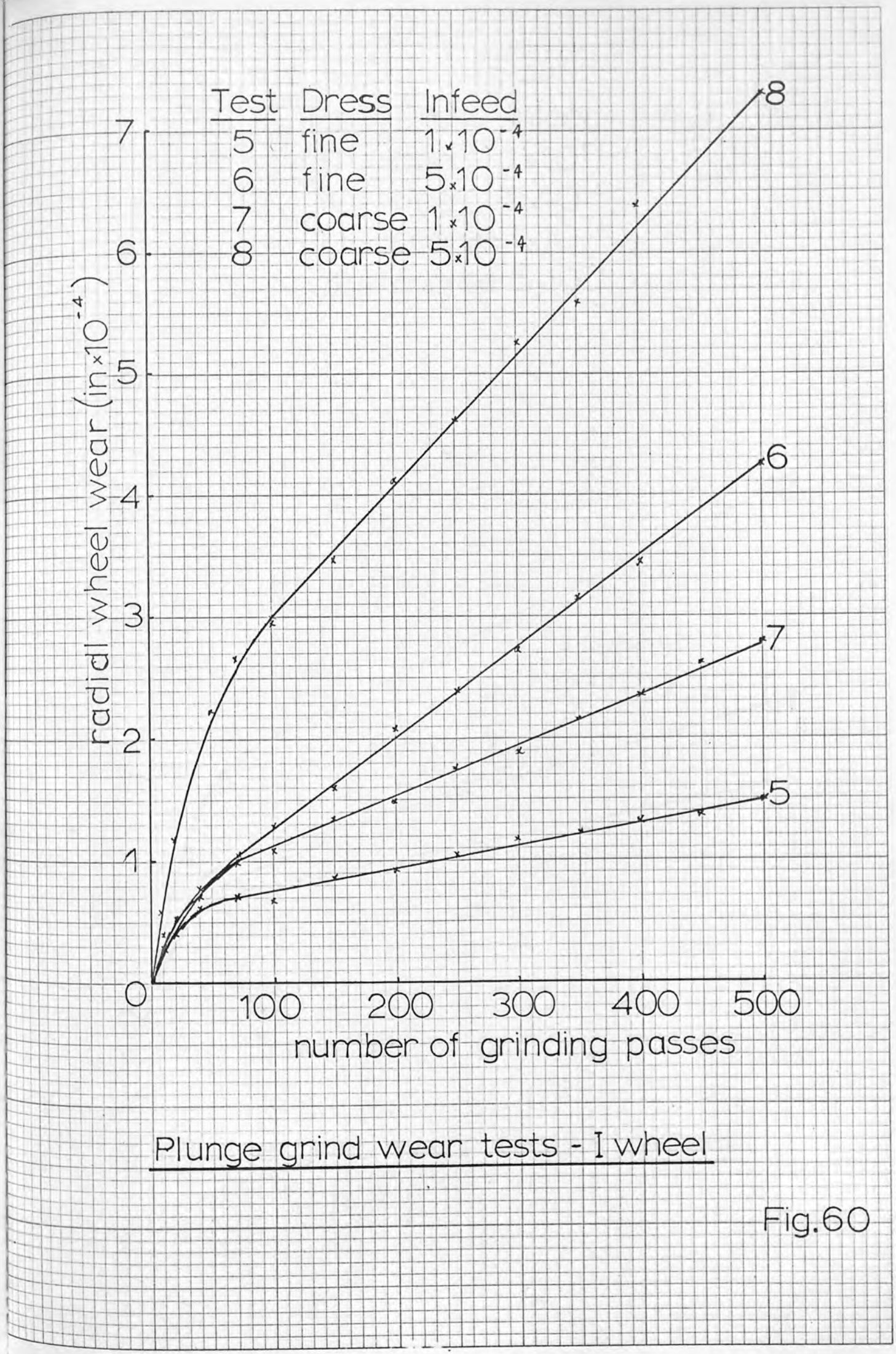

Plunge grind wear tests - I wheel

Fig.60

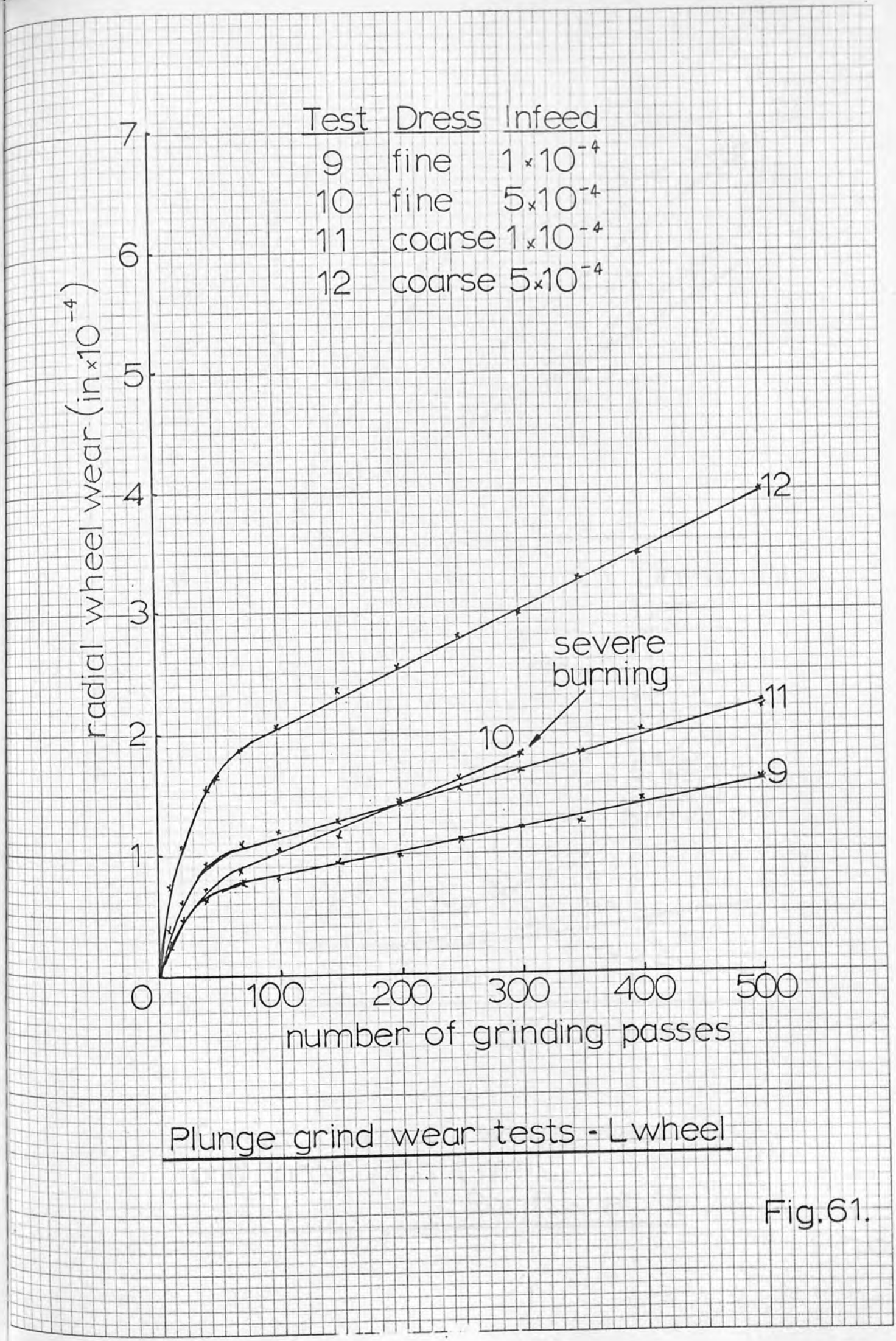

Plunge grind wear tests - L wheel

Fig.61.

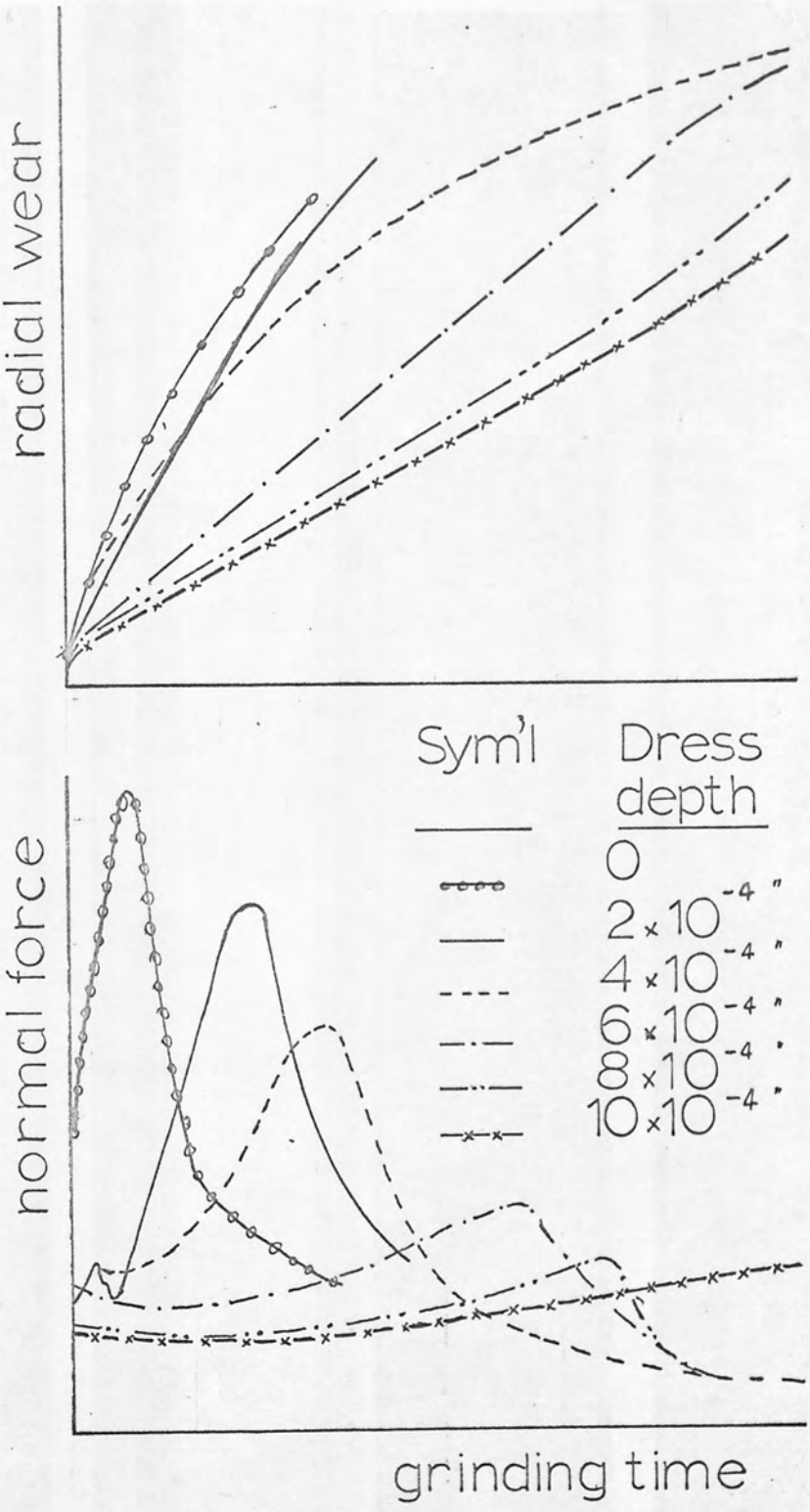

The variation of wheel wear and force with time
Racitti-ref. 15

Fig.62.

Wheel wear test results - Fine dressing

Fig. 63.

Wheel wear test results - Fine dressing

Fig. 64.

Wheel wear test results - Coarse dressing

Fig. 65.

Wheel wear test results - Coarse dressing

Fig. 66.

Wheel wear test results - Fine dressing

Fig. 67.

Wheel wear test results - Coarse dressing

Fig.68.

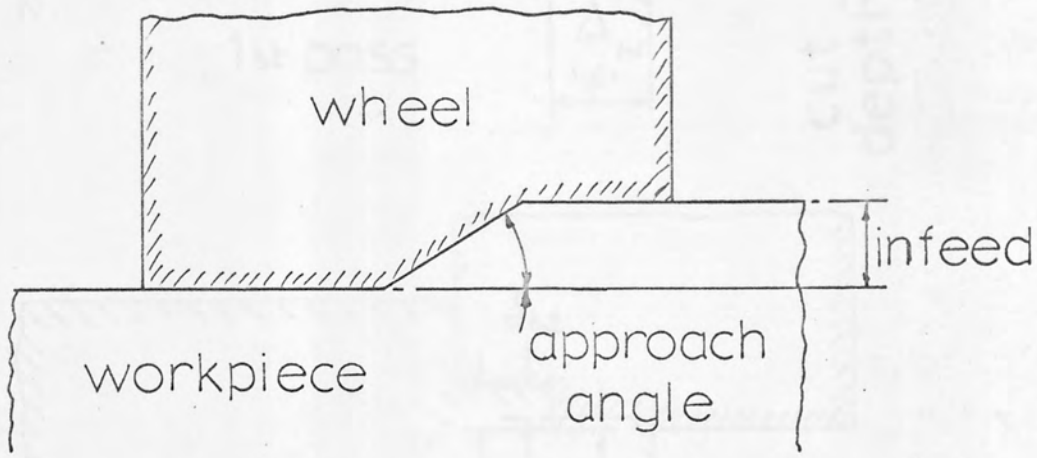

Stable grinding condition

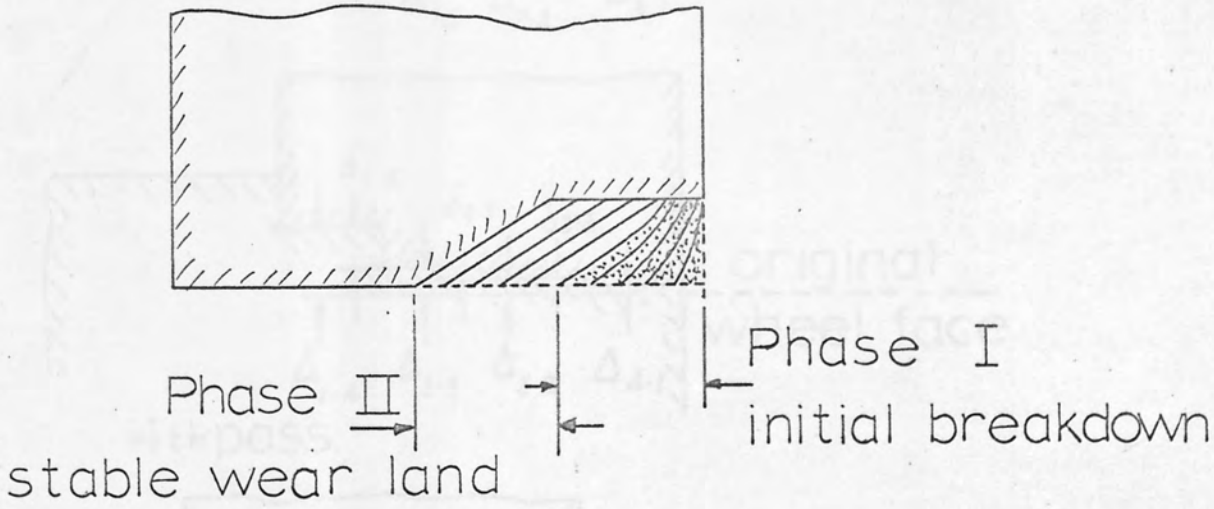

Development of wear in crossfeed surface grinding Purcell-ref. 47

Fig. 69.

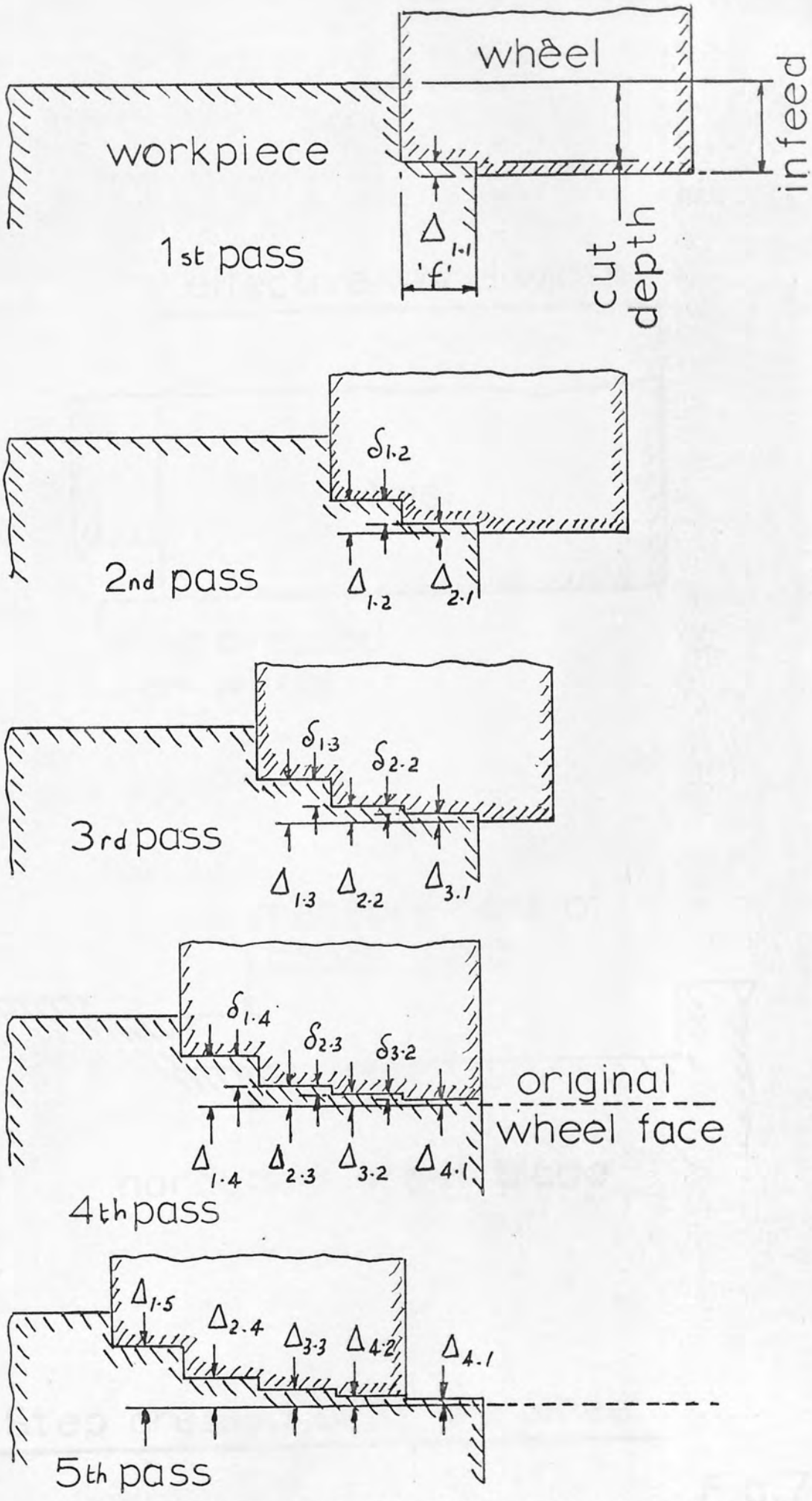

Wheel wear in crossfeed surface grinding

Fig.70.

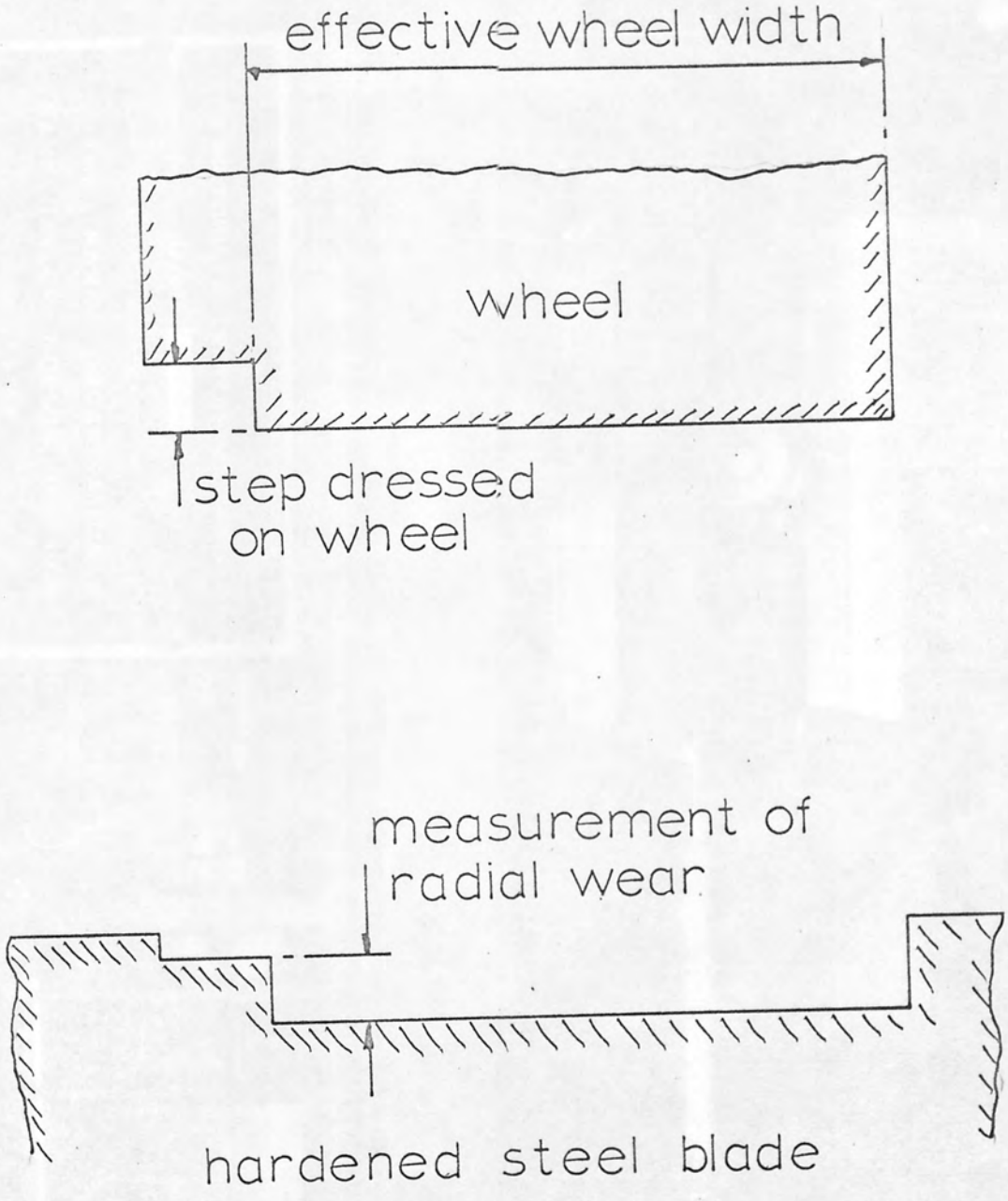

Step dressed onto the wheel

Fig.71.

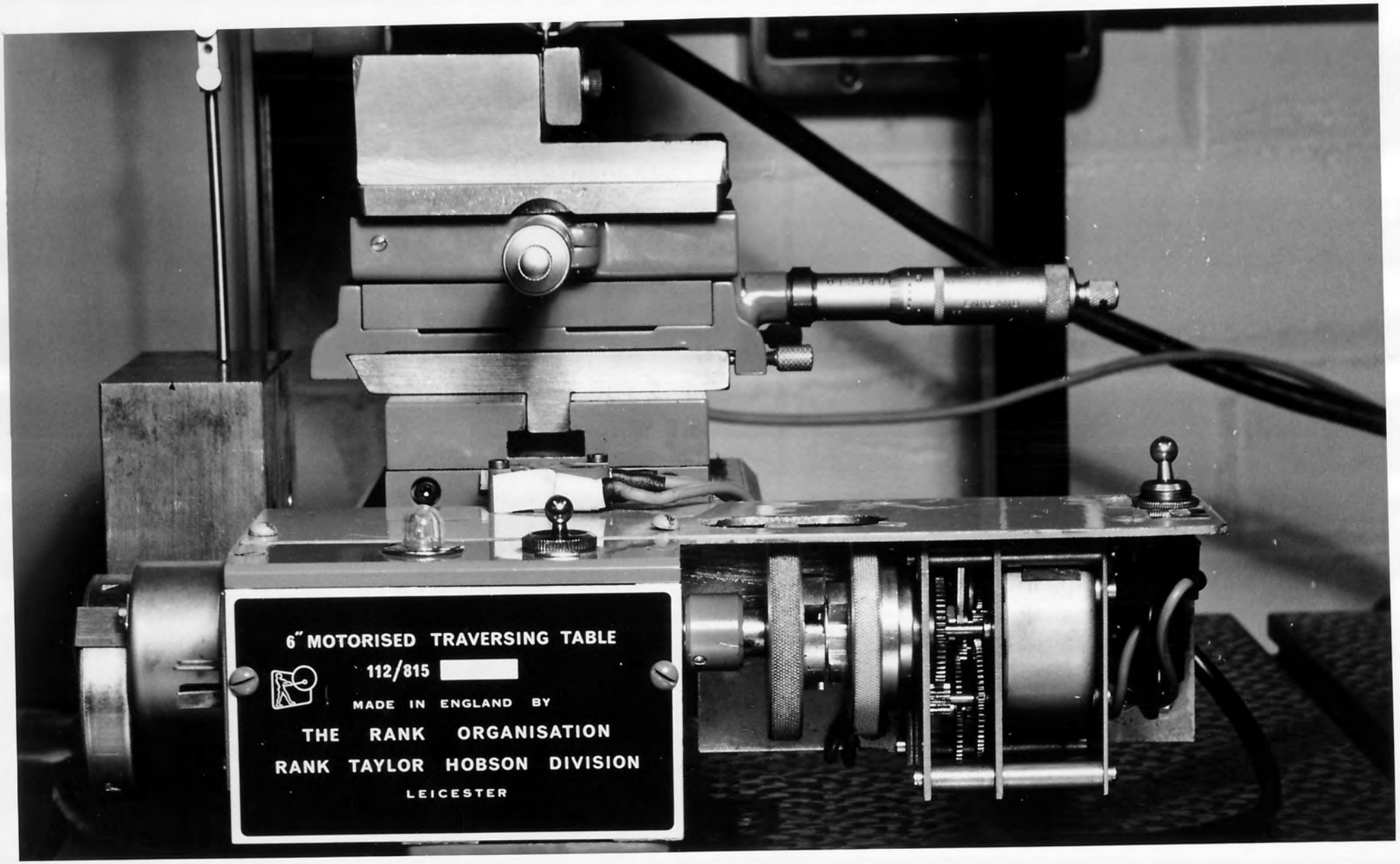
6" MOTORISED TRAVERSING TABLE
112/815
MADE IN ENGLAND BY
THE RANK ORGANISATION
RANK TAYLOR HOBSON DIVISION
LEICESTER

Fig.72

Fig.73

Coarse dressing		
Infeed	in.	0.001
Diamond traverse rate	in./rev.	0.007
Fine dressing		
Infeed	in.	0.001
Diamond traverse rate	in./rev.	0.002
Grinding		
Crossfeed	in	0.030
		0.070
		0.170
Wheel width/crossfeed increment ratio		4 : 1
		9 : 1
Infeed	in.	0.001
		0.0005
Table speed	ft./min.	56
		40

Test conditions for crossfeed surface grinding

Fig.74

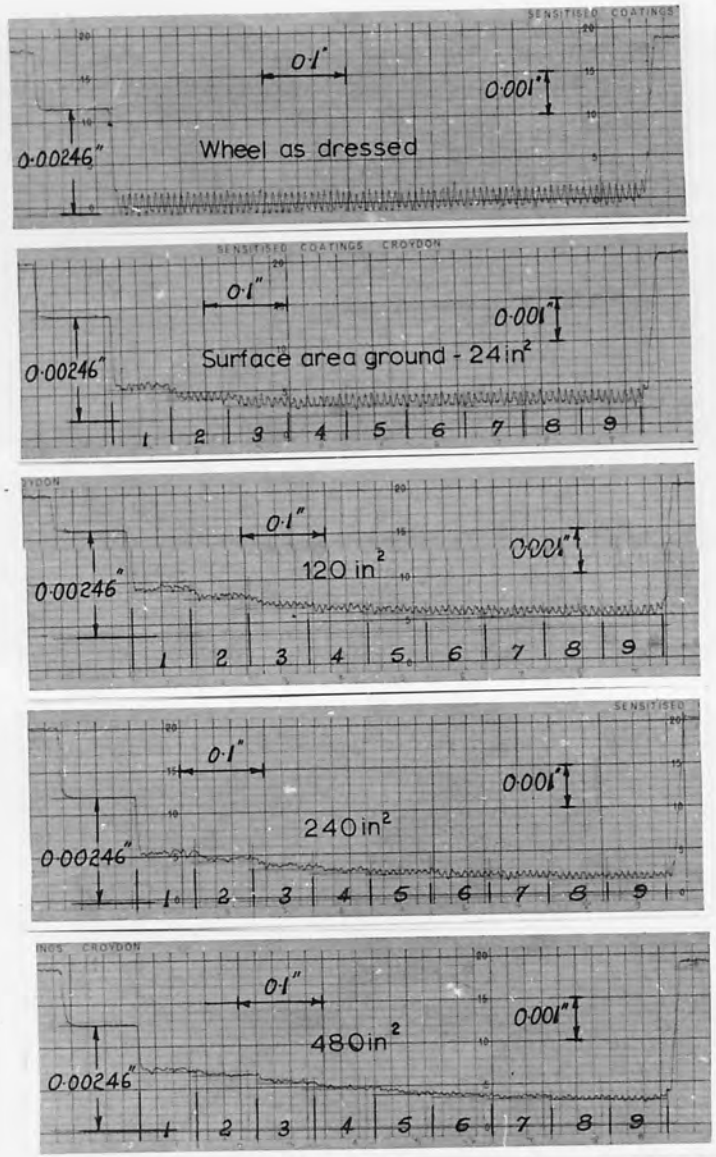

'a' $\frac{\text{wheel width}}{\text{cross feed}} = 9$

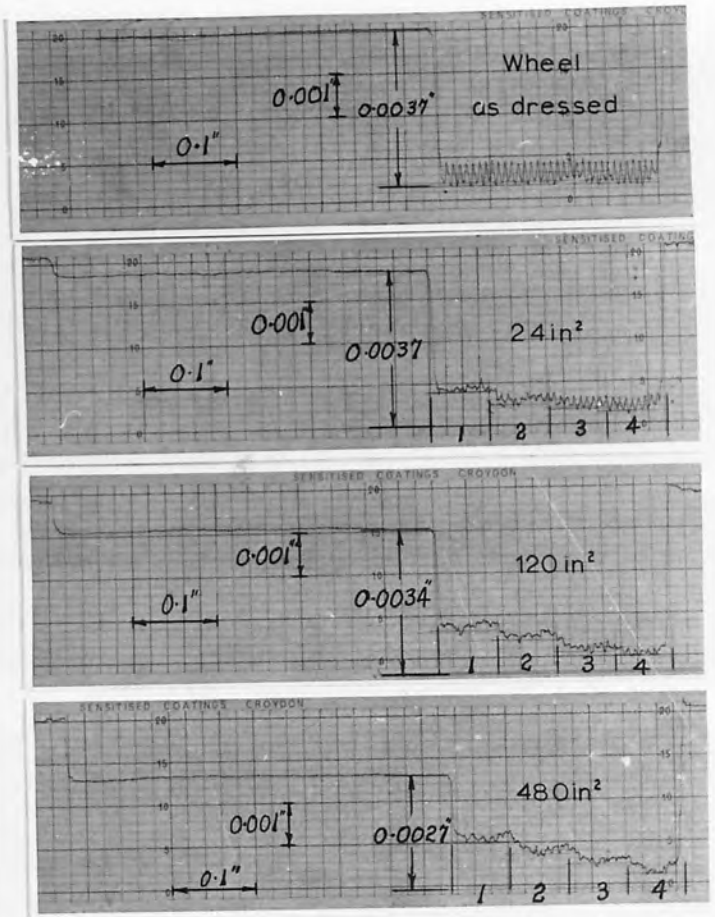

'b' $\frac{\text{wheel width}}{\text{cross feed}} = 4$

coarse dress
wheel infeed - 0·001 in
table speed - 56 ft/min
cross feed - 0·070 in

Fig. 75

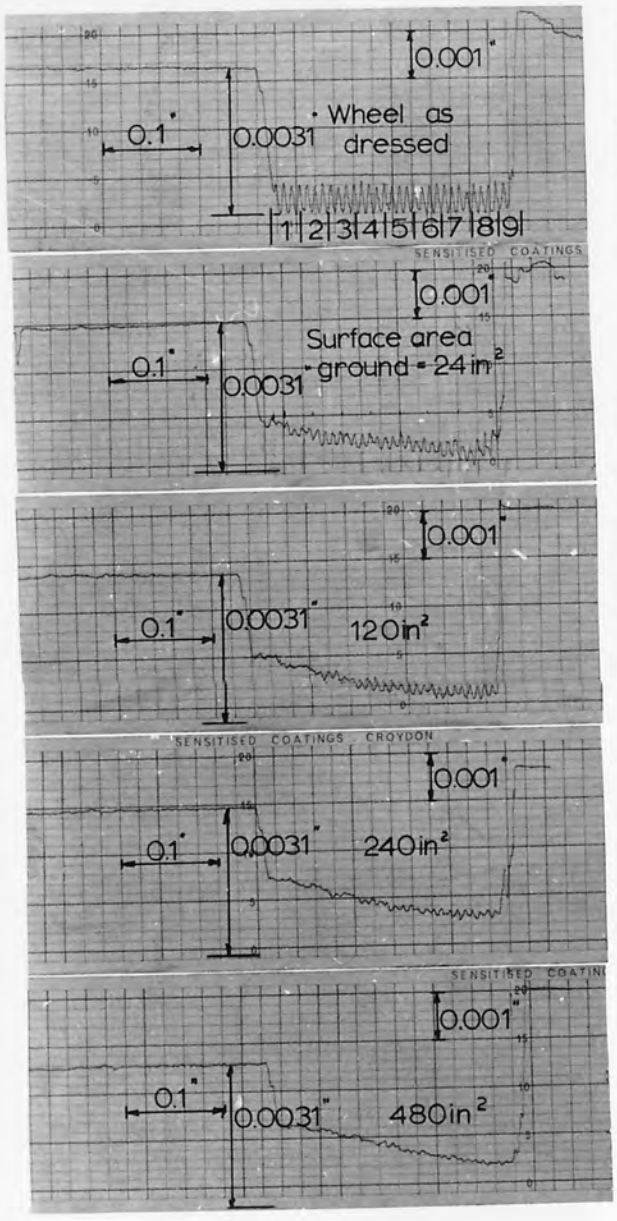

'a' $\frac{\text{wheel width}}{\text{cross feed}} = 9$

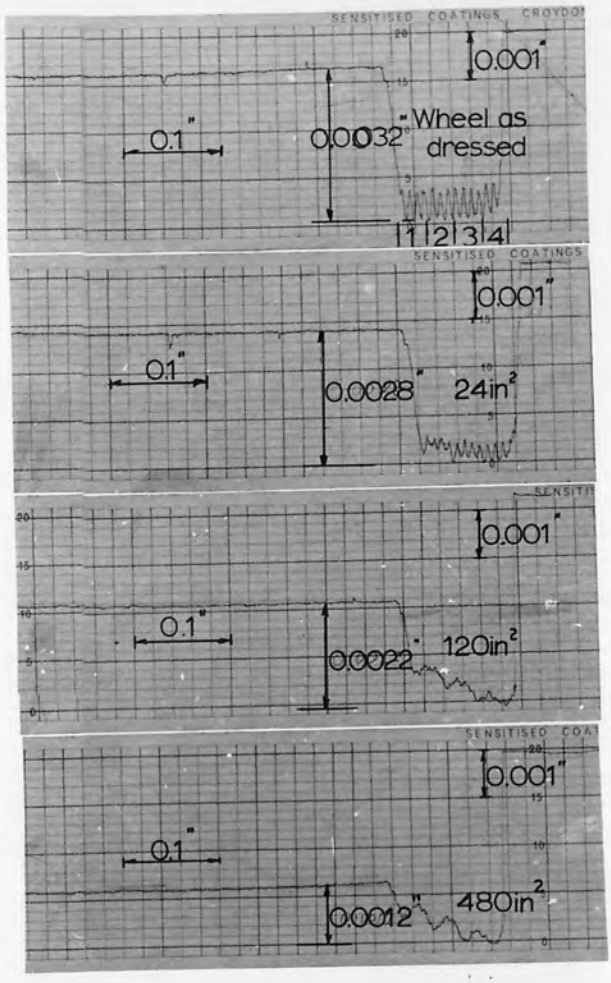

'b' $\frac{\text{wheel width}}{\text{cross feed}} = 4$

coarse dress
wheel infeed - 0.001"in
table speed - 56 ft/min
cross feed - 0.030 in

Fig.76

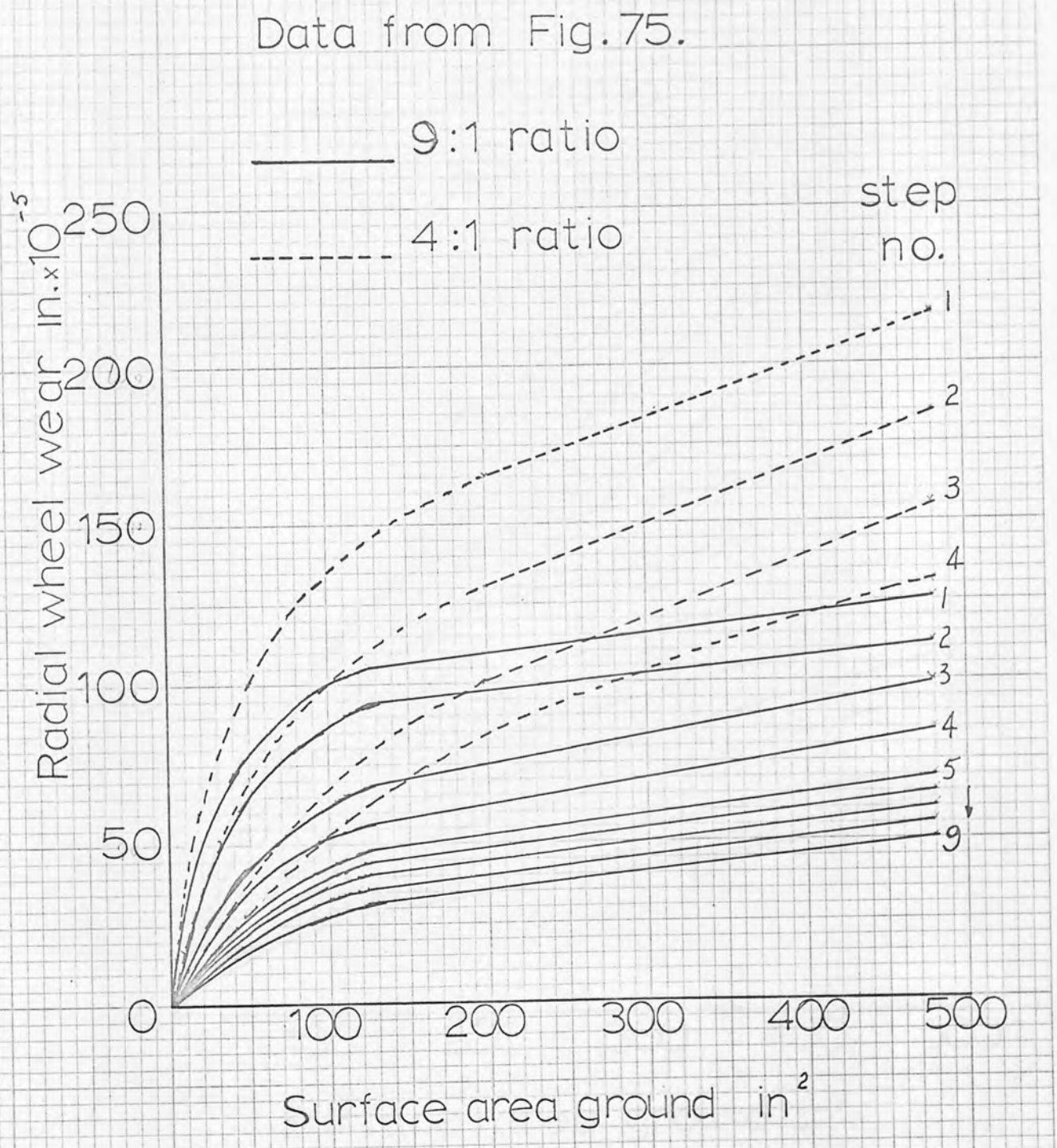

Wear on wheel sections

Fig. 77.

Data from Fig.76.

_____ 9:1 ratio

--------- 4:1 ratio

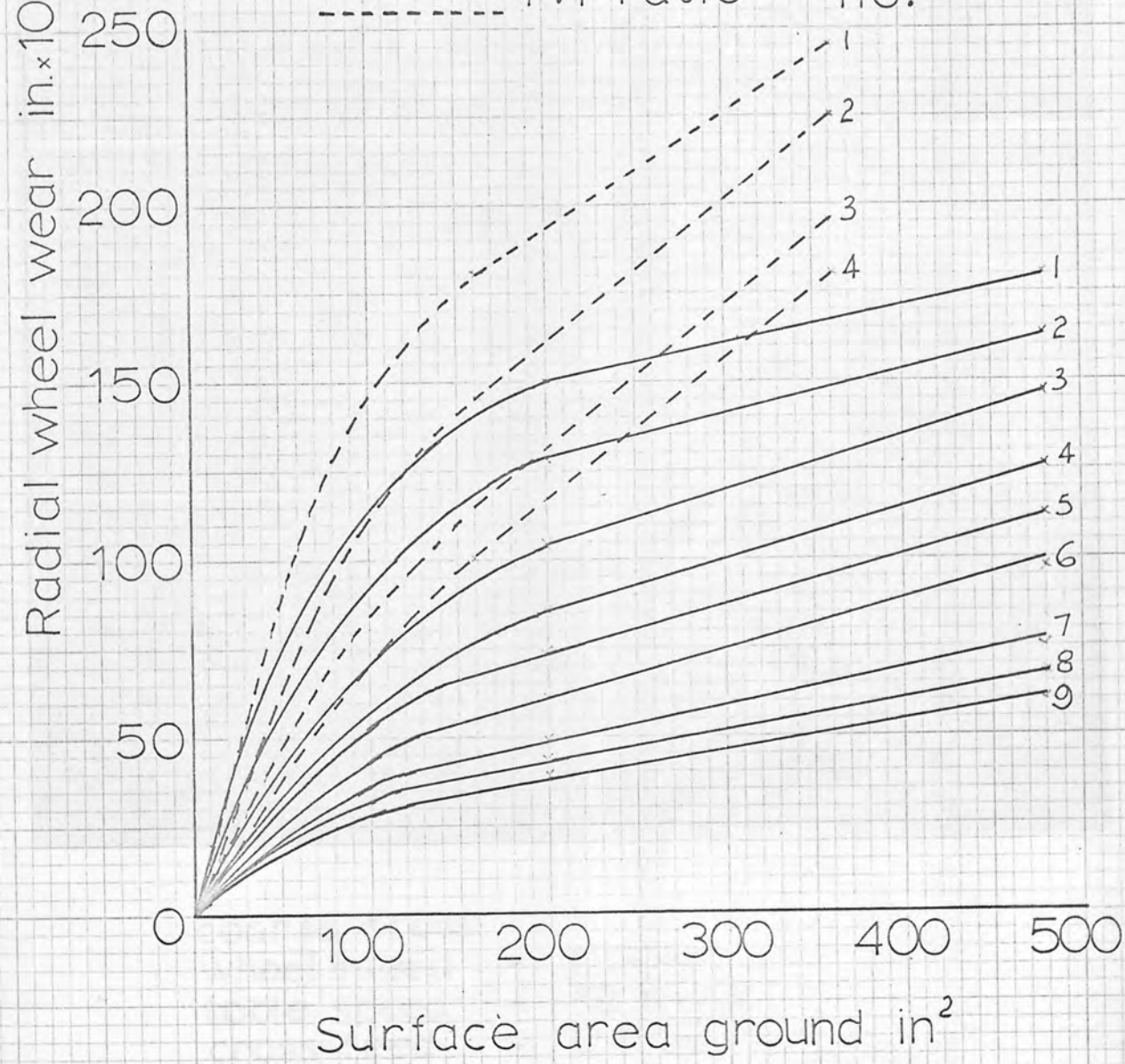

Wear on wheel sections

Fig.78.

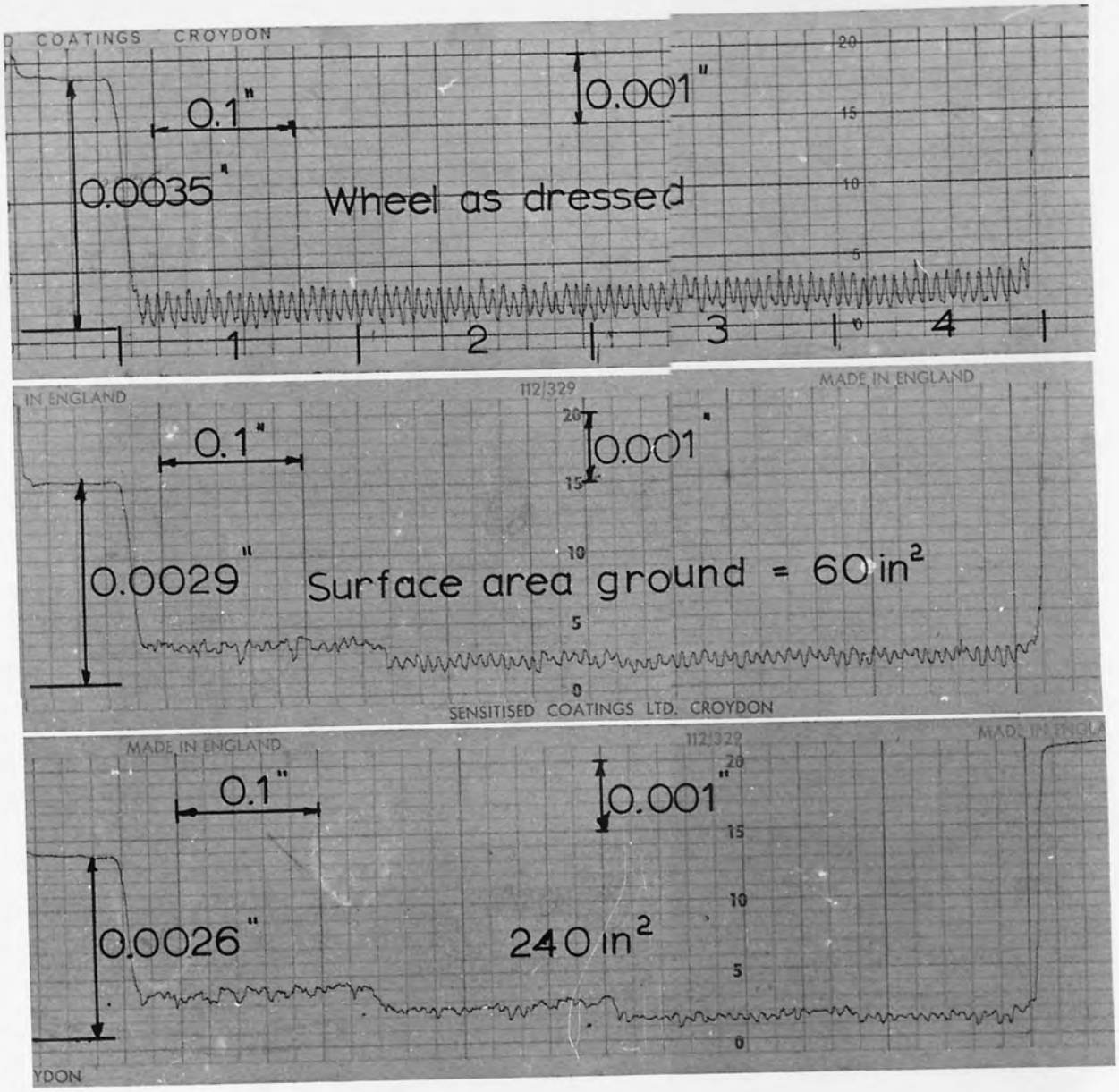

coarse dress
wheel infeed - 0.001 in
table speed - 56 ft min
cross feed - 0.170 in

$$\frac{\text{wheel width}}{\text{cross feed}} - 4$$

Fig.79

Leading section only
Data from Figs 77b, 78b, 79.

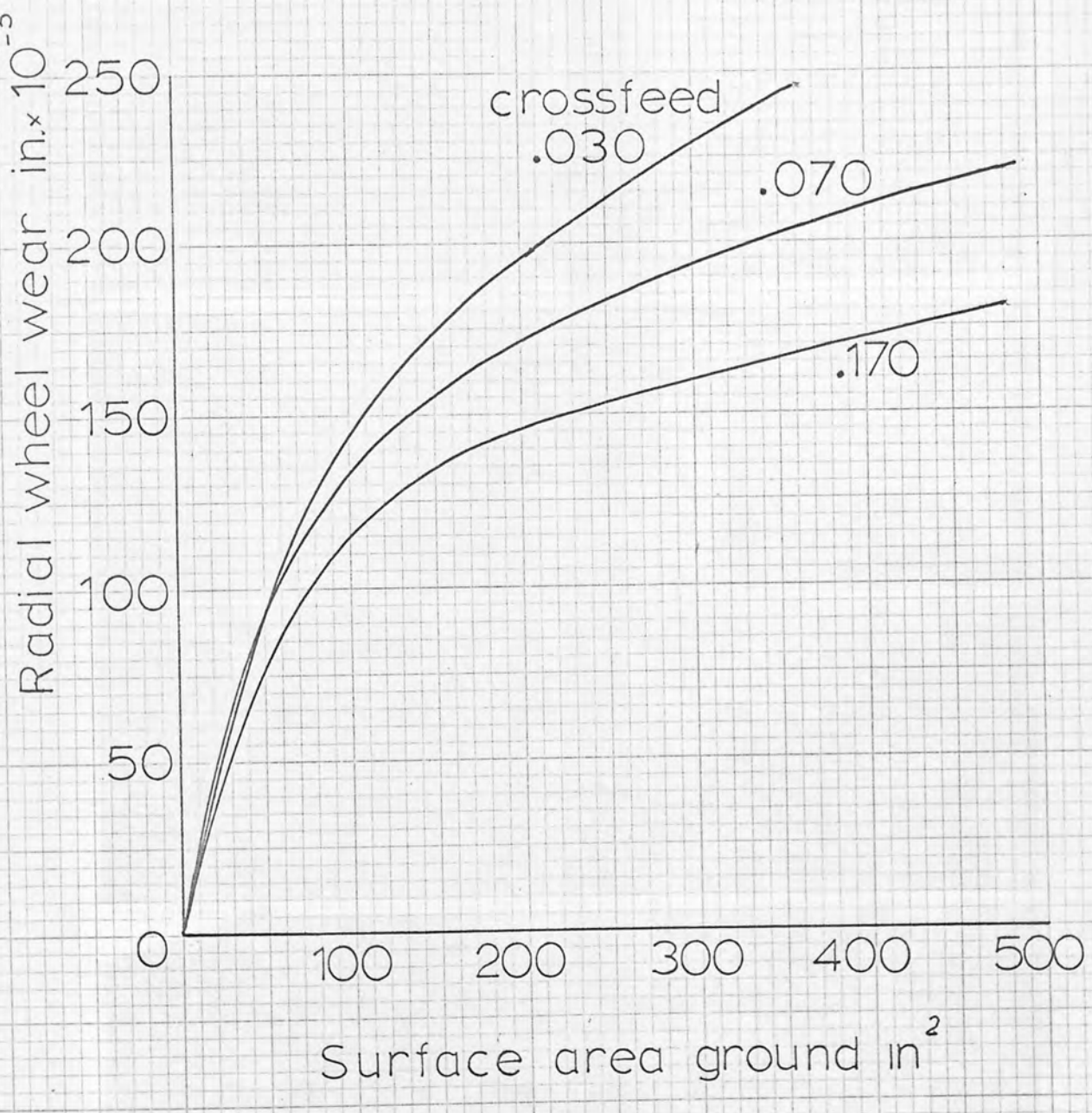

Wear on leading wheel section for various crossfeed increments

Fig. 80.

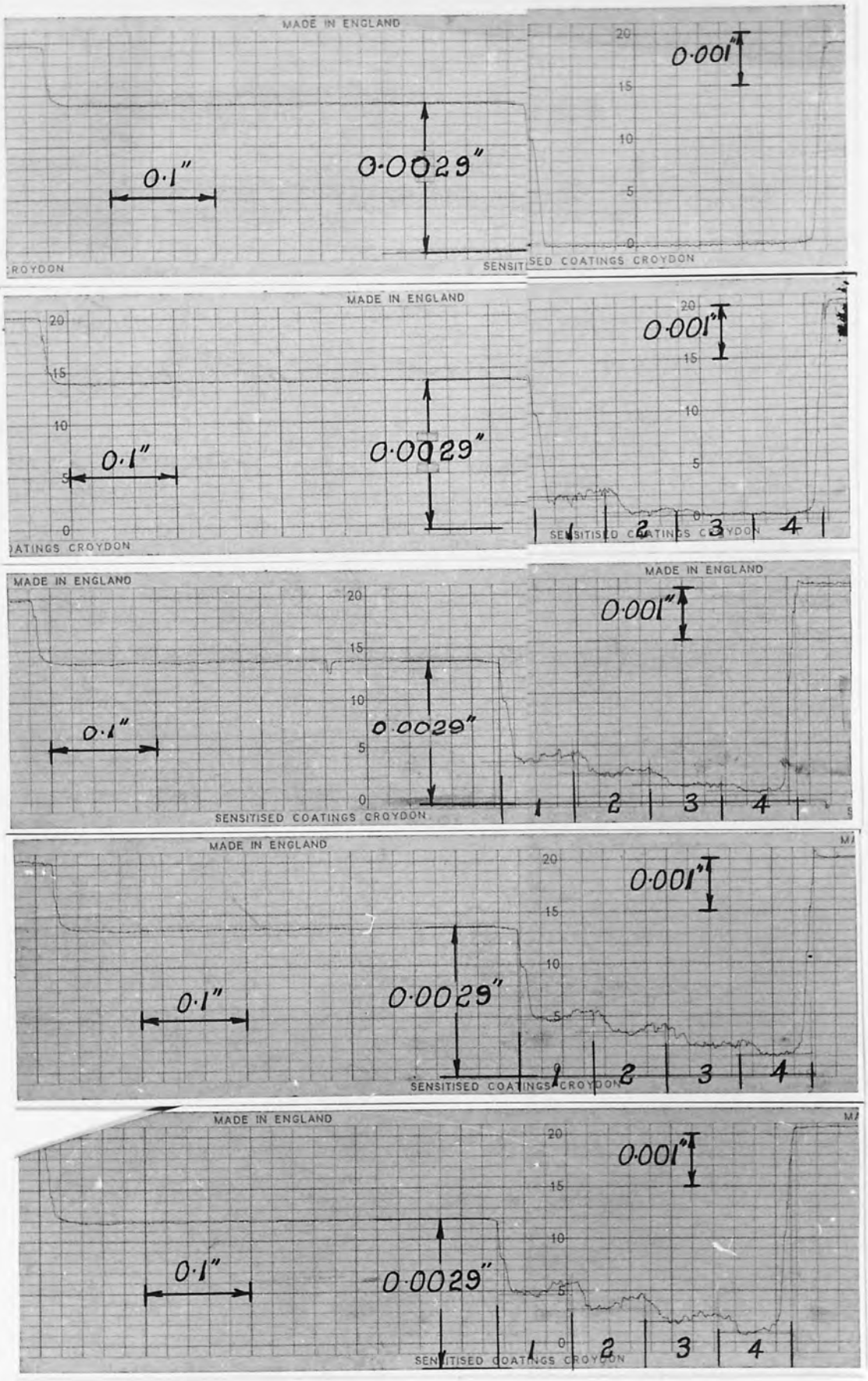

fine dress
wheel infeed 0.001 in
table speed 56 ft/min
cross feed 0.070 in

$$\frac{\text{wheel width}}{\text{cross feed}} - 4$$

Fig.81

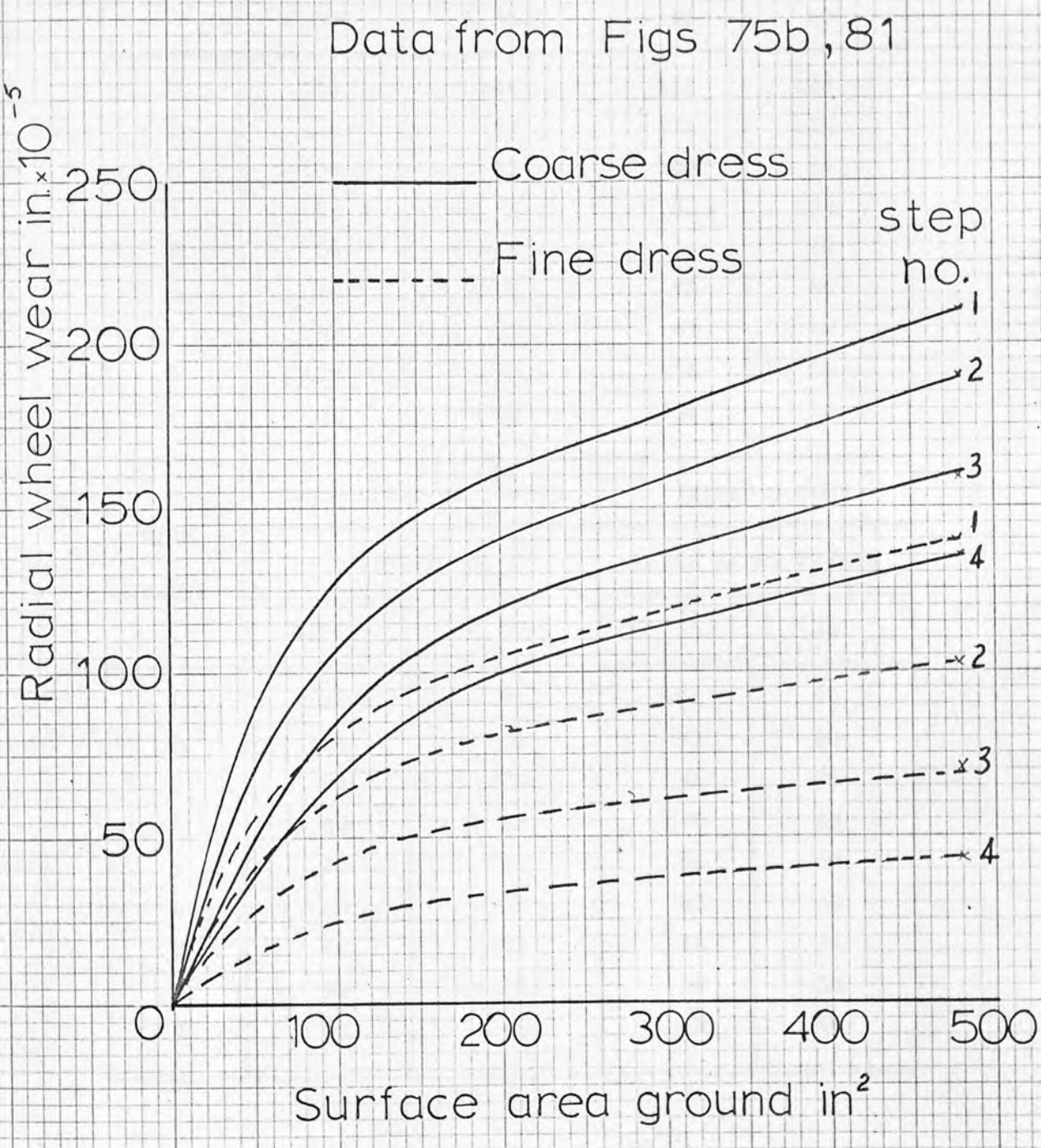

Wheel wear after coarse and fine dressing

Fig. 82.

STEP NUMBER	TABLE SPEED 56 FT/MIN		INFEED 0.001"	
	INFEED IN.		TABLE SPEED FT/MIN	
	0.001	0.0005	56	40
1	136	104	136	128
2	124	92	124	116
3	106	86	106	94
4	92	76	92	82
5	76	66	76	70
6	70	62	70	66
7	62	58	62	60
8	58	50	58	56
9	56	48	56	52

STEP NUMBER	TABLE SPEED 40 FT/MIN		INFEED 0.0005"	
	INFEED IN.		TABLE SPEED FT/MIN	
	0.001	0.0005	56	40
1	128	99	104	99
2	116	90	92	90
3	94	75	86	75
4	82	68	76	68
5	70	60	66	60
6	66	58	62	58
7	60	54	58	54
8	56	50	50	50
9	52	48	48	48

Radial wheel wear (in x 10^{-5})

Effect of grinding conditions on wheel wear

Fig.83

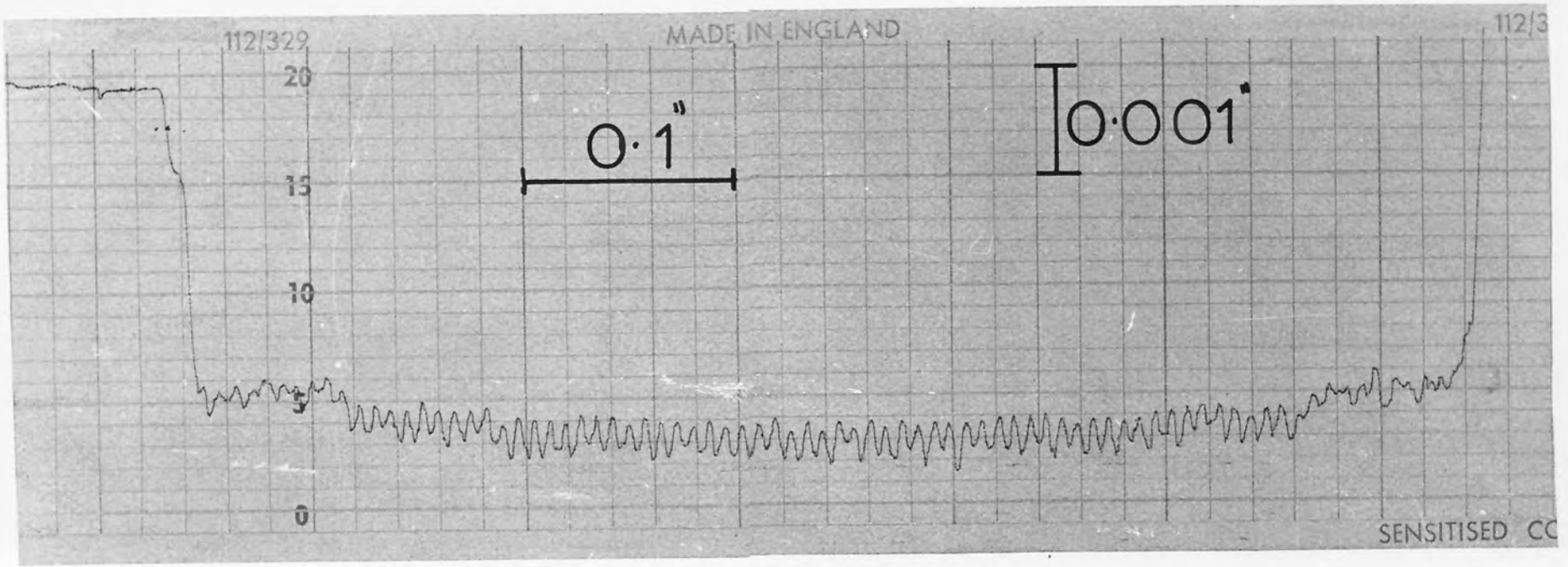

Cross feed increment = 0·070"

Surface area ground = 48 in^2 – 2 complete cross traverses in each direction

Fig. 84

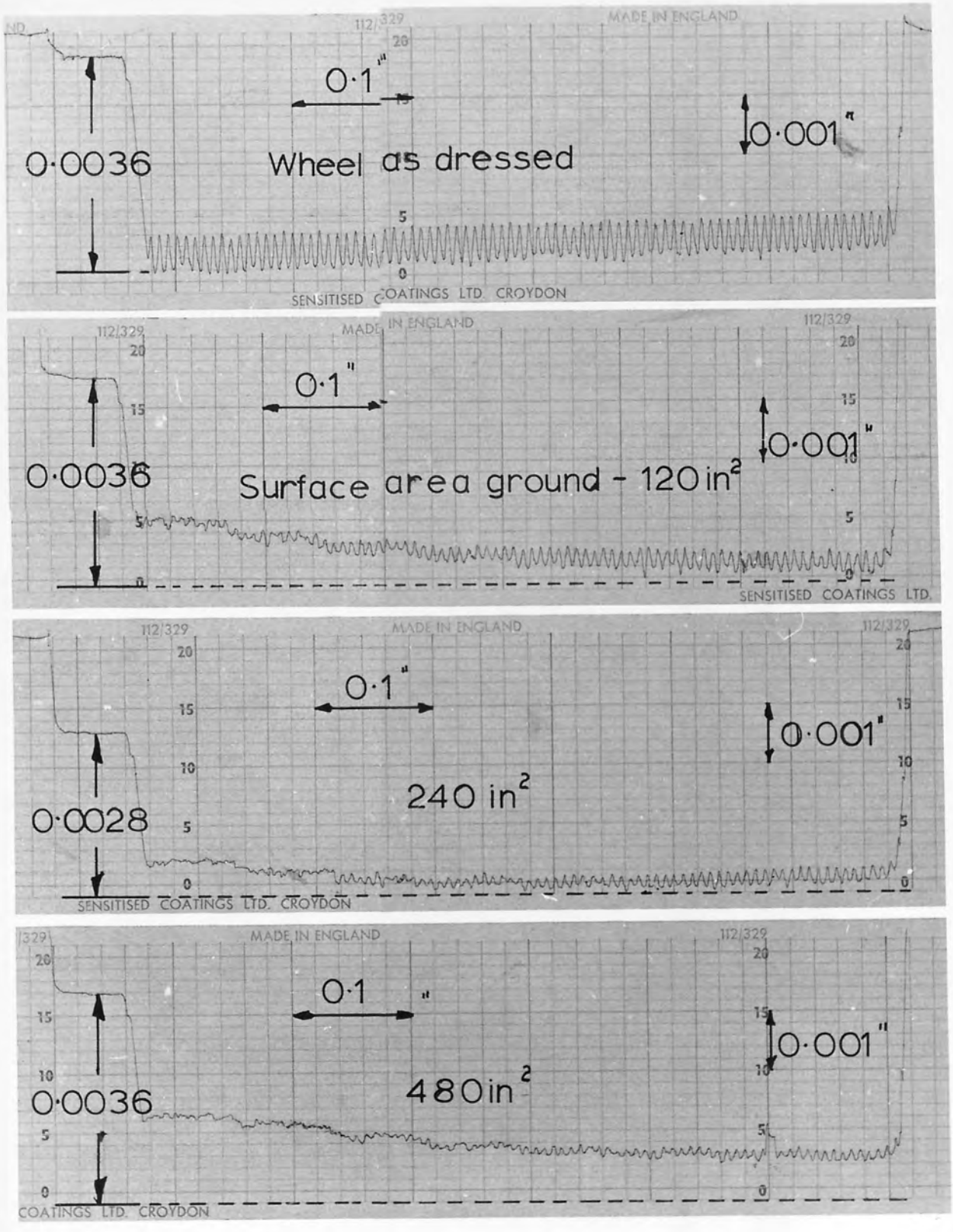
MADE IN ENGLAND
112/329
0·1"
0·001"
0·0036
Wheel as dressed
SENSITISED COATINGS LTD. CROYDON
MADE IN ENGLAND
112/329
0·1"
0·001"
0·0036
Surface area ground - 120 in²
SENSITISED COATINGS LTD.
MADE IN ENGLAND
112/329
0·1"
0·001"
0·0028
240 in²
SENSITISED COATINGS LTD. CROYDON
MADE IN ENGLAND
112/329
0·1"
0·001"
0·0036
480 in²
COATINGS LTD. CROYDON

Fig.85

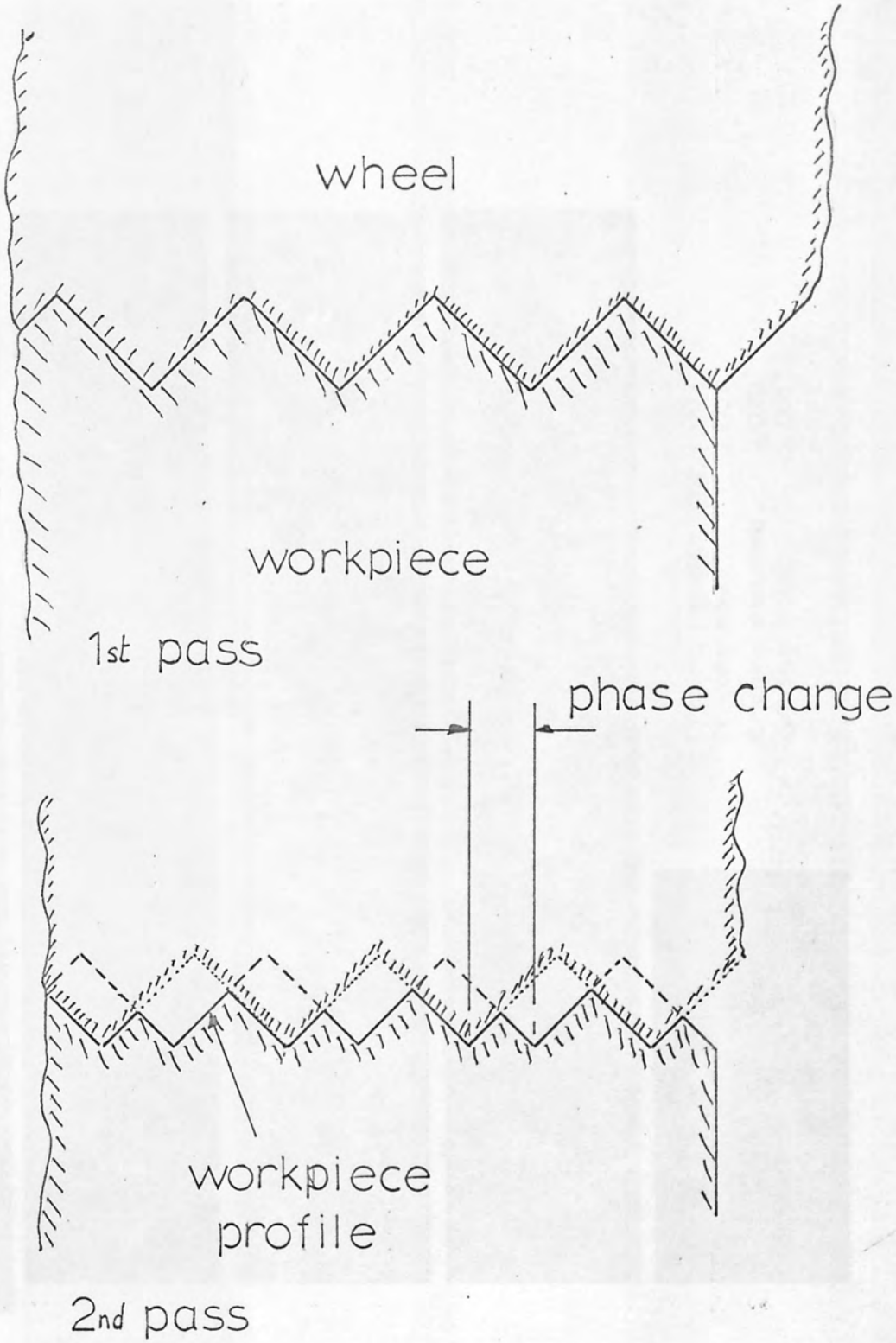

The influence of a phase change on the workpiece surface

Fig. 86.

Crossfeed grinding - workpiece surface

Fig. 87.

Crossfeed grinding - workpiece surface

Fig. 88.

Crossfeed grinding - workpiece surface

Fig. 89.

COARSE DRESSING Infeed 0.001 in		Traverse rate 0.0055 in/rev	
$\frac{\text{Wheel width}}{\text{Crossfeed}}$ = 7:1		$\frac{\text{Wheel width}}{\text{Crossfeed}}$ = 4:1	
55.0	71.0	76.0	74.0
37.0	57.0	76.0	70.0
38.0	50.0	74.0	52.0
43.0	50.0	73.0	54.0
44.0	58.0	63.0	53.0
42.0	75.0	63.0	58.0
45.0	63.0	65.0	58.0
60.0	42.0	71.0	60.0
56.0	50.0	66.0	67.0
57.0	52.0	63.0	62.0
68.0	66.0	75.0	65.0
82.0	81.0	68.0	54.0
83.0		61.0	

Crossfeed increment = 0.070 in.

Centre line average values taken over 0.070 in. intervals perpendicular to grinding direction.

After Vickerstaff[17]

Fig.90

FINE DRESSING

Infeed 0.001 in Traverse rate 0.0015 in/rev

$\frac{\text{Wheel width}}{\text{Crossfeed}}$ = 7:1		$\frac{\text{Wheel width}}{\text{Crossfeed}}$ = 4:1	
20.0	18.7	23.0	23.0
19.0	20.0	23.0	24.0
19.2	22.0	23.0	22.0
22.0	22.0	24.5	20.5
17.0	21.8	24.0	20.3
19.0	21.3	22.2	21.5
23.0	20.0	21.8	23.2
22.0	23.0	24.2	21.0
22.0	28.0	22.5	22.0
19.5	24.0	21.5	21.5
19.2	26.0	23.8	23.0
22.0	21.5	21.8	21.0
18.5		20.0	

Crossfeed increment = 0.070 in.

Centre line average values taken over 0.070 in. intervals perpendicular to grinding direction.

After Vickerstaff[17]

Fig.91

	A	B	C	D
Dressing	c'se	fine	c'se	c'se
Wheel infeed in	.001	.001	.001	.001
Table speed ft/m	56	56	56	56
Wheel width / Cross feed	9	9	9	4
Cross feed in	.070	.070	.030	.070

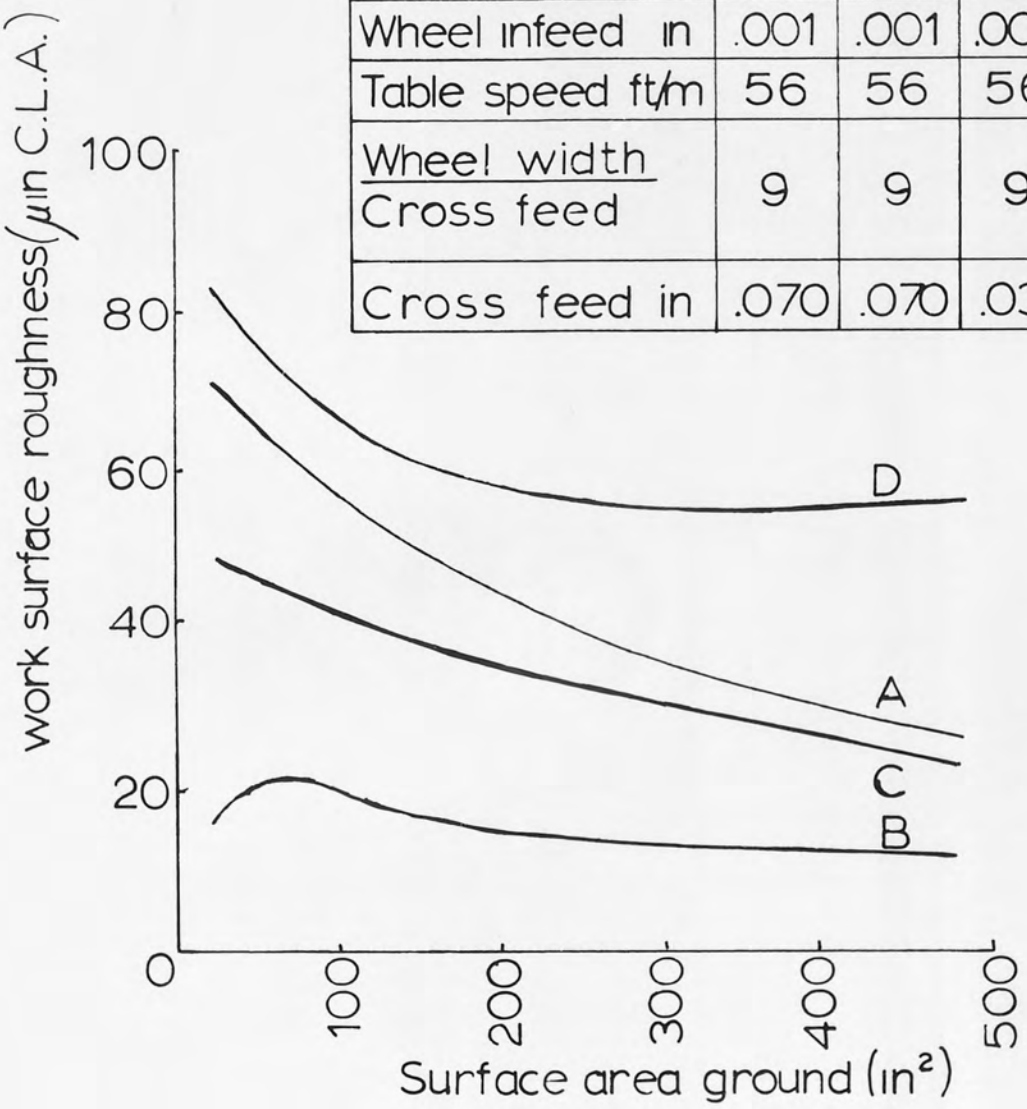

Fig.92

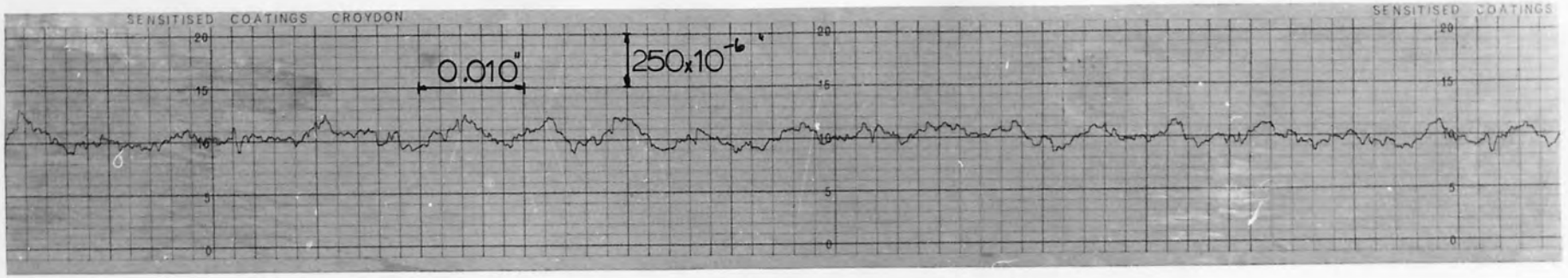

cross feed - 0.030 in. $\frac{\text{wheel width}}{\text{cross feed}}$ - 9

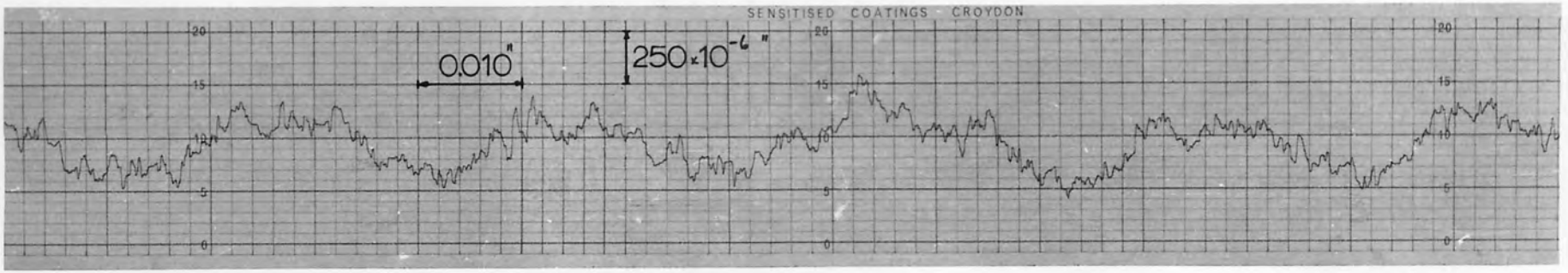

cross feed - 0.030 in. $\frac{\text{wheel width}}{\text{cross feed}}$ - 4

coarse dress
wheel infeed - 0.001 in
table speed - 56 ft/min
surface area
ground - 360 in²

Fig. 93